

1 **Ice, Cloud, and Land Elevation Satellite-2 (ICESat-2)**

2  
3 **Algorithm Theoretical Basis Document (ATBD)**

4  
5 **for**

6  
7 **Land - Vegetation Along-Track Products (ATL08)**

8  
9  
10  
11 **Contributions by Land/Vegetation SDT Team Members**  
12 **and ICESat-2 Project Science Office**

13 **(Amy Neuenschwander, Katherine Pitts, Benjamin Jelley, John Robbins,**  
14 **Jonathan Markel, Sorin Popescu, Ross Nelson, David Harding, Dylan**  
15 **Pederson, Brad Klotz, and Ryan Sheridan)**

16  
17  
18 **ATBD prepared by**

19 **Amy Neuenschwander**

20  
21  
22 **5 April 2022**

23 **(This ATBD Version corresponds to release 005 of the ICESat-2 ATL08**  
24 **data)**

25  
26  
27 **Content reviewed: technical approach, assumptions, scientific soundness,**  
28 **maturity, scientific utility of the data product**



31  
32

## ATL08 algorithm and product change history

ATBD Version	Change
2016 Nov	Product segment size changed from 250 signal photons to 100 m using five 20m segments from ATL03 (Sec 2)
2016 Nov	Filtered signal classification flag removed from classed_pc_flag (Sec 2.3.2)
2016 Nov	DRAGANN signal flag added (Sec 2.3.5)
2016 Nov	Do not report segment statistics if too few ground photons within segment (Sec 4.14 (3))
2016 Nov	Product parameters added: h_canopy_uncertainty, landsat_flag, d_flag, delta_time_beg, delta_time_end, night_flag, msw_flag (Sec 2)
2017 May	Revised region boundaries to be separated by continent (Sec 2)
2017 May	Alternative DRAGANN parameter calculation added (Sec 4.3.1)
2017 May	Set canopy flag = 0 when <i>L-km</i> segment is over Antarctica or Greenland regions (Sec 4.4 (1))
2017 May	Change initial canopy filter search radius from 3 m to 15 m (Sec 4.8 (6))
2017 May	Product parameters removed: h_rel_ph, terrain_thresh
2017 May	Product parameters added: segment_id, segment_id_beg, segment_id_end, dem_flag, surf_type (Sec 2)
2017 July	Urban flag added (Sec 2.4.20)
2017 July	Dynamic point spread function added (Sec 4.10 (6))
2017 July	Methodology for processing <i>L-km</i> segments with buffer added (Sec 4.1 (2), Sec 4.16)
2017 July	Revised alternative DRAGANN methodology ( <del>see bolded text in</del> Sec 4.3.1)
2017 July	Added post-DRAGANN filtering methodology (Sec 4.6)
2017 July	Updated SNR to be estimated from superset of ATL03 and DRAGANN found signal used for processing ATL08 (Sec 2.5.18)
2017 September	More details added to DRAGANN description (Sec 4.3), and corrections to DRAGANN implementation (Sec 3.1.1, Sec 4.3 (9))
2017 September	Added Appendix A – very detailed DRAGANN description
2017 September	Revised alternative DRAGANN methodology ( <del>see bolded text in</del> Sec 4.3.1)
2017 September	Clarified SNR calculation (Sec 2.5.18, Sec 4.3 (18))
2017 September	Added cloud flag filtering option (Sec 1)
2017 September	Added top of canopy median surface filter (Sec 3.5 (a), Sec 4.9 (3), Sec 4.11 (1-3))

2017 September	Modified 500 canopy photon segment filter (Sec 3.5 (c), Sec 4.11 (6))
2017 November	Added solar_azimuth, solar_elevation, and n_seg_ph to Reference Data group; parameters were already in product (Sec 2.4)
2017 November	Specified number of ground photons threshold for relative canopy product calculations (Sec 4.15 (2)); no number of ground photons threshold for absolute canopy heights (Sec 4.15.1 (1))
2017 November	Changed the ATL03 signal used in superset from all ATL03 signal (signal_conf_ph flags 1-4) to the medium-high confidence flags (signal_conf_ph flags 3-4) (Sec 3.1, Sec 4.3 (17))
2017 November	Removed Date parameter from Table 2.4 since UTC date is in file metadata
2018 March	Clarified that cloud flag filtering option should be turned off by default (Sec 1)
2018 March	Changed h_diff_ref QA threshold from 10 m to 25 m (Table 5.2)
2018 March	Added absolute canopy height quartiles, canopy_h_quartile_abs ( <i>Later removed</i> )
2018 March	Removed psf_flag from main product; psf_flag will only be a QAQC alert (Sec 5.2)
2018 March	Added an Asmooth filter based on the reference DEM value (Sec 4.5 (4-5))
2018 March	Changed relief calculation to 95 <sup>th</sup> – 5 <sup>th</sup> signal photon heights. (Sec 4.5 (6))
2018 March	Adjusted the Asmooth smoothing methodology (Sec 4.5 (8))
2018 March	Recalculate the Asmooth surface after filtering outlying noise from signal, then detrend signal height data (Sec 4.6 (3-4))
2018 March	Added option to run alternative DRAGANN process again in high noise cases (Sec 4.3.3)
2018 March	Changed global land cover reference to MODIS Global Mosaics product (Sec 2.4.16)
2018 March	Adjusted the top of canopy median filter thresholds based on SNR (Sec 4.11 (1-2))
2018 March	Added a final photon classification QA check (Sec 4.13, Table 5.2)
2018 March	Added slope adjusted terrain parameters ( <i>Later removed</i> )
2018 June	Replaced slope adjusted terrain parameters with terrain best fit parameter (Sec 2.1.14, 4.14 (2.e))
2018 June	Clarified source for water mask (Sec 2.4.18)
2018 June	Clarified source for urban mask (Sec 2.4.20)
2018 June	Added expansion to the terrain_slope calculation (Sec 4.14)
2018 June	Removed canopy_d_quartile

2018 June	Removed canopy_quartile_heights and canopy_quartile_heights_abs, replaced with canopy_h_metrics (Secs 2.2.3, 4.15 (6), 4.15.1 (5))
2018 *** draft 1	Delta_time specified as mid-segment time, rather than mean segment time (Sec 2.4.7)
2018 *** draft 1	QA/QC products to be reported on a per orbit basis, rather than per region (Sec 5.2)
2018 *** draft 1	Added more detail to landsat_flag description (Sec. 2.2.23)
2018 *** draft 1	Added psf_flag back into ATL08 product, as it is also needed for the QA product (Sec 2.5.12)
2018 *** draft 1	Specified that the sigma_h value reported here is the mean of the ATL03 reported sigma_h values (Sec 2.5.7)
2018 *** draft 1	Removed n_photons from all subgroups
2018 *** draft 1	Better defined the interpolation and smoothing methods used throughout: <ul style="list-style-type: none"> <li>• 1 (3): Interpolation – nearest</li> <li>• 4.5 (5): Interpolation – PCHIP</li> <li>• 4.5 (8): Smoothing – moving average</li> <li>• 4.6 (3): Interpolation – PCHIP</li> <li>• 4.6 (3): Smoothing – moving average</li> <li>• 4.7 (10): Smoothing – moving average</li> <li>• 4.7 (11): Interpolation – linear</li> <li>• 4.7 (12): Smoothing – moving average</li> <li>• 4.7 (13): Interpolation – linear</li> <li>• 4.7 (14): Smoothing – moving average</li> <li>• 4.7 (15): Smoothing – Savitzky-Golay</li> <li>• 4.7 (16): Interpolation – linear</li> <li>• 4.7 (21): Interpolation – PCHIP</li> <li>• 4.9 (10): Interpolation – linear</li> <li>• 4.10 (all): Smoothing – moving average</li> <li>• 4.10 (6.b): Interpolation – linear</li> <li>• 4.11 (1.a): Interpolation – linear</li> <li>• 4.11 (1.c): Smoothing – lowess</li> <li>• 4.11 (4): Interpolation – PCHIP</li> <li>• 4.11 (7): Interpolation – PCHIP</li> <li>• 4.11 (9): Smoothing – moving average</li> <li>• 4.14 (2.e.i.1): Interpolation – linear</li> </ul>
2018 *** draft 1	Added ref_elev and ref_azimuth back in (it was mistakenly removed in a previous version; Secs 2.5.3, 2.5.4)
2018 *** draft 1	Clarified wording of h_canopy_quad definition (Sec 2.2.18)
2018 *** draft 1	Updated segment_snowcover description to match the ATL09 snow_ice parameter it references (Sec 2.4.19) and added product reference to Table 4.2

2018 *** draft 1	Added ph_ndx_beg (Sec 2.5.22); parameter was already on product
2018 *** draft 1	Added dem_removal_flag for QA purposes (Sec 2.4.13; Table 5.2)
2018 *** draft 2	Reformatted QA/QC trending and trigger alert list into a table for better clarification (Table 5.3)
2018 *** draft 2	Replaced n_photons in Table 5.2 with n_te_photons, n_ca_photons, and n_toc_photons
2018 *** draft 2	Removed beam_number from Table 2.5. Beam number and weak/strong designation within gtx group attributes.
2018 *** draft 2	Clarified calculation of h_te_best_fit (Sec 4.14 (2.e))
2018 *** draft 2	Changed h_canopy and h_canopy_abs to be 98 <sup>th</sup> percentile height (Table 2.2, Sec 2.2.5, Sec 2.2.6, Sec 4.15 (4), Sec 4.15.1 (3))
2018 *** draft 2	Separated h_canopy_metrics_abs from h_canopy_metrics (Table 2.2, Sec 2.2.3, Sec 4.15.1 (5))
2018 October	Removed 99 <sup>th</sup> percentile from h_canopy_metrics and h_canopy_metrics_abs (Table 2.2, Sec 2.2.3, Sec 2.2.4, Sec 4.15 (4), Sec 4.15.1 (5))
2018 December	Renamed and reworded Section 4.3.1 to better indicate that the DRAGANN preprocessing step is not optional
2018 December	Specified that DRAGANN should use along-track time, and added time rescaling step (Sec 4.3 (1 - 4))
2018 December	Added DRAGANN changes made to better capture sparse canopy in cases of low noise rates (Sec 4.3, Appendix A)
2018 December	Made corrections to DRAGANN description regarding the determination of the noise Gaussian (Sec 3.1.1, Sec 4.3)
2018 December	Removed h_median_canopy and h_median_canopy_abs, as they are equivalent to canopy_h_metrics(50) and canopy_h_metrics_abs(50) (Table 2.2, Sec 4.15 (5), Sec 4.15.1 (4))
2018 December	Removed the requirement that > 5% ground photons required to calculate relative canopy height parameters (Table 2.2, Sec 4.15 (2))
2018 December	Added canopy relative height confidence flag (canopy_rh_conf) based on the percentage of ground and canopy photons in a segment (Table 2.2, Sec 4.15 (2))
2018 December	Added ATL09 layer_flag to ATL08 output (Table 2.5, Table 4.2)
2019 February	Adjusted cloud filtering to be based on ATL09 backscatter analysis rather than cloud flags (Sec 4.1)
2019 March 5	Updated ATL09-based product descriptions reported on ATL08 product (Secs 2.5.13, 2.5.14, 2.5.15, 2.5.16)
2019 March 5	Updated cloud-based low signal filter methodology, and moved to first step of ATL08 processing (Sec 4.1)

2019 March 13	Replace canopy_closure with new landsat_perc parameter (Table 2.2, Sec 2.2.24)
2019 March 13	Change ATL08 product output regions to match ATL03 regions (Sec 2), but keep ATL08 regions internally and report in new parameter atl08_regions (Table 2.4, Sec 2.4.22)
2019 March 13	Add methodology for handling short ATL08 processing segments at the end of an ATL03 granule (Sec 4.2), and output distance the processing segment length is extended into new parameter last_seg_extend (Table 2.4, Sec 2.4.23)
2019 March 13	Add preprocessing step for removing atmospheric and ocean tide corrections from ATL03 heights ( <i>Later removed</i> )
2019 March 27	Remove preprocessing step for removing atmospheric and ocean tide corrections from ATL03 heights, since those values are now removed from the ATL03 photon heights.
2019 March 27	Replaced ATL03 region figure with corrected version (Figure 2.2)
2019 March 27	Specified that at least 50 classed photons are required to create the 100 m land and canopy products (Secs 2, 4.14(1), 4.15(1))
2019 March 27	Clarified that any non-extended segments would report a land_seg_extend value of 0 (Sec 4.2, Sec 2.4.23)
2019 April 30	Fixed the error in Eqn 1.4 for the sigma topo value
2019 May 13	Specified for cloud flag carry-over from ATL09 that ATL08 will report the highest cloud flag if an 08 segment straddles two 09 segments. (Section 2.5)
2019 May 13	Changed parameter cloud_flag_asr to cloud_flag_atm since the cloud_flag_asr is likely not to work over land due to varying surface reflectance (Sec, 2.5)
2019 May 13	Add ATL09 parameter cloud_fold_flag to the ATL08 data product for future qa/qc checks for low clouds. (Secs, 2.5)
2019 May 13	Clarification on the calculation of gradient for slope that feeds into the calculation of the point spread function (Sec 4.11)
2019 July 8	Changed Landsat canopy cover percentage to 3 % (from original value of 5%) (Section 4.4)
2019 July 8	Added a QA method for DRAGANN flags to help remove false positives (now Section 4.3.1)
2019 July 8	Set the window size to 9 rather than SmoothSize for the final ground finding step. (Section 4.11 and 4.12)
2019 July 8	Added a brightness flag to land segments. (Section 2.4.21)
2019 November 12	Added subset_te_flag to (Section 2.1) which indicate 100 m segments that are populated by less than 100 m worth of data

2019 November 12	Added subset_can_flag (section 2.2) which indicate 100 m segments that are populated by less than 100 m worth of data
2020 January 5	Clarified the interpolation of values (latitude, longitude, delta time) when the 100 m segments are populated by less than 100 m worth of data. (Section 2.4.3 and 2.4.4)
2020 January 13	Fine-tuned the methodology to improve ground finding by first histogramming the photons to improve detecting the ground in cases of dense canopy. (Section 4.8)
2020 January 13	Updated ATL08 HDF5 file organization figure in Section 2.1
2020 February 14	Added sentence to avoid ATL03 data having a degraded PPD flag to beginning of Section 4
2020 February 14	Added documentation for removing signal photons due to cloud contamination by checking the reference DEM to beginning of Section 4
2020 February 14	Added full saturation flag and near saturation flag from ATL03 to ATL08 data product to Section 2.
2020 February 14	Added statement to clarify handling of remaining geosegments that do not fit within a 100 m window at the end of a 10-km processing window in Section 4.2
2020 April 15	Added ph_h parameter to photon group on data structure. ph_h is the photon height above the interpolated ground surface.
2020 May 15	Added sat_flag which is derived from the ATL03 product. The saturation flag indicates that the ATL08 segment experienced some saturation which is often an indicator for water
2020 May 15	Canopy height metrics (relative and absolute heights) were expanded to every 5% ranging from 5 – 95%.
2020 May 15	The Landsat canopy cover check to determine whether the algorithm should search for both ground and canopy or just ground has been disabled. Now the ATL08 algorithm will search for both ground and canopy points everywhere.
2020 June 15	Corrected the calculation of the absolute canopy heights
2020 June 15	Changed the search radius for initial top of canopy determination (Section 4.9)
2020 September 1	Incorporate the quality_ph flag from ATL03 into the ATL08 workflow (beginning of Section 4)
2020 September 1	Added the calculation of Terrain photon rate (photon_rate_te) for each ATL08 segment to the land product (Section 2.1.16)
2020 September 1	Added the calculation of canopy photon rate (photon_rate_can) for each ATL08 segment to the land product (Section 2.2.26)



2020 September 1	Changed the k-d tree search radius for the top of canopy from 15 m to 100 m. Section 4.9.6
2020 September 15	Added new parameter for terrain heights (h_te_rh25) which represents the height of the 25% of ground cumulative distribution.
<b>2021 March 15</b>	Added terrain_best_fit_geosegment (h_te_best_fit_20m) parameter to the data product. 20 m estimate of best fit terrain height
<b>2021 March 15</b>	Added canopy_height_geosegment (h_canopy_20m) to the data product. 20 m estimate of relative canopy height
2021 March 15	Added latitude_20m to the data product.
2021 March 15	Added longitude_20m to the data product
<b>2021 March 15</b>	Updated the urban_flag parameter. Inclusion of the DLR Global Urban Footprint (GUF) as a potential indicator of man-made/built structures. Section 2.4.20
<b>2021 March 15</b>	Updated the Segment_landcover with Copernicus. Replace the MODIS landcover value with the landcover classification from the 100 m Copernicus landcover. Section 2.4.16
<b>2021 March 15</b>	Added the Segment_Woody_Vegetation_Fractional_cover. Inclusion of a woody vegetation fraction cover derived from the 2019 Copernicus fractional cover data products. Section 2.4.17
<b>2021 March 15</b>	Removed Landsat_perc (Landsat Percentage Calculation), Landsat_flag, and Canopy_flag from the ATL08 data product and from the algorithm. Removed all reference to Landsat from the ATBD.

33  
34

35 **Contents**

36 List of Tables..... 16

37 List of Figures..... 17

38 1 INTRODUCTION ..... 19

39 1.1. Background ..... 20

40 1.2 Photon Counting Lidar ..... 22

41 1.3 The ICESat-2 concept..... 23

42 1.4 Height Retrieval from ATLAS ..... 26

43 1.5 Accuracy Expected from ATLAS..... 28

44 1.6 Additional Potential Height Errors from ATLAS..... 30

45 1.7 Dense Canopy Cases ..... 30

46 1.8 Sparse Canopy Cases ..... 31

47 2. ATL08: DATA PRODUCT ..... 32

48 2.1 Subgroup: Land Parameters ..... 35

49 2.1.1 Georeferenced\_segment\_number\_beg..... 36

50 2.1.2 Georeferenced\_segment\_number\_end ..... 37

51 2.1.3 Segment\_terrain\_height\_mean..... 37

52 2.1.4 Segment\_terrain\_height\_med ..... 37

53 2.1.5 Segment\_terrain\_height\_min ..... 38

54 2.1.6 Segment\_terrain\_height\_max..... 38

55 2.1.7 Segment\_terrain\_height\_mode..... 38

56 2.1.8 Segment\_terrain\_height\_skew ..... 38

57 2.1.9 Segment\_number\_terrain\_photons..... 39

58 2.1.10 Segment height\_interp..... 39

59 2.1.11 Segment h\_te\_std..... 39

60 2.1.12 Segment\_terrain\_height\_uncertainty ..... 39

61 2.1.13 Segment\_terrain\_slope ..... 39

62	2.1.14	Segment_terrain_height_best_fit .....	40
63	2.1.15	Segment_terrain_height_25 .....	40
64	2.1.16	Subset_te_flag {1:5} .....	40
65	2.1.17	Segment Terrain Photon Rate .....	41
66	2.1.18	Terrain Best Fit GeoSegment {1:5} .....	41
67	2.2	Subgroup: Vegetation Parameters .....	41
68	2.2.1	Georeferenced_segment_number_beg .....	44
69	2.2.2	Georeferenced_segment_number_end .....	44
70	2.2.3	Canopy_height_metrics_abs .....	44
71	2.2.4	Canopy_height_metrics .....	45
72	2.2.5	Absolute_segment_canopy_height .....	45
73	2.2.6	Segment_canopy_height .....	46
74	2.2.7	canopy_height GeoSegment {1:5} .....	46
75	2.2.8	Absolute_segment_mean_canopy .....	46
76	2.2.9	Segment_mean_canopy .....	47
77	2.2.10	Segment_dif_canopy .....	47
78	2.2.11	Absolute_segment_min_canopy .....	47
79	2.2.12	Segment_min_canopy .....	47
80	2.2.13	Absolute_segment_max_canopy .....	47
81	2.2.14	Segment_max_canopy .....	48
82	2.2.15	Segment_canopy_height_uncertainty .....	48
83	2.2.16	Segment_canopy_openness .....	49
84	2.2.17	Segment_top_of_canopy_roughness .....	49
85	2.2.18	Segment_canopy_quadratic_height .....	49
86	2.2.19	Segment_number_canopy_photons .....	49
87	2.2.20	Segment_number_top_canopy_photons .....	50
88	2.2.21	Centroid_height .....	50

89	2.2.22	Segment_rel_canopy_conf .....	50
90	2.2.23	Subset_can_flag {1:5}.....	50
91	2.2.24	Segment Canopy Photon Rate .....	51
92	2.3	Subgroup: Photons.....	51
93	2.3.1	Indices_of_classed_photons.....	52
94	2.3.2	Photon_class.....	52
95	2.3.3	Georeferenced_segment_number .....	52
96	2.3.4	Photon Height.....	53
97	2.3.5	DRAGANN_flag.....	53
98	2.4	Subgroup: Reference data.....	53
99	2.4.1	Georeferenced_segment_number_beg.....	55
100	2.4.2	Georeferenced_segment_number_end .....	55
101	2.4.3	Segment_latitude .....	55
102	2.4.4	Geosegment_latitude{1:5} .....	56
103	2.4.5	Segment_longitude.....	56
104	2.4.6	Geosegment_longitude{1:5}.....	57
105	2.4.7	Delta_time .....	57
106	2.4.8	Delta_time_beg.....	57
107	2.4.9	Delta_time_end.....	57
108	2.4.10	Night_Flag .....	57
109	2.4.11	Segment_reference_DTM.....	57
110	2.4.12	Segment_reference_DEM_source .....	58
111	2.4.13	Segment_reference_DEM_removal_flag .....	58
112	2.4.14	Segment_terrain_difference .....	58
113	2.4.15	Segment_terrain flag .....	58
114	2.4.16	Segment_landcover.....	58
115	2.4.17	Segment_Woody Vegetation Fractional Cover.....	60

116	2.4.18	Segment_watermask .....	60
117	2.4.19	Segment_snowcover .....	60
118	2.4.20	Urban_flag .....	60
119		Surface_Type .....	<b>Error! Bookmark not defined.</b>
120	2.4.21	ATL08_region .....	61
121	2.4.22	Last_segment_extend .....	61
122	2.4.23	Brightness_flag.....	62
123	2.5	Subgroup: Beam data.....	62
124	2.5.1	Georeferenced_segment_number_beg.....	65
125	2.5.2	Georeferenced_segment_number_end .....	65
126	2.5.3	Beam_coelevation.....	65
127	2.5.4	Beam_azimuth.....	65
128	2.5.5	ATLAS_Pointing_Angle .....	66
129	2.5.6	Reference_ground_track.....	66
130	2.5.7	Sigma_h .....	66
131	2.5.8	Sigma_along.....	66
132	2.5.9	Sigma_across.....	66
133	2.5.10	Sigma_topo .....	67
134	2.5.11	Sigma_ATLAS_LAND .....	67
135	2.5.12	PSF_flag .....	67
136	2.5.13	Layer_flag .....	67
137	2.5.14	Cloud_flag_atm .....	68
138	2.5.15	MSW.....	68
139	2.5.16	Cloud Fold Flag .....	68
140	2.5.17	Computed_Apparent_Surface_Reflectance .....	68
141	2.5.18	Signal_to_Noise_Ratio .....	69
142	2.5.19	Solar_Azimuth .....	69

143	2.5.20	Solar_Elevation .....	69
144	2.5.21	Number_of_segment_photons .....	69
145	2.5.22	Photon_Index_Begin .....	69
146	2.5.23	Saturation Flag.....	69
147	3	ALGORITHM METHODOLOGY.....	71
148	3.1	Noise Filtering.....	71
149	3.1.1	DRAGANN .....	72
150	3.2	Surface Finding.....	76
151	3.2.1	De-trending the Signal Photons.....	78
152	3.2.2	Canopy Determination .....	78
153	3.2.3	Variable Window Determination.....	79
154	3.2.4	Compute descriptive statistics.....	80
155	3.2.5	Ground Finding Filter (Iterative median filtering) .....	82
156	3.3	Top of Canopy Finding Filter .....	83
157	3.4	Classifying the Photons .....	84
158	3.5	Refining the Photon Labels.....	84
159	3.6	Canopy Height Determination .....	89
160	3.7	Link Scale for Data products.....	89
161	4.	ALGORITHM IMPLEMENTATION .....	90
162	4.1	Cloud based filtering .....	93
163	4.2	Preparing ATL03 data for input to ATL08 algorithm .....	95
164	4.3	Noise filtering via DRAGANN.....	97
165	4.3.1	DRAGANN Quality Assurance.....	99
166	4.3.2	Preprocessing to dynamically determine a DRAGANN parameter .....	101
167	4.3.3	Iterative DRAGANN processing.....	104
168	4.4	Compute Filtering Window .....	104
169	4.5	De-trend Data .....	105

170	4.6	Filter outlier noise from signal .....	106
171	4.7	Finding the initial ground estimate .....	106
172	4.8	Find the top of the canopy (if canopy_flag = 1) .....	109
173	4.9	Compute statistics on de-trended (Asmooth) data.....	110
174	4.10	Refine Ground Estimates.....	111
175	4.11	Canopy Photon Filtering.....	113
176	4.12	Compute individual Canopy Heights.....	115
177	4.13	Final photon classification QA check .....	116
178	4.14	Compute segment parameters for the Land Products .....	116
179	4.15	Compute segment parameters for the Canopy Products .....	119
180	4.15.1	Canopy Products calculated with absolute heights .....	120
181	4.16	Record final product without buffer .....	121
182	5	DATA PRODUCT VALIDATION STRATEGY.....	122
183	5.1	Validation Data .....	122
184	5.2	Internal QC Monitoring .....	125
185	6	REFERENCES .....	131
186			

187	<b>List of Tables</b>	
188	Table 2.1. Summary table of land parameters on ATL08.....	35
189	Table 2.2. Summary table of canopy parameters on ATL08.....	42
190	Table 2.3. Summary table for photon parameters for the ATL08 product.....	51
191	Table 2.4. Summary table for reference parameters for the ATL08 product.....	53
192	Table 2.5. Summary table for beam parameters for the ATL08 product.....	62
193	Table 3.1. Standard deviation ranges utilized to qualify the spread of photons within	
194	moving window.....	81
195	Table 4.1. Input parameters to ATL08 classification algorithm.....	91
196	Table 4.2. Additional external parameters referenced in ATL08 product. ....	92
197	Table 5.1. Airborne lidar data vertical height (Z accuracy) requirements for	
198	validation data. ....	122
199	Table 5.2. ATL08 parameter monitoring.....	125
200	Table 5.3. QA/QC trending and triggers. ....	129
201		



202	<b>List of Figures</b>	
203	Figure 1.1. Various modalities of lidar detection. Adapted from Harding, 2009.....	23
204	Figure 1.2. Schematic of 6-beam configuration for ICESat-2 mission. The laser	
205	energy will be split into 3 laser beam pairs – each pair having a weak spot (1X) and a	
206	strong spot (4X). .....	25
207	Figure 1.3. Illustration of off-nadir pointing scenarios. Over land (green regions) in	
208	the mid-latitudes, ICESat-2 will be pointed away from the repeat ground tracks to	
209	increase the density of measurements over terrestrial surfaces. ....	26
210	Figure 1.4. Illustration of the point spread function, also referred to as Znoise, for a	
211	series of photons about a surface. ....	28
212	Figure 2.1. HDF5 data structure for ATL08 products.....	33
213	Figure 2.2. ATL03 granule regions; graphic from ATL03 ATBD (Neumann et al.). ....	34
214	Figure 2.3. ATL08 product regions. ....	35
215	Figure 2.4. Illustration of canopy photons (red dots) interaction in a vegetated area.	
216	Relative canopy heights, $H_i$ , are computed by differencing the canopy photon height	
217	from an interpolated terrain surface. ....	42
218	Figure 3.1. Combination of noise filtering algorithms to create a superset of input	
219	data for surface finding algorithms. ....	72
220	Figure 3.2. Histogram of the number of photons within a search radius. This	
221	histogram is used to determine the threshold for the DRAGANN approach.....	74
222	Figure 3.3. Output from DRAGANN filtering. Signal photons are shown as blue. ....	76
223	Figure 3.4. Flowchart of overall surface finding method. ....	77
224	Figure 3.5. Plot of Signal Photons (black) from 2014 MABEL flight over Alaska and	
225	de-trended photons (red). ....	78
226	Figure 3.6. Shape Parameter for variable window size. ....	80
227	Figure 3.7. Illustration of the standard deviations calculated for each moving	
228	window to identify the amount of spread of signal photons within a given window.	
229	.....	82
230	Figure 3.8. Three iterations of the ground finding concept for $L$ -km segments with	
231	canopy. ....	83

232	Figure 3.9. Example of the intermediate ground and top of canopy surfaces	
233	calculated from MABEL flight data over Alaska during July 2014.....	86
234	Figure 3.10. Example of classified photons from MABEL data collected in Alaska	
235	2014. Red photons are photons classified as terrain. Green photons are classified as	
236	top of canopy. Canopy photons (shown as blue) are considered as photons lying	
237	between the terrain surface and top of canopy.....	87
238	Figure 3.11. Example of classified photons from MABEL data collected in Alaska	
239	2014. Red photons are photons classified as terrain. Green photons are classified as	
240	top of canopy. Canopy photons (shown as blue) are considered as photons lying	
241	between the terrain surface and top of canopy.....	88
242	Figure 3.12. Example of classified photons from MABEL data collected in Alaska	
243	2014. Red photons are photons classified as terrain. Green photons are classified as	
244	top of canopy. Canopy photons (shown as blue) are considered as photons lying	
245	between the terrain surface and top of canopy.....	88
246	Figure 5.1. Example of <i>L-km</i> segment classifications and interpolated ground	
247	surface.....	128
248		

249 **1 INTRODUCTION**

250 This document describes the theoretical basis and implementation of the  
251 processing algorithms and data parameters for Level 3 land and vegetation heights  
252 for the non-polar regions of the Earth. The ATL08 product contains heights for both  
253 terrain and canopy in the along-track direction as well as other descriptive  
254 parameters derived from the measurements. At the most basic level, a derived surface  
255 height from the ATLAS instrument at a given time is provided relative to the WGS-84  
256 ellipsoid. Height estimates from ATL08 can be compared with other geodetic data and  
257 used as input to higher-level ICESat-2 products, namely ATL13 and ATL18. ATL13  
258 will provide estimates of inland water-related heights and associated descriptive  
259 parameters. ATL18 will consist of gridded maps for terrain and canopy features.

260 The ATL08 product will provide estimates of terrain heights, canopy heights,  
261 and canopy cover at fine spatial scales in the along-track direction. Along-track is  
262 defined as the direction of travel of the ICESat-2 satellite in the velocity vector.  
263 Parameters for the terrain and canopy will be provided at a fixed step-size of 100 m  
264 along the ground track referred to as a segment. A fixed segment size of 100 m was  
265 chosen to provide continuity of data parameters on the ATL08 data product. From an  
266 analysis perspective, it is difficult and cumbersome to attempt to relate canopy cover  
267 over variable lengths. Furthermore, a segment size of 100 m will facilitate a simpler  
268 combination of along-track data to create the gridded products.

269 We anticipate that the signal returned from the weak beam will be sufficiently  
270 weak and may prohibit the determination of both a terrain and canopy segment  
271 height, particularly over areas of dense vegetation. However, in more arid regions we  
272 anticipate producing a terrain height for both the weak and strong beams.

273 In this document, section 1 provides a background of lidar in the ecosystem  
274 community as well as describing photon counting systems and how they differ from  
275 discrete return lidar systems. Section 2 provides an overview of the Land and  
276 Vegetation parameters and how they are defined on the data product. Section 3  
277 describes the basic methodology that will be used to derive the parameters for ATL08.

278 Section 4 describes the processing steps, input data, and procedure to derive the data  
279 parameters. Section 5 will describe the test data and specific tests that NASA's  
280 implementation of the algorithm should pass in order to determine a successful  
281 implementation of the algorithm.

282

### 283 ***1.1. Background***

284 The Earth's land surface is a complex mosaic of geomorphic units and land  
285 cover types resulting in large variations in terrain height, slope, roughness, vegetation  
286 height and reflectance, often with the variations occurring over very small spatial  
287 scales. Documentation of these landscape properties is a first step in understanding  
288 the interplay between the formative processes and response to changing conditions.  
289 Characterization of the landscape is also necessary to establish boundary conditions  
290 for models which are sensitive to these properties, such as predictive models of  
291 atmospheric change that depend on land-atmosphere interactions. Topography, or  
292 land surface height, is an important component for many height applications, both to  
293 the scientific and commercial sectors. The most accurate global terrain product was  
294 produced by the Shuttle Radar Topography Mission (SRTM) launched in 2000;  
295 however, elevation data are limited to non-polar regions. The accuracy of SRTM  
296 derived elevations range from 5 – 10 m, depending upon the amount of topography  
297 and vegetation cover over a particular area. ICESat-2 will provide a global distribution  
298 of geodetic measurements (of both the terrain surface and relative canopy heights)  
299 which will provide a significant benefit to society through a variety of applications  
300 including sea level change monitoring, forest structural mapping and biomass  
301 estimation, and improved global digital terrain models.

302 In addition to producing a global terrain product, monitoring the amount and  
303 distribution of above ground vegetation and carbon pools enables improved  
304 characterization of the global carbon budget. Forests play a significant role in the  
305 terrestrial carbon cycle as carbon pools. Events, such as management activities  
306 (Krankina et al. 2012) and disturbances can release carbon stored in forest above

307 ground biomass (AGB) into the atmosphere as carbon dioxide, a greenhouse gas that  
308 contributes to climate change (Ahmed et al. 2013). While carbon stocks in nations  
309 with continuous national forest inventories (NFIs) are known, complications with NFI  
310 carbon stock estimates exist, including: (1) ground-based inventory measurements  
311 are time consuming, expensive, and difficult to collect at large-scales (Houghton  
312 2005; Ahmed et al. 2013); (2) asynchronously collected data; (3) extended time  
313 between repeat measurements (Houghton 2005); and (4) the lack of information on  
314 the spatial distribution of forest AGB, required for monitoring sources and sinks of  
315 carbon (Houghton 2005). Airborne lidar has been used for small studies to capture  
316 canopy height and in those studies canopy height variation for multiple forest types  
317 is measured to approximately 7 m standard deviation (Hall et al., 2011).

318         Although the spatial extent and changes to forests can be mapped with existing  
319 satellite remote sensing data, the lack of information on forest vertical structure and  
320 biomass limits the knowledge of biomass/biomass change within the global carbon  
321 budget. Based on the global carbon budget for 2015 (Quere et al., 2015), the largest  
322 remaining uncertainties about the Earth's carbon budget are in its terrestrial  
323 components, the global residual terrestrial carbon sink, estimated at  $3.0 \pm 0.8$   
324 GtC/year for the last decade (2005-2014). Similarly, carbon emissions from land-use  
325 changes, including deforestation, afforestation, logging, forest degradation and  
326 shifting cultivation are estimated at  $0.9 \pm 0.5$  GtC /year. By providing information on  
327 vegetation canopy height globally with a higher spatial resolution than previously  
328 afforded by other spaceborne sensors, the ICESat-2 mission can contribute  
329 significantly to reducing uncertainties associated with forest vegetation carbon.

330         Although ICESat-2 is not positioned to provide global biomass estimates due  
331 to its profiling configuration and somewhat limited detection capabilities, it is  
332 anticipated that the data products for vegetation will be complementary to ongoing  
333 biomass and vegetation mapping efforts. Synergistic use of ICESat-2 data with other  
334 space-based mapping systems is one solution for extended use of ICESat-2 data.  
335 Possibilities include NASA's Global Ecosystems Dynamics Investigation (GEDI) lidar

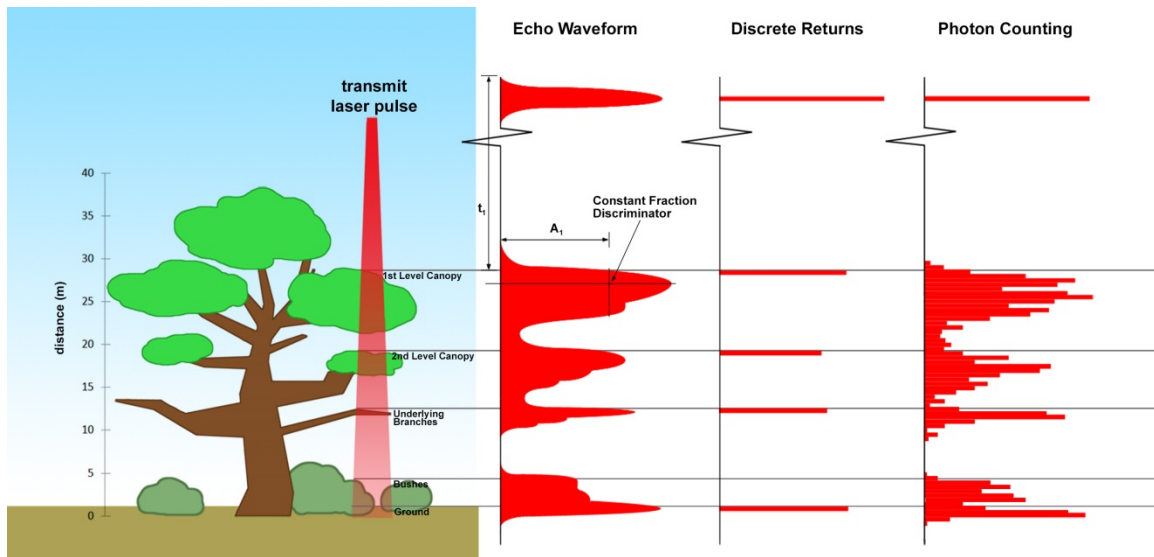
336 planned to fly onboard the International Space Station (ISS) or imaging sensors, such  
337 as Landsat 8, or NASA/ISRO –NISAR radar mission.

338

## 339 **1.2 Photon Counting Lidar**

340 Rather than using an analog, full waveform system similar to what was utilized  
341 on the ICESat/GLAS mission, ICESat-2 will employ a photon counting lidar. Photon  
342 counting lidar has been used successfully for ranging for several decades in both the  
343 science and defense communities. Photon counting lidar systems operate on the  
344 concept that a low power laser pulse is transmitted and the detectors used are  
345 sensitive at the single photon level. Due to this type of detector, any returned photon  
346 whether from the reflected signal or solar background can trigger an event within the  
347 detector. A discussion regarding discriminating between signal and background noise  
348 photons is discussed later in this document. A question of interest to the ecosystem  
349 community is to understand where within the canopy is the photon likely to be  
350 reflected. Figure 1.1 is an example of three different laser detector modalities: full  
351 waveform, discrete return, and photon counting. Full waveform sensors record the  
352 entire temporal profile of the reflected laser energy through the canopy. In contrast,  
353 discrete return systems have timing hardware that record the time when the  
354 amplitude of the reflected signal energy exceeds a certain threshold amount. A photon  
355 counting system, however, will record the arrival time associated with a single  
356 photon detection that can occur anywhere within the vertical distribution of the  
357 reflected signal. If a photon counting lidar system were to dwell over a surface for a  
358 significant number of shots (i.e. hundreds or more), the vertical distribution of the  
359 reflected photons will resemble a full waveform. Thus, while an individual photon  
360 could be reflected from anywhere within the vertical canopy, the probability  
361 distribution function (PDF) of that reflected photon would be the full waveform.  
362 Furthermore, the probability of detecting the top of the tree is not as great as  
363 detecting reflective surfaces positioned deeper into the canopy where the bulk of  
364 leaves and branches are located. As one might imagine, the PDF will differ according

365 to canopy structure and vegetation physiology. For example, the PDF of a conifer tree  
366 will look different than broadleaf trees.



367

368 Figure 1.1. Various modalities of lidar detection. Adapted from Harding, 2009.

369 A cautionary note, the photon counting PDF that is illustrated in Figure 1.1 is  
370 merely an illustration if enough photons (i.e. hundreds of photons or more) were to  
371 be reflected from a target. In reality, due to the spacecraft speed, ATLAS will record 0  
372 – 4 photons per transmit laser pulse over vegetation.

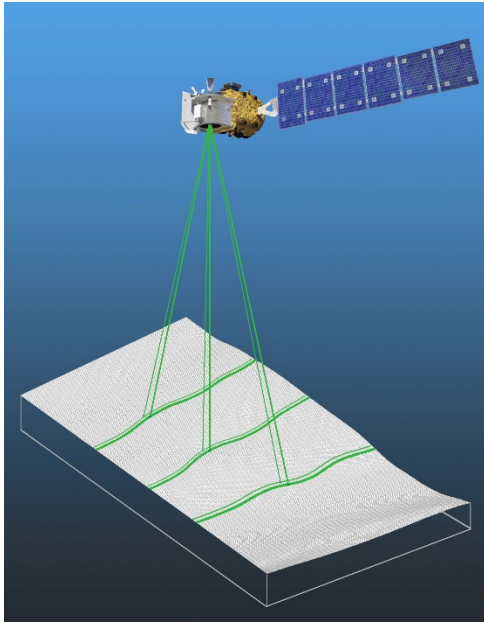
373

### 374 1.3 The ICESat-2 concept

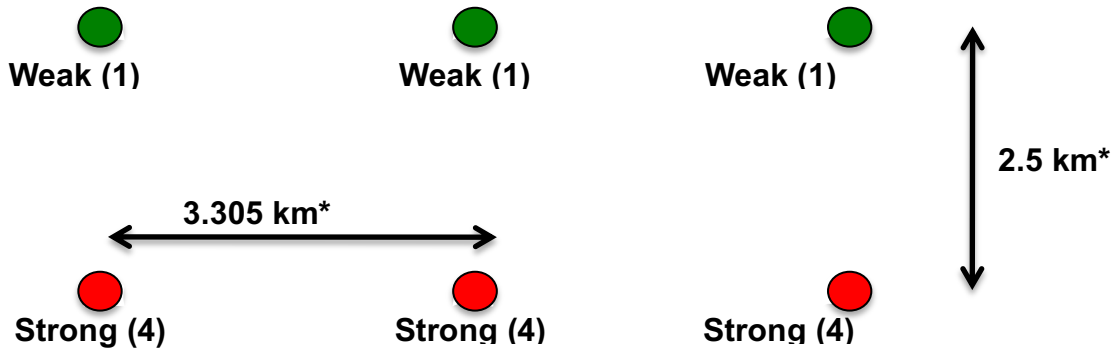
375 The Advanced Topographic Laser Altimeter System (ATLAS) instrument  
376 designed for ICESat-2 will utilize a different technology than the GLAS instrument  
377 used for ICESat. Instead of using a high-energy, single-beam laser and digitizing the  
378 entire temporal profile of returned laser energy, ATLAS will use a multi-beam,  
379 micropulse laser (sometimes referred to as photon-counting). The travel time of each  
380 detected photon is used to determine a range to the surface which, when combined  
381 with satellite attitude and pointing information, can be geolocated into a unique XYZ  
382 location on or near the Earth's surface. For more information on how the photons  
383 from ICESat-2 are geolocated, refer to ATL03 ATBD. The XYZ positions from ATLAS

384 are subsequently used to derive surface and vegetation properties. The ATLAS  
385 instrument will operate at 532 nm in the green range of the electromagnetic (EM)  
386 spectrum and will have a laser repetition rate of 10 kHz. The combination of the laser  
387 repetition rate and satellite velocity will result in one outgoing laser pulse  
388 approximately every 70 cm on the Earth's surface and each spot on the surface is ~13  
389 m in diameter. Each transmitted laser pulse is split by a diffractive optical element in  
390 ATLAS to generate six individual beams, arranged in three pairs (Figure 1.2). The  
391 beams within each pair have different transmit energies ('weak' and 'strong', with an  
392 energy ratio of approximately 1:4) to compensate for varying surface reflectance. The  
393 beam pairs are separated by ~3.3 km in the across-track direction and the strong and  
394 weak beams are separated by ~2.5 km in the along-track direction. As ICESat-2 moves  
395 along its orbit, the ATLAS beams describe six tracks on the Earth's surface; the array  
396 is rotated slightly with respect to the satellite's flight direction so that tracks for the  
397 fore and aft beams in each column produce pairs of tracks – each separated by  
398 approximately 90 m.





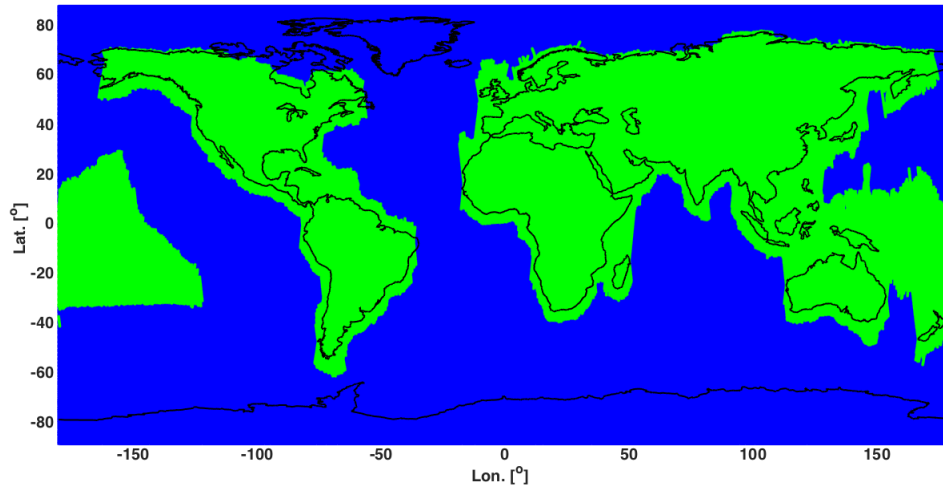
399



400

401 Figure 1.2. Schematic of 6-beam configuration for ICESat-2 mission. The laser energy will  
 402 be split into 3 laser beam pairs – each pair having a weak spot (1X) and a strong spot (4X).

403 The motivation behind this multi-beam design is its capability to compute  
 404 cross-track slopes on a per-orbit basis, which contributes to an improved  
 405 understanding of ice dynamics. Previously, slope measurements of the terrain were  
 406 determined via repeat-track and crossover analysis. The laser beam configuration as  
 407 proposed for ICESat-2 is also beneficial for terrestrial ecosystems compared to GLAS  
 408 as it enables a denser spatial sampling in the non-polar regions. To achieve a spatial  
 409 sampling goal of no more than 2 km between equatorial ground tracks, ICESat-2 will  
 410 be off-nadir pointed a maximum of 1.8 degrees from the reference ground track  
 411 during the entire mission.



412

413 Figure 1.3. Illustration of off-nadir pointing scenarios. Over land (green regions) in the  
 414 mid-latitudes, ICESat-2 will be pointed away from the repeat ground tracks to increase the  
 415 density of measurements over terrestrial surfaces.

416 ICESat-2 is designed to densely sample the Earth's surface, permitting  
 417 scientists to measure and quantitatively characterize vegetation across vast  
 418 expanses, e.g., nations, continents, globally. ICESat-2 will acquire synoptic  
 419 measurements of vegetation canopy height, density, the vertical distribution of  
 420 photosynthetically active material, leading to improved estimates of forest biomass,  
 421 carbon, and volume. In addition, the orbital density, i.e., the number of orbits per unit  
 422 area, at the end of the three year mission will facilitate the production of gridded  
 423 global products. ICESat-2 will provide the means by which an accurate "snapshot" of  
 424 global biomass and carbon may be constructed for the mission period.

425

#### 426 **1.4 Height Retrieval from ATLAS**

427 Light from the ATLAS lasers reaches the earth's surface as flat disks of down-  
 428 traveling photons approximately 50 cm in vertical extent and spread over  
 429 approximately 14 m horizontally. Upon hitting the earth's surface, the photons are  
 430 reflected and scattered in every direction and a handful of photons return to the

431 ATLAS telescope's focal plane. The number of photon events per laser pulse is a  
432 function of outgoing laser energy, surface reflectance, solar conditions, and scattering  
433 and attenuation in the atmosphere. For highly reflective surfaces (such as land ice)  
434 and clear skies, approximately 10 signal photons from a single strong beam are  
435 expected to be recorded by the ATLAS instrument for a given transmit laser pulse.  
436 Over vegetated land where the surface reflectance is considerably less than snow or  
437 ice surfaces, we expect to see fewer returned photons from the surface. Whereas  
438 snow and ice surfaces have high reflectance at 532 nm (typical Lambertian  
439 reflectance between 0.8 and 0.98 (Martino, GSFC internal report, 2010)), canopy and  
440 terrain surfaces have much lower reflectance (typically around 0.3 for soil and 0.1 for  
441 vegetation) at 532 nm. As a consequence we expect to see 1/3 to 1/9 as many photons  
442 returned from terrestrial surfaces as from ice and snow surfaces. For vegetated  
443 surfaces, the number of reflected signal photon events per transmitted laser pulse is  
444 estimated to range between 0 to 4 photons.

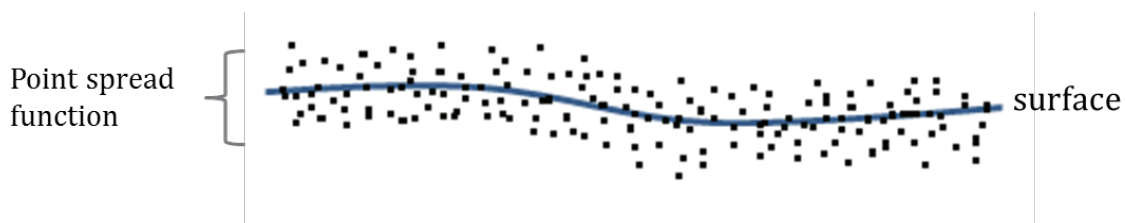
445 The time measured from the detected photon events are used to compute a  
446 range, or distance, from the satellite. Combined with the precise pointing and attitude  
447 information about the satellite, the range can be geolocated into a XYZ point (known  
448 as a geolocated photon) above the WGS-84 reference ellipsoid. In addition to  
449 recording photons from the reflected signal, the ATLAS instrument will detect  
450 background photons from sunlight which are continually entering the telescope. A  
451 primary objective of the ICESat-2 data processing software is to correctly  
452 discriminate between signal photons and background photons. Some of this  
453 processing occurs at the ATL03 level and some of it also occurs within the software  
454 for ATL08. At ATL03, this discrimination is done through a series of three steps of  
455 progressively finer resolution with some processing occurring onboard the satellite  
456 prior to downlink of the raw data. The ATL03 data product produces a classification  
457 between signal and background (i.e. noise) photons, and further discussion on that  
458 classification process can be read in the ATL03 ATBD. In addition, not all geophysical  
459 corrections (e.g. ocean tide) are applied to the position of the individual geolocated  
460 photons at the ATL03 level, but they are provided on the ATL03 data product if there

461 exists a need to apply them. Thus, in general, all of the heights processed in the ATL08  
462 algorithm consists of the ATL03 heights with respect to the WGS-84 ellipsoid, with  
463 geophysical corrections applied, as specified in Chapter 6 of the ATL03 ATBD.

464

### 465 **1.5 Accuracy Expected from ATLAS**

466 There are a variety of elements that contribute to the elevation accuracy that  
467 are expected from ATLAS and the derived data products. Elevation accuracy is a  
468 composite of ranging precision of the instrument, radial orbital uncertainty,  
469 geolocation knowledge, forward scattering in the atmosphere, and tropospheric path  
470 delay uncertainty. The ranging precision seen by ATLAS will be a function of the laser  
471 pulse width, the surface area potentially illuminated by the laser, and uncertainty in  
472 the timing electronics. The requirement on radial orbital uncertainty is specified to  
473 be less than 4 cm and tropospheric path delay uncertainty is estimated to be 3 cm. In  
474 the case of ATLAS, the ranging precision for flat surfaces, is expected to have a  
475 standard deviation of approximately 25 cm. The composite of each of the errors can  
476 also be thought of as the spread of photons about a surface (see Figure 1.4) and is  
477 referred to as the point spread function or Znoise.



478

479 Figure 1.4. Illustration of the point spread function, also referred to as Znoise, for a series  
480 of photons about a surface.

481 The estimates of  $\sigma_{orbit}$ ,  $\sigma_{troposphere}$ ,  $\sigma_{forwardscattering}$ ,  $\sigma_{pointing}$ , and  $\sigma_{timing}$   
482 for a photon will be represented on the ATL03 data product as the final geolocated  
483 accuracy in the X, Y, and Z (or height) direction. In reality, these parameters have  
484 different temporal and spatial scales, however until ICESat-2 is on orbit, it is uncertain  
485 how these parameters will vary over time. As such, Equation 1.1 may change once the

486 temporal aspects of these parameters are better understood. For a preliminary  
 487 quantification of the uncertainties, Equation 1.1 is valid to incorporate the instrument  
 488 related factors.

$$489 \quad \sigma_Z = \sqrt{\sigma_{Orbit}^2 + \sigma_{trop}^2 + \sigma_{forwardscattering}^2 + \sigma_{pointing}^2 + \sigma_{timing}^2} \quad \text{Eqn. 1.1}$$

490

491 Although  $\sigma_Z$  on the ATL03 product represents the best understanding of the  
 492 uncertainty for each geolocated photon, it does not incorporate the uncertainty  
 493 associated with local slope of the topography. The slope component to the geolocation  
 494 uncertainty is a function of both the geolocation knowledge of the pointing (which is  
 495 required to be less than 6.5 m) multiplied by the tangent of the surface slope. In a case  
 496 of flat topography ( $\leq 1$  degree slope),  $\sigma_Z \leq 25$  cm, whereas in the case of a 10 degree  
 497 surface slope,  $\sigma_Z = 119$  cm. The uncertainty associated with the local slope will be  
 498 combined with  $\sigma_Z$  to produce the term  $\sigma_{AtlasLand}$ .

$$499 \quad \sigma_{AtlasLand} = \sqrt{\sigma_Z^2 + \sigma_{topo}^2} \quad \text{Eqn. 1.2}$$

$$500 \quad \sigma_{topo} = \sigma_{topo} = \sqrt{(6.5 \tan(\theta_{surfaceslope}))^2} \quad \text{Eqn. 1.3}$$

501 Ultimately, the uncertainty that will be reported on the data product ATL08  
 502 will include the  $\sigma_{AtlasLand}$  term and the local rms values of heights computed within  
 503 each data parameter segment. For example, calculations of terrain height will be  
 504 made on photons classified as terrain photons (this process is described in the  
 505 following sections). The uncertainty of the terrain height for a segment is described  
 506 in Equation 1.4, where the root mean square term of  $\sigma_{AtlasLand}$  and rms of terrain  
 507 heights are normalized by the number of terrain photons for that given segment.

$$508 \quad \sigma_{ATL08segment} = \sqrt{\sigma_{AtlasLand}^2 + \sigma_{Zrmssegmentclass}^2} \quad \text{Eqn. 1.4}$$

509

510 **1.6 Additional Potential Height Errors from ATLAS**

511 Some additional potential height errors in the ATL08 terrain and vegetation  
512 product can come from a variety of sources including:

- 513 a. Vertical sampling error. ATLAS height estimates are based on a  
514 random sampling of the surface height distribution. Photons may  
515 be reflected from anywhere within the PDF of the reflecting surface;  
516 more specifically, anywhere from within the canopy. A detailed  
517 look at the potential effect of vertical sampling error is provided in  
518 Neuenschwander and Magruder (2016).
- 519 b. Background noise. Random noise photons are mixed with the  
520 signal photons so classified photons will include random outliers.
- 521 c. Complex topography. The along-track product may not always  
522 represent complex surfaces, particularly if the density of ground  
523 photons does not support an accurate representation.
- 524 d. Vegetation. Dense vegetation may preclude reflected photon  
525 events from reaching the underlying ground surface. An incorrect  
526 estimation of the underlying ground surface will subsequently lead  
527 to an incorrect canopy height determination.
- 528 e. Misidentified photons. The product from ATL03 combined with  
529 additional noise filtering may not identify the correct photons as  
530 signal photons.

531

532 **1.7 Dense Canopy Cases**

533 Although the height accuracy produced from ICESat-2 is anticipated to be  
534 superior to other global height products (e.g. SRTM), for certain biomes photon  
535 counting lidar data as it will be collected by the ATLAS instrument present a challenge  
536 for extracting both the terrain and canopy heights, particularly for areas of dense

537 vegetation. Due to the relatively low laser power, we anticipate that the along-track  
538 signal from ATLAS may lose ground signal under dense forest (e.g. >96% canopy  
539 closure) and in situations where cloud cover obscures the terrestrial signal. In areas  
540 having dense vegetation, it is likely that only a handful of photons will be returned  
541 from the ground surface with the majority of reflections occurring from the canopy.  
542 A possible source of error can occur with both the canopy height estimates and the  
543 terrain heights if the vegetation is particularly dense and the ground photons were  
544 not correctly identified.

545

### 546 **1.8 *Sparse Canopy Cases***

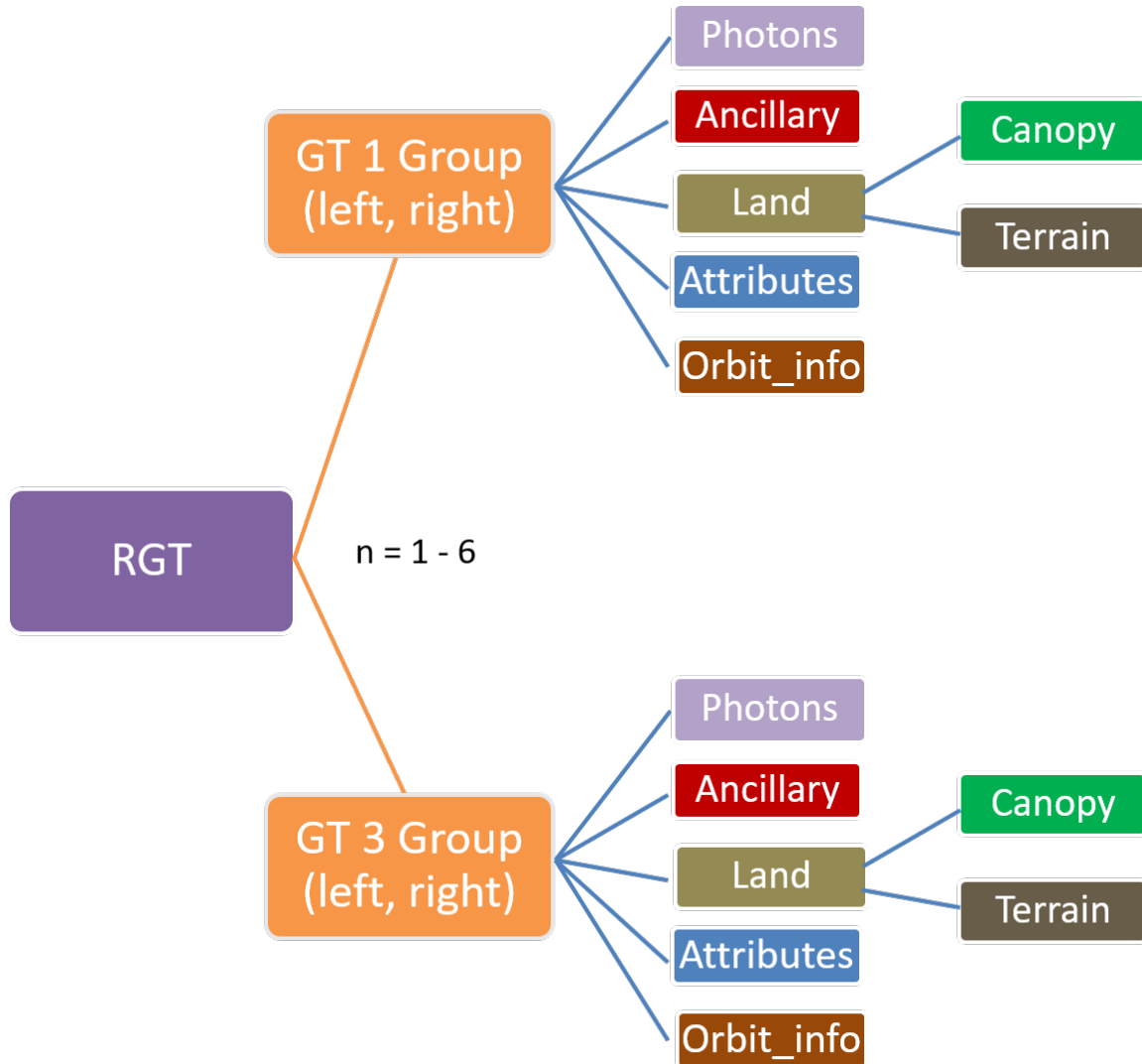
547 Conversely, sparse canopy cases also pose a challenge to vegetation height  
548 retrievals. In these cases, expected reflected photon events from sparse trees or  
549 shrubs may be difficult to discriminate between solar background noise photons. The  
550 algorithms being developed for ATL08 operate under the assumption that signal  
551 photons are close together and noise photons will be more isolated in nature. Thus,  
552 signal (in this case canopy) photons may be incorrectly identified as solar background  
553 noise on the data product. Due to the nature of the photon counting processing,  
554 canopy photons identified in areas that have extremely low canopy cover <15% will  
555 be filtered out and reassigned as noise photons.

556

## 557 **2. ATL08: DATA PRODUCT**

558           The ATL08 product will provide estimates of terrain height, canopy height,  
559 and canopy cover at fine spatial scales in the along-track direction. In accordance with  
560 the HDF-driven structure of the ICESat-2 products, the ATL08 product will  
561 characterize each of the six Ground Tracks (GT) associated with each Reference  
562 Ground Track (RGT) for each cycle and orbit number. Each ground track group has a  
563 distinct beam number, distance from the reference track, and transmit energy  
564 strength, and all beams will be processed independently using the same sequence of  
565 steps described within ATL08. Each ground track group (GT) on the ATL08 product  
566 contains subgroups for land and canopy heights segments as well as beam and  
567 reference parameters useful in the ATL08 processing. In addition, the labeled photons  
568 that are used to determine the data parameters will be indexed back to the ATL03  
569 products such that they are available for further, independent analysis. A layout of  
570 the ATL08 HDF product is shown in Figure 2.1. The six GTs are numbered from left to  
571 right, regardless of satellite orientation.





572

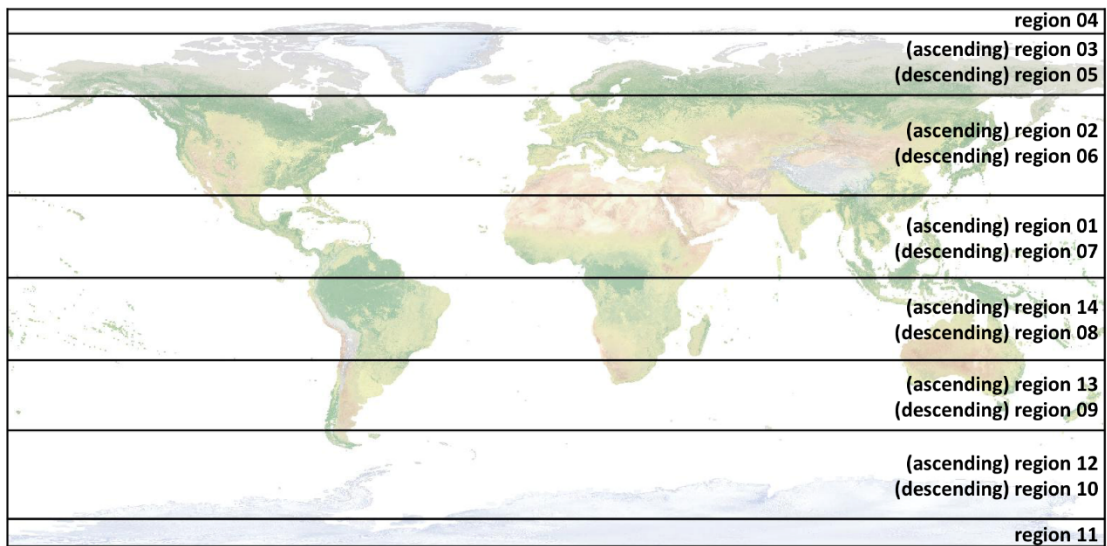
573 Figure 2.1. HDF5 data structure for ATL08 products

574

575 For each data parameter, terrain surface elevation and canopy heights will be  
 576 provided at a fixed segment size of 100 meters along the ground track. Based on the  
 577 satellite velocity and the expected number of reflected photons for land surfaces, each  
 578 segment should have more than 100 signal photons, but in some instances there may  
 579 be less than 100 signal photons per segment. If a segment has less than 50 classed  
 580 (i.e., labeled by ATL08 as ground, canopy, or top of canopy) photons we feel this  
 581 would not accurately represent the surface. Thus, an invalid value will be reported in

582 all height fields. In the event that there are more than 50 classed photons, but a terrain  
 583 height cannot be determined due to an insufficient number of ground photons, (e.g.  
 584 lack of photons penetrating through dense canopy), the only reported terrain height  
 585 will be the interpolated surface height.

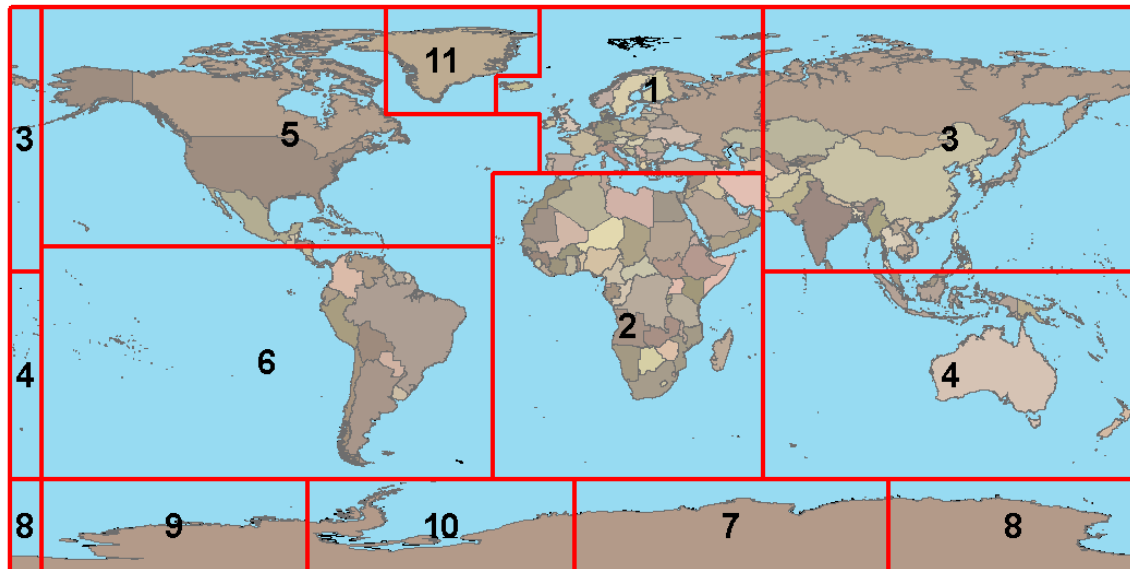
586 The ATL08 product will be produced per granule based on the ATL03 defined  
 587 regions (see Figure 2.2). Thus, the ATL08 file/name convention scheme will match  
 588 the file/naming convention for ATL03 –in attempt for reducing complexity to allow  
 589 users to examine both data products.



590

591 Figure 2.2. ATL03 granule regions; graphic from ATL03 ATBD (Neumann et al.).

592 The ATL08 product additionally has its own internal regions, which are  
 593 roughly assigned by continent, as shown by Figure 2.3. For the regions covering  
 594 Antarctica (regions 7, 8, 9, 10) and Greenland (region 11), the ATL08 algorithm will  
 595 assume that no canopy is present. These internal ATL08 regions will be noted in the  
 596 ATL08 product (see parameter atl08\_region in Section 2.4.22). Note that the regions  
 597 for each ICESat-2 product are not the same.



598

599 Figure 2.3. ATL08 product regions.

600

601 **2.1 Subgroup: Land Parameters**

602 ATL08 terrain height parameters are defined in terms of the absolute height  
 603 above the reference ellipsoid.

604 Table 2.1. Summary table of land parameters on ATL08.

Group	Data type	Description	Source
<b>segment_id_beg</b>	Integer	First along-track segment_id number in 100-m segment	ATL03
<b>segment_id_end</b>	Integer	Last along-track segment_id number in 100-m segment	ATL03
<b>h_te_mean</b>	Float	Mean terrain height for segment	computed
<b>h_te_median</b>	Float	Median terrain height for segment	computed
<b>h_te_min</b>	Float	Minimum terrain height for segment	computed
<b>h_te_max</b>	Float	Maximum terrain height for segment	computed
<b>h_te_mode</b>	Float	Mode of terrain height for segment	computed
<b>h_te_skew</b>	Float	Skew of terrain height for segment	computed

<b>n_te_photons</b>	Integer	Number of ground photons in segment	computed
<b>h_te_interp</b>	Float	Interpolated terrain surface height at mid-point of segment	computed
<b>h_te_std</b>	Float	Standard deviation of ground heights about the interpolated ground surface	computed
<b>h_te_uncertainty</b>	Float	Uncertainty of ground height estimates. Includes all known uncertainties such as geolocation, pointing angle, timing, radial orbit errors, etc.	computed from Equation 1.4
<b>terrain_slope</b>	Float	Slope of terrain within segment	computed
<b>h_te_best_fit</b>	Float	Best fit terrain elevation at the 100 m segment mid-point location	computed
<b>h_te_best_fit_20m</b>	Float	Best fit terrain elevation at the 20 m geosegment mid-point location	computed
<b>h_te_rh25</b>	float	The relative height from classified canopy photons are sorted into a cumulative distribution, and the height associated with the 98% height above the h_te_bestfit for that segment is reported.	computed
<b>subset_te_flag</b>	Integer	Quality flag indicating the terrain photons populating the 100 m segment statistics are derived from less than 100 m worth of photons	computed
<b>photon_rate_te</b>	Float	Calculated photon rate for ground photons within each segment	computed

605

606 **2.1.1** Georeferenced\_segment\_number\_beg

607 (parameter = segment\_id\_beg). The first along-track segment\_id in each 100-m  
608 segment. Each 100-m segment consists of five sequential 20-m segments provided  
609 from the ATL03 product, which are labeled as segment\_id. The segment\_id is a seven  
610 digit number that uniquely identifies each along track segment, and is written at the  
611 along-track geolocation segment rate (i.e. ~20m along track). The four digit RGT

612 number can be combined with the seven digit segment\_id number to uniquely define  
613 any along-track segment number. Values are sequential, with 0000001 referring to  
614 the first segment after the equatorial crossing of the ascending node.

615 **2.1.2 Georeferenced\_segment\_number\_end**

616 (parameter = segment\_id\_end). The last along-track segment\_id in each 100-m  
617 segment. Each 100-m segment consists of five sequential 20-m segments provided  
618 from the ATL03 product, which are labeled as segment\_id. The segment\_id is a seven  
619 digit number that uniquely identifies each along track segment, and is written at the  
620 along-track geolocation segment rate (i.e. ~20m along track). The four digit RGT  
621 number can be combined with the seven digit segment\_id number to uniquely define  
622 any along-track segment number. Values are sequential, with 0000001 referring to  
623 the first segment after the equatorial crossing of the ascending node.

624 **2.1.3 Segment\_terrain\_height\_mean**

625 (parameter = h\_te\_mean). Estimated mean of the terrain height above the  
626 reference ellipsoid derived from classified ground photons within the 100 m segment.  
627 If a terrain height cannot be directly determined within the segment (i.e. there are not  
628 a sufficient number of ground photons), only the interpolated terrain height will be  
629 reported. Required input data is classified point cloud (i.e. photons labeled as either  
630 canopy or ground in the ATL08 processing). This parameter will be derived from only  
631 classified ground photons.

632 **2.1.4 Segment\_terrain\_height\_med**

633 (parameter = h\_te\_median). Median terrain height above the reference  
634 ellipsoid derived from the classified ground photons within the 100 m segment. If  
635 there are not a sufficient number of ground photons, an invalid value will be reported  
636 –no interpolation will be done. Required input data is classified point cloud (i.e.  
637 photons labeled as either canopy or ground in the ATL08 processing). This parameter  
638 will be derived from only classified ground photons.

639           **2.1.5** Segment\_terrain\_height\_min

640           (parameter = h\_te\_min). Minimum terrain height above the reference ellipsoid  
641 derived from the classified ground photons within the 100 m segment. If there are  
642 not a sufficient number of ground photons, an invalid value will be reported –no  
643 interpolation will be done. Required input data is classified point cloud (i.e. photons  
644 labeled as either canopy or ground in the ATL08 processing). This parameter will be  
645 derived from only classified ground photons.

646           **2.1.6** Segment\_terrain\_height\_max

647           (parameter = h\_te\_max). Maximum terrain height above the reference  
648 ellipsoid derived from the classified ground photons within the 100 m segment. If  
649 there are not a sufficient number of ground photons, an invalid value will be reported  
650 –no interpolation will be done. Required input data is classified point cloud (i.e.  
651 photons labeled as either canopy or ground in the ATL08 processing). This parameter  
652 will be derived from only classified ground photons.

653           **2.1.7** Segment\_terrain\_height\_mode

654           (parameter = h\_te\_mode). Mode of the classified ground photon heights above  
655 the reference ellipsoid within the 100 m segment. If there are not a sufficient number  
656 of ground photons, an invalid value will be reported –no interpolation will be done.  
657 Required input data is classified point cloud (i.e. photons labeled as either canopy or  
658 ground in the ATL08 processing). This parameter will be derived from only classified  
659 ground photons.

660           **2.1.8** Segment\_terrain\_height\_skew

661           (parameter = h\_te\_skew). The skew of the classified ground photons within the  
662 100 m segment. If there are not a sufficient number of ground photons, an invalid  
663 value will be reported –no interpolation will be done. Required input data is classified  
664 point cloud (i.e. photons labeled as either canopy or ground in the ATL08 processing).  
665 This parameter will be derived from only classified ground photons.

666           **2.1.9** Segment\_number\_terrain\_photons  
667           (parameter = n\_te\_photons). Number of terrain photons identified in segment.

668           **2.1.10** Segment\_height\_interp  
669           (parameter = h\_te\_interp). Interpolated terrain surface height above the  
670 reference ellipsoid from ATL08 processing at the mid-point of each segment. This  
671 interpolated surface is the FINALGROUND estimate (described in section 4.9).

672           **2.1.11** Segment\_h\_te\_std  
673           (parameter = h\_te\_std). Standard deviations of terrain points about the  
674 interpolated ground surface within the segment. Provides an indication of surface  
675 roughness.

676           **2.1.12** Segment\_terrain\_height\_uncertainty  
677           (parameter = h\_te\_uncertainty). Uncertainty of the mean terrain height for the  
678 segment. This uncertainty incorporates all systematic uncertainties (e.g. timing,  
679 orbits, geolocation, etc.) as well as uncertainty from errors of identified photons. This  
680 parameter is described in Section 1, Equation 1.4. If there are not a sufficient number  
681 of ground photons, an invalid value will be reported –no interpolation will be done.  
682 Required input data is classified point cloud (i.e. photons labeled as either canopy or  
683 ground in the ATL08 processing). This parameter will be derived from only classified  
684 ground photons. The  $\sigma_{segmentclass}$  term in Equation 1.4 represents the standard  
685 deviation of the terrain height residuals about the FINALGROUND estimate.

686           **2.1.13** Segment\_terrain\_slope  
687           (parameter = terrain\_slope). Slope of terrain within each segment. Slope is  
688 computed from a linear fit of the terrain photons. It estimates the rise [m] in relief  
689 over each segment [100 m]; e.g., if the slope value is 0.04, there is a 4 m rise over the  
690 100 m segment. Required input data are the classified terrain photons.





717 inform the user that, in this example, the 100 m estimate are being derived from only  
718 40 m worth of data.

#### 719 **2.1.17 Segment Terrain Photon Rate**

720 (parameter = photon\_rate\_te). This value indicates the terrain photon rate  
721 within each ATL08 segment. This value is calculated as the total number of terrain  
722 photons divided by the total number of laser shots within each ATL08 segment. The  
723 number of laser shots is defined as the number of unique Delta\_Time values within  
724 each segment.

#### 725 **2.1.18 Terrain Best Fit GeoSegment {1:5}**

726 (parameter = h\_te\_best\_fit\_20m). The best fit terrain elevation at the mid-point  
727 location of each 20 m geosegment. The mid-segment terrain elevation is determined  
728 by selecting the best of three fits – linear, 3<sup>rd</sup> order and 4<sup>th</sup> order polynomials – to the  
729 terrain photons and interpolating the elevation at each 20 m along a 100 m segment.  
730 For the linear fit, a slope correction and weighting is applied to each ground photon  
731 based on the distance to the slope height at the center of the segment. For segments  
732 that do not have a sufficient number of photons, an invalid (or fill) value will be  
733 reported. Each 20 m geo-segment shall have 10 signal photons as a minimum number  
734 to be used for calculations and a minimum of 3 terrain photons are required to  
735 estimate a height.

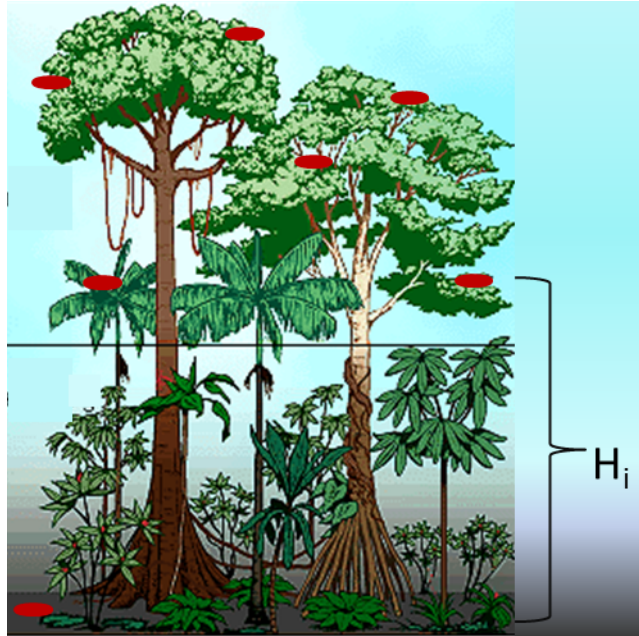
736

### 737 **2.2 Subgroup: Vegetation Parameters**

738 Canopy parameters will be reported on the ATL08 data product in terms of both  
739 the absolute height above the reference ellipsoid as well as the relative height above  
740 an estimated ground. The relative canopy height,  $H_i$ , is computed as the height from  
741 an identified canopy photon minus the interpolated ground surface for the same  
742 horizontal geolocation (see Figure 2.3). Thus, each identified signal photon above an  
743 interpolated surface (including a buffer distance based on the instrument point  
744 spread function) is by default considered a canopy photon. Canopy parameters will

745 only be computed for segments where more than 5% of the classed photons are  
 746 classified as canopy photons.

747



748

749 Figure 2.4. Illustration of canopy photons (red dots) interaction in a vegetated area.  
 750 Relative canopy heights,  $H_i$ , are computed by differencing the canopy photon height from  
 751 an interpolated terrain surface.

752 Table 2.2. Summary table of canopy parameters on ATL08.

Group	Data type	Description	Source
<b>segment_id_beg</b>	Integer	First along-track segment_id number in 100-m segment	ATL03
<b>segment_id_end</b>	Integer	Last along-track segment_id number in 100-m segment	ATL03
<b>canopy_h_metrics_abs</b>	Float	Absolute (H##) canopy height metrics calculated at the following percentiles: 5, 10, 15, 20, 25, 30, 35, 40, 45, 50, 55, 60, 65, 70, 75, 80, 85, 90, 95.	computed
<b>canopy_h_metrics</b>	Float	Relative (RH##) canopy height metrics calculated at the following percentiles: 5, 10, 15, 20, 25, 30, 35, 40, 45, 50, 55, 60, 65, 70, 75, 80, 85, 90, 95.	computed

<b>h_canopy_abs</b>	Float	98% height of all the individual absolute canopy heights (height above WGS84 ellipsoid) for segment.	computed
<b>h_canopy</b>	Float	98% height of all the individual relative canopy heights (height above terrain) for segment.	computed
<b>h_canopy_20m</b>	Float	98% height of all the individual relative canopy heights (height above terrain) for 20m geosegment.	
<b>h_mean_canopy_abs</b>	Float	Mean of individual absolute canopy heights within segment	computed
<b>h_mean_canopy</b>	Float	Mean of individual relative canopy heights within segment	computed
<b>h_dif_canopy</b>	Float	Difference between h_canopy and canopy_h_metrics(50)	computed
<b>h_min_canopy_abs</b>	Float	Minimum of individual absolute canopy heights within segment	computed
<b>h_min_canopy</b>	Float	Minimum of individual relative canopy heights within segment	computed
<b>h_max_canopy_abs</b>	Float	Maximum of individual absolute canopy heights within segment. Should be equivalent to H100	computed
<b>h_max_canopy</b>	Float	Maximum of individual relative canopy heights within segment. Should be equivalent to RH100	computed
<b>h_canopy_uncertainty</b>	Float	Uncertainty of the relative canopy height (h_canopy)	computed
<b>canopy_openness</b>	Float	STD of relative heights for all photons classified as canopy photons within the segment to provide inference of canopy openness	computed
<b>toc_roughness</b>	Float	STD of relative heights of all photons classified as top of canopy within the segment	computed
<b>h_canopy_quad</b>	Float	Quadratic mean canopy height	computed
<b>n_ca_photons</b>	Integer4	Number of canopy photons within 100 m segment	computed
<b>n_toc_photons</b>	Integer4	Number of top of canopy photons within 100 m segment	computed
<b>centroid_height</b>	Float	Absolute height above reference ellipsoid associated with the centroid of all signal photons	computed
<b>canopy_rh_conf</b>	Integer	Canopy relative height confidence flag based on percentage of ground and canopy photons within a segment: 0 (<5% canopy), 1 (>5% canopy, <5% ground), 2 (>5% canopy, >5% ground)	computed

<b>subset_can_flag</b>	Integer	Quality flag indicating the canopy photons populating the 100 m segment statistics are derived from less than 100 m worth of photons	computed
<b>photon_rate_can</b>	Float	Photon rate of canopy photons within each 100 m segment	computed

753

754 **2.2.1 Georeferenced\_segment\_number\_beg**

755 (parameter = segment\_id\_beg). The first along-track segment\_id in each 100-m  
756 segment. Each 100-m segment consists of five sequential 20-m segments provided  
757 from the ATL03 product, which are labeled as segment\_id. The segment\_id is a seven  
758 digit number that uniquely identifies each along track segment, and is written at the  
759 along-track geolocation segment rate (i.e. ~20m along track). The four digit RGT  
760 number can be combined with the seven digit segment\_id number to uniquely define  
761 any along-track segment number. Values are sequential, with 0000001 referring to  
762 the first segment after the equatorial crossing of the ascending node.

763 **2.2.2 Georeferenced\_segment\_number\_end**

764 (parameter = segment\_id\_end). The last along-track segment\_id in each 100-m  
765 segment. Each 100-m segment consists of five sequential 20-m segments provided  
766 from the ATL03 product, which are labeled as segment\_id. The segment\_id is a seven  
767 digit number that uniquely identifies each along track segment, and is written at the  
768 along-track geolocation segment rate (i.e. ~20m along track). The four digit RGT  
769 number can be combined with the seven digit segment\_id number to uniquely define  
770 any along-track segment number. Values are sequential, with 0000001 referring to  
771 the first segment after the equatorial crossing of the ascending node.

772 **2.2.3 Canopy\_height\_metrics\_abs**

773 (parameter = canopy\_h\_metrics\_abs). The absolute height metrics (H##) of  
774 classified canopy photons (labels 2 and 3) above the ellipsoid. The height metrics are  
775 sorted based on a cumulative distribution and calculated at the following percentiles:  
776 10, 15, 20, 25, 30, 35, 40, 45, 50, 55, 60, 65, 70, 75, 80, 85, 90, 95. These height metrics

777 are often used in the literature to characterize vertical structure of vegetation. One  
778 important distinction of these canopy height metrics compared to those derived from  
779 other lidar systems (e.g., LVIS or GEDI) is that the ICESat-2 canopy height metrics are  
780 heights above the ground surface. These metrics do not include the ground photons.  
781 Required input data are the relative canopy heights of all canopy photons above the  
782 estimated terrain surface and the mid-segment elevation. The absolute canopy  
783 heights metrics are determined by adding the relative canopy height metric to the  
784 best-fit terrain (`h_te_bestfit`). For cases where the `h_te_bestfit` is invalid, the  
785 cumulative distribution will be calculated for the absolute canopy heights (not the  
786 relative canopy heights) and those cumulative heights will be reported.

787

#### 788 **2.2.4** `Canopy_height_metrics`

789 (`parameter = canopy_h_metrics`). Relative height metrics above the estimated  
790 terrain surface (`RH##`) of classified canopy photons (labels 2 and 3). The height  
791 metrics are sorted based on a cumulative distribution and calculated at the following  
792 percentiles: 10, 15, 20, 25, 30, 35, 40, 45, 50, 55, 60, 65, 70, 75, 80, 85, 90, 95. These  
793 height metrics are often used in the literature to characterize vertical structure of  
794 vegetation. One important distinction of these canopy height metrics compared to  
795 those derived from other lidar systems (e.g., LVIS or GEDI) is that the ICESat-2 canopy  
796 height metrics are heights above the ground surface. These metrics do not include the  
797 ground photons. Required input data are relative canopy heights above the estimated  
798 terrain surface for all canopy photons.

#### 799 **2.2.5** `Absolute_segment_canopy_height`

800 (`parameter = h_canopy_abs`). The absolute 98% height of classified canopy  
801 photon heights (labels 2 and 3) above the ellipsoid. The relative height from classified  
802 canopy photons are sorted into a cumulative distribution, and the height associated  
803 with the 98% height above the `h_te_bestfit` for that segment is reported. For cases

804 where the `h_te_bestfit` is invalid, the cumulative distribution will be calculated for the  
805 absolute canopy heights and the 98% absolute height will be reported.

#### 806 **2.2.6** `Segment_canopy_height`

807 (parameter = `h_canopy`). The relative 98% height of classified canopy photon  
808 heights (labels 2 and 3) above the estimated terrain surface. Relative canopy heights  
809 have been computed by differencing the canopy photon height from the estimated  
810 terrain surface in the ATL08 processing. The relative canopy heights are sorted into  
811 a cumulative distribution, and the height associated with the 98% height is reported.

#### 812 **2.2.7** `canopy_height GeoSegment {1:5}`

813 (parameter = `h_canopy_20m`). The relative 98% height of classified canopy  
814 photon heights (labels 2 and 3) above the estimated terrain surface in each 20 m  
815 geosegment. Relative canopy heights have been computed by differencing the canopy  
816 photon height from the estimated terrain surface in the ATL08 processing. The  
817 relative canopy heights are sorted into a cumulative distribution, and the height  
818 associated with the 98% height is reported. For segments that do not have a sufficient  
819 number of photons, an invalid (or fill) value will be reported. Each 20 m geo-segment  
820 shall have 10 signal photons as a minimum number to be used for calculations and a  
821 minimum of 3 canopy photons are required to estimate a height.

822

823

#### 824 **2.2.8** `Absolute_segment_mean_canopy`

825 (parameter = `h_mean_canopy_abs`). The absolute mean canopy height for the  
826 segment. relative canopy heights are the photons heights for canopy photons (labels  
827 2 and 3) above the estimated terrain surface. These relative heights are averaged and  
828 then added to `h_te_bestfit`.

829           **2.2.9** Segment\_mean\_canopy

830           (parameter = h\_mean\_canopy). The mean canopy height for the segment.  
831 Relative canopy heights have been computed by differencing the canopy photon  
832 height (labels 2 and 3) from the estimated terrain surface in the ATL08 processing.  
833 These heights are averaged.

834           **2.2.10** Segment\_dif\_canopy

835           (parameter = h\_dif\_canopy). Difference between h\_canopy and  
836 canopy\_h\_metrics(50). This parameter is one metric used to describe the vertical  
837 distribution of the canopy within the segment.

838           **2.2.11** Absolute\_segment\_min\_canopy

839           (parameter = h\_min\_canopy\_abs). The minimum absolute canopy height for  
840 the segment. Relative canopy heights are the photons heights for canopy photons  
841 (labels 2 and 3) above the estimated terrain surface. Required input data is classified  
842 point cloud (i.e. photons labeled as either canopy or ground in the ATL08 processing).  
843 The minimum relative canopy height for each segment is added to h\_te\_bestfit and  
844 reported as the absolute minimum canopy height.

845           **2.2.12** Segment\_min\_canopy

846           (parameter = h\_min\_canopy). The minimum relative canopy height for the  
847 segment. Canopy heights are the photons heights for canopy photons (labels 2 and 3)  
848 differenced from the estimated terrain surface. Required input data is classified point  
849 cloud (i.e. photons labeled as either canopy or ground in the ATL08 processing).

850           **2.2.13** Absolute\_segment\_max\_canopy

851           (parameter = h\_max\_canopy\_abs). The maximum absolute canopy height for  
852 the segment. This parameter is equivalent to H100 metric reported in the literature.  
853 This parameter, however, has the potential for error as random solar background  
854 noise may not have been fully rejected. It is recommended that h\_canopy or  
855 h\_canopy\_abs (i.e., the 98% canopy height) be considered as the top of canopy

856 measurement. Required input data is classified point cloud (i.e. photons labeled as  
 857 either canopy or ground in the ATL08 processing). The absolute max canopy height  
 858 is the maximum relative canopy height added to `h_te_bestfit`.

859 **2.2.14 Segment\_max\_canopy**

860 (parameter = `h_max_canopy`). The maximum relative canopy height for the  
 861 segment. Canopy heights are the photons heights for canopy photons (labels 2 and 3)  
 862 differenced from the estimated terrain surface. This product is equivalent to RH100  
 863 metric reported in the literature. This parameter, however, has the potential for error  
 864 as random solar background noise may not have been fully rejected. It is  
 865 recommended that `h_canopy` or `h_canopy_abs` (i.e., the 98% canopy height) be  
 866 considered as the top of canopy measurement. Required input data is classified point  
 867 cloud (i.e. photons labeled as either canopy or ground in the ATL08 processing).

868 **2.2.15 Segment\_canopy\_height\_uncertainty**

869 (parameter = `h_canopy_uncertainty`). Uncertainty of the relative canopy  
 870 height for the segment. This uncertainty incorporates all systematic uncertainties  
 871 (e.g. timing, orbits, geolocation, etc.) as well as uncertainty from errors of identified  
 872 photons. This parameter is described in Section 1, Equation 1.4. If there are not a  
 873 sufficient number of ground photons, an invalid value will be reported –no  
 874 interpolation will be done. In the case for canopy height uncertainty, the parameter  
 875  $\sigma_{segmentclass}$  is comprised of both the terrain uncertainty within the segment but also  
 876 the top of canopy residuals. Required input data is classified point cloud (i.e. photons  
 877 labeled as either top of canopy or ground in the ATL08 processing). This parameter  
 878 will be derived from only classified top of canopy photons, label = 3. The canopy  
 879 height uncertainty is derived from Equation 1.4, shown below as Equation 1.5,  
 880 represents the standard deviation of the terrain points and the standard deviation of  
 881 the top of canopy height photons.

882 
$$\sigma_{ATL08_{segment\_ch}} = \frac{\sqrt{\sigma_{AtlasLand}^2 + \sigma_{Zrms_{segment\_terrain}}^2 + \sigma_{Zrms_{segment\_toc}}^2}}{n_{photons_{segment\_terrain}} + n_{photons_{segment\_toc}}} \quad \text{Eqn 1.5}$$



883

884 **2.2.16 Segment\_canopy\_openness**

885 (parameter = canopy\_openness). Standard deviation of relative canopy  
886 heights within each segment. This parameter will potentially provide an indicator of  
887 canopy openness (label = 2 and 3) as a greater standard deviation of heights indicates  
888 greater penetration of the laser energy into the canopy. Required input data is  
889 classified point cloud (i.e. photons labeled as either canopy or ground in the ATL08  
890 processing).

891 **2.2.17 Segment\_top\_of\_canopy\_roughness**

892 (parameter = toc\_roughness). Standard deviation of relative top of canopy  
893 heights (label = 3) within each segment. This parameter will potentially provide an  
894 indicator of canopy variability. Required input data is classified point cloud (i.e.  
895 photons labeled as the top of the canopy in the ATL08 processing).

896 **2.2.18 Segment\_canopy\_quadratic\_height**

897 (parameter = h\_canopy\_quad). The quadratic mean relative height of relative  
898 canopy heights. The quadratic mean height is computed as:

899 
$$qmh = \sqrt{\sum_{i=1}^{n_{ca\_photons}} \frac{h_i^2}{n_{ca\_photons}}}$$

900 **2.2.19 Segment\_number\_canopy\_photons**

901 (parameter = n\_ca\_photons). Number of canopy photons (label = 2) within  
902 each segment. Required input data is classified point cloud (i.e. photons labeled as  
903 either canopy or ground in the ATL08 processing). This parameter does not include  
904 the top of canopy photons. To determine the total number of canopy photons, add  
905 n\_ca\_photons to n\_toc\_photons within each segment.

906 **2.2.20** Segment\_number\_top\_canopy\_photons

907 (parameter = n\_toc\_photons). Number of top of canopy photons (label = 3)  
908 within each segment. Required input data is classified point cloud (i.e. photons  
909 labeled as top of canopy in the ATL08 processing). To determine the total number of  
910 canopy photons, add n\_ca\_photons to n\_toc\_photons within each segment.

911 **2.2.21** Centroid\_height

912 (parameter = centroid\_height). Optical centroid of all photons classified as  
913 either canopy or ground points (label = 1 2 or 3) within a segment. The heights used  
914 in this calculation are absolute heights above the reference ellipsoid. This parameter  
915 is equivalent to the centroid height produced on ICESat GLA14.

916 **2.2.22** Segment\_rel\_canopy\_conf

917 (parameter = canopy\_rh\_conf). Canopy relative height confidence flag based  
918 on percentage of ground photons and percentage of canopy photons (label 2 and 3),  
919 relative to the total classified (ground and canopy, label = 1 2 and 3) photons within  
920 a segment: 0 (<5% canopy), 1 (>5% canopy and <5% ground), 2 (>5% canopy and  
921 >5% ground). This is a measure based on the quantity, not the quality, of the  
922 classified photons in each segment.

923 **2.2.23** Subset\_can\_flag {1:5}

924 (parameter = subset\_can\_flag). This flag indicates the distribution of identified  
925 canopy photons (label 2 and 3) within each 100 m. The purpose of this flag is to  
926 provide the user with an indication whether the photons contributing to the canopy  
927 height estimates are evenly distributed or only partially distributed (i.e. due to cloud  
928 cover or signal attenuation). A 100 m ATL08 segment is comprised of 5 geo-segments.  
929 subset\_can\_flags:

930 -1: no data within geosegment available for analysis

931 0: indicates no canopy photons within geosegment

932 1: indicates canopy photons within geosegment

933 For example, a 100 m ATL08 segment might have the following  
934 subset\_can\_flags: {-1 -1 -1 1 1} which would translate that no photons (canopy or  
935 ground) were available for processing in the first three geosegments. Geosegment 4  
936 and 5 had valid labeled canopy photons. Again, the motivation behind this flag is to  
937 inform the user that, in this example, the 100 m estimate are being derived from only  
938 40 m worth of data.

939 **2.2.24 Segment Canopy Photon Rate**

940 (parameter = photon\_rate\_can). This value indicates the canopy photon rate  
941 within each ATL08 segment. This value is calculated as the total number of canopy  
942 photons (label =2 and 3) divided by the total number of unique laser shots within  
943 each ATL08 segment. The number of laser shots is defined as the number of unique  
944 Delta\_Time values within each segment.

945

946

947 **2.3 Subgroup: Photons**

948 The subgroup for photons contains the classified photons that were used to  
949 generate the parameters within the land or canopy subgroups. Each photon that is  
950 identified as being likely signal will be classified as: 0 = noise, 1 = ground, 2 = canopy,  
951 or 3 = top of canopy. The index values for each classified photon will be provided such  
952 that they can be extracted from the ATL03 data product for independent evaluation.

953 Table 2.3. Summary table for photon parameters for the ATL08 product.

Group	Data Type	Description	Source
classified_PC_indx	Float	Indices of photons tracking back to ATL03 that surface finding software identified and used within the creation of the data products.	ATL03

<b>classified_PC_flag</b>	Integer	Classification flag for each photon as either noise, ground, canopy, or top of canopy.	computed
<b>ph_segment_id</b>	Integer	Georeferenced bin number (20-m) associated with each photon	ATL03
<b>ph_h</b>	Float	Height of photon above interpolated ground surface	computed
<b>d_flag</b>	Integer	Flag indicating whether DRAGANN labeled the photon as noise or signal	computed

954

### 955       **2.3.1** Indices\_of\_classed\_photons

956       (parameter = `classified_PC_indx`). Indices of photons tracking back to ATL03 that  
957 surface finding software identified and used within the creation of the data products  
958 for a given segment.

### 959       **2.3.2** Photon\_class

960       (parameter = `classified_PC_flag`). Classification flags for a given segment. 0 =  
961 noise, 1 = ground, 2 = canopy, 3 = top of canopy. The final ground and canopy  
962 classification are flags 1-3. The full canopy is the combination of flags 2 and 3.

### 963       **2.3.3** Georeferenced\_segment\_number

964       (parameter = `ph_segment_id`). The `segment_id` associated with every photon in  
965 each 100-m segment. Each 100-m segment consists of five sequential 20-m segments  
966 provided from the ATL03 product, which are labeled as `segment_id`. The `segment_id`  
967 is a seven digit number that uniquely identifies each along track segment, and is  
968 written at the along-track geolocation segment rate (i.e. ~20m along track). The four  
969 digit RGT number can be combined with the seven digit `segment_id` number to  
970 uniquely define any along-track segment number. Values are sequential, with  
971 0000001 referring to the first segment after the equatorial crossing of the ascending  
972 node.

973           **2.3.4** Photon Height  
 974           (parameter = ph\_h). Height of the photon above the interpolated ground  
 975           surface at the location of the photon.

976           **2.3.5** DRAGANN\_flag  
 977           (parameter = d\_flag). Flag indicating the labeling of DRAGANN noise filtering for  
 978           a given photon. 0 = noise, 1=signal.

979

980   **2.4 Subgroup: Reference data**

981           The reference data subgroup contains parameters and information that are  
 982           useful for determining the terrain and canopy heights that are reported on the  
 983           product. In addition to position and timing information, these parameters include the  
 984           reference DEM height, reference landcover type, and flags indicating water or snow.

985   Table 2.4. Summary table for reference parameters for the ATL08 product.

Group	Data Type	Description	Source
<b>segment_id_beg</b>	Integer	First along-track segment_id number in 100-m segment	ATL03
<b>segment_id_end</b>	Integer	Last along-track segment_id number in 100-m segment	ATL03
<b>latitude</b>	Float	Center latitude of signal photons within each segment	ATL03
<b>longitude</b>	Float	Center longitude of signal photons within each segment	ATL03
<b>delta_time</b>	Float	Mid-segment GPS time in seconds past an epoch. The epoch is provided in the metadata at the file level	ATL03
<b>delta_time_beg</b>	Float	Delta time of the first photon in the segment	ATL03
<b>delta_time_end</b>	Float	Delta time of the last photon in the segment	ATL03
<b>night_flag</b>	Integer	Flag indicating whether the measurements were	computed

---

		acquired during night time conditions	
<b>dem_h</b>	Float4	Reference DEM elevation	external
<b>dem_flag</b>		Source of reference DEM	external
<b>dem_removal_flag</b>	Integer	Quality check flag to indicate > 20% photons removed due to large distance from dem_h	computed
<b>h_dif_ref</b>	Float4	Difference between h_te_median and dem_h	computed
<b>terrain_flg</b>	Integer	Terrain flag quality check to indicate a deviation from the reference DTM	computed
<b>segment_landcover</b>	Integer4	Reference landcover for segment derived from best global landcover product available	external
<b>segment_watermask</b>	Integer4	Water mask indicating inland water produced from best sources available	external
<b>segment_snowcover</b>	Integer4	Daily snow cover mask derived from best sources	external
<b>urban_flag</b>	Integer	Flag indicating segment is located in an urban area	external
<b>surf_type</b>	Integer1	Flags describing surface types: 0=not type, 1=is type. Order of array is land, ocean, sea ice, land ice, inland water.	ATL03
<b>atl08_region</b>	Integer	ATL08 region(s) encompassed by ATL03 granule being processed	computed
<b>last_seg_extend</b>	Float	The distance (km) that the last ATL08 processing segment in a file is either extended or overlapped with the previous ATL08 processing segment	computed
<b>brightness_flag</b>	Integer	Flag indicating that the ground surface is bright (e.g. snow-covered or other bright surfaces)	computed

---

987           **2.4.1** Georeferenced\_segment\_number\_beg

988           (parameter = segment\_id\_beg). The first along-track segment\_id in each 100-m  
989 segment. Each 100-m segment consists of five sequential 20-m segments provided  
990 from the ATL03 product, which are labeled as segment\_id. The segment\_id is a seven  
991 digit number that uniquely identifies each along track segment, and is written at the  
992 along-track geolocation segment rate (i.e. ~20m along track). The four digit RGT  
993 number can be combined with the seven digit segment\_id number to uniquely define  
994 any along-track segment number. Values are sequential, with 0000001 referring to  
995 the first segment after the equatorial crossing of the ascending node.

996           **2.4.2** Georeferenced\_segment\_number\_end

997           (parameter = segment\_id\_end). The last along-track segment\_id in each 100-m  
998 segment. Each 100-m segment consists of five sequential 20-m segments provided  
999 from the ATL03 product, which are labeled as segment\_id. The segment\_id is a seven  
1000 digit number that uniquely identifies each along track segment, and is written at the  
1001 along-track geolocation segment rate (i.e. ~20m along track). The four digit RGT  
1002 number can be combined with the seven digit segment\_id number to uniquely define  
1003 any along-track segment number. Values are sequential, with 0000001 referring to  
1004 the first segment after the equatorial crossing of the ascending node.

1005           **2.4.3** Segment\_latitude

1006           (parameter = latitude). Center latitude of signal photons within each segment.  
1007 Each 100 m segment consists of 5 20m ATL03 geosegments. In most cases, there will  
1008 be signal photons in each of the 5 geosegments necessary for calculating a latitude  
1009 value. For instances where the 100 m ATL08 is not fully populated with photons (e.g.  
1010 photons drop out due to clouds or signal attenuation), the latitude will be interpolated  
1011 to the mid-point of the 100 m segment. To implement this interpolation, we confirm  
1012 that each 100 m segment is comprised of at least 3 unique ATL03 geosegments IDs,  
1013 indicating that data is available near the mid-point of the land segment. If less than 3  
1014 ATL03 segments are available, the coordinate is interpolated based on the ratio of  
1015 delta time at the centermost ATL03 segment and that of the centermost photon, thus

1016 applying the centermost photon's coordinates to represent the land segment with a  
1017 slight adjustment. In some instances, the latitude and longitude will require  
1018 extrapolation to estimate a mid-100 m segment location. It is possible that in these  
1019 extremely rare cases, the latitude and longitude could not represent the true center  
1020 of the 100 m segment. We encourage the user to investigate the parameters  
1021 segment\_te\_flag and segment\_can\_flag which provide information as to the number  
1022 and distribution of signal photons within each 100 m segment.

#### 1023 **2.4.4** Geosegment\_latitude{1:5}

1024 (parameter = latitude\_20m). Interpolated center latitude of each 20 m  
1025 geosegment.

#### 1026 **2.4.5** Segment\_longitude

1027 (parameter = longitude). Center longitude of signal photons within each  
1028 segment. Each 100 m segment consists of 5 20m geosegments. In most cases, there  
1029 will be signal photons in each of the 5 geosegments necessary for calculating a  
1030 longitude value. For instances where the 100 m ATL08 is not fully populated with  
1031 photons (e.g. photons drop out due to clouds or signal attenuation), the latitude will  
1032 be interpolated to the mid-point of the 100 m segment. To implement this  
1033 interpolation, we confirm that each 100 m segment is comprised of at least 3 unique  
1034 ATL03 geosegments IDs, indicating that data is available near the mid-point of the  
1035 land segment. If less than 3 ATL03 segments are available, the coordinate is  
1036 interpolated based on the ratio of delta time at the centermost ATL03 segment and  
1037 that of the centermost photon, thus applying the centermost photon's coordinates to  
1038 represent the land segment with a slight adjustment. In some instances, the latitude  
1039 and longitude will require extrapolation to estimate a mid-100 m segment location. It  
1040 is possible that in these extremely rare cases, the latitude and longitude could not  
1041 represent the true center of the 100 m segment. We encourage the user to investigate  
1042 the parameters segment\_te\_flag and segment\_can\_flag which provide information as to  
1043 the number and distribution of signal photons within each 100 m segment.



1044           **2.4.6** Geosegment\_longitude{1:5}  
1045           (parameter = longitude\_20m). Interpolated center longitude of each 20 m  
1046 geosegment.  
1047  
1048           **2.4.7** Delta\_time  
1049           (parameter = delta\_time). Mid-segment GPS time for the segment in seconds  
1050 past an epoch. The epoch is listed in the metadata at the file level.  
1051           **2.4.8** Delta\_time\_beg  
1052           (parameter = delta\_time\_beg). Delta time for the first photon in the segment  
1053 in seconds past an epoch. The epoch is listed in the metadata at the file level.  
1054           **2.4.9** Delta\_time\_end  
1055           (parameter = delta\_time\_end). Delta time for the last photon in the segment  
1056 in seconds past an epoch. The epoch is listed in the metadata at the file level.  
1057           **2.4.10** Night\_Flag  
1058           (parameter = night\_flag). Flag indicating the data were acquired in night  
1059 conditions: 0 = day, 1 = night. Night flag is set when solar elevation is below 0.0  
1060 degrees.  
1061           **2.4.11** Segment\_reference\_DTM  
1062           (parameter = dem\_h). Reference terrain height value for segment determined  
1063 by the “best” DEM available based on data location. All heights in ICESat-2 are  
1064 referenced to the WGS 84 ellipsoid unless clearly noted otherwise. DEM is taken from  
1065 a variety of ancillary data sources: MERIT, GIMP, GMTED, MSS. The DEM source flag  
1066 indicates which source was used.

1067           **2.4.12** Segment\_reference\_DEM\_source  
 1068           (parameter = dem\_flag). Indicates source of the reference DEM height. Values:  
 1069           0=None, 1=GIMP, 2=GMTED, 3=MSS, 4=MERIT.

1070           **2.4.13** Segment\_reference\_DEM\_removal\_flag  
 1071           (parameter = dem\_removal\_flag). Quality check flag to indicate > 20%  
 1072           classified photons removed from land segment due to large distance from dem\_h.

1073           **2.4.14** Segment\_terrain\_difference  
 1074           (parameter = h\_dif\_ref). Difference between h\_te\_median and dem\_h. Since the  
 1075           mean terrain height is more sensitive to outliers, the median terrain height will be  
 1076           evaluated against the reference DEM. This parameter will be used as an internal data  
 1077           quality check with the notion being that if the difference exceeds a threshold (TBD) a  
 1078           terrain quality flag (terrain\_flg) will be triggered.

1079           **2.4.15** Segment\_terrain flag  
 1080           (parameter = terrain\_flg). Terrain flag to indicate confidence in the derived  
 1081           terrain height estimate. If h\_dif\_ref exceeds a threshold (TBD) the terrain\_flg  
 1082           parameter will be set to 1. Otherwise, it is 0.

1083           **2.4.16** Segment\_landcover  
 1084           (parameter = segment\_landcover). Updating the segment landcover with the  
 1085           2019 Copernicus Landcover 100 m discrete landcover product which incorporates 23  
 1086           discrete landcover classes which follow the UN-FAO's Land Cover Classification  
 1087           System. The ATL08 landcover segment will be the Copernicus Landcover value at the  
 1088           segment     latitude/longitude.     <https://land.copernicus.eu/global/products/lc>  
 1089           (<https://doi.org/10.5281/zenodo.3939050>).

Map Code	Landcover Class	Definition according to UN LCCS
0	No data	

111	Closed forest, evergreen needle leaf	Tree canopy >70%, almost all needle leaf trees remain green all year. Canopy is never without green foliage
113	Closed forest, deciduous needle leaf	Tree canopy >70%, consists of seasonal needle leaf communities with an annual cycle of leaf-on and leaf-off periods.
112	Closed forest, evergreen broad leaf	Tree canopy >70%, almost all broadleaf trees remain green year round. Canopy is never without green foliage
114	Closed forest, deciduous broad leaf	Tree canopy >70%, consists of seasonal broad leaf communities with an annual cycle of leaf-on and leaf-off periods.
115	Closed forest, mixed	Closed forest, mix of types
116	Closed forest, unknown	Closed forest, not matching any of the other definitions
121	Open forest, evergreen needle leaf	Top layer- trees 15-70% and second layer mixed of shrubs and grassland, almost all needle leaf trees remain green all year. Canopy is never without green foliage
123	Open forest, deciduous needle leaf	Top layer- trees 15-70% and second layer mixed of shrubs and grassland, consists of seasonal needle leaf tree communities with an annual cycle of leaf-on and leaf-off
122	Open forest, evergreen broad leaf	Top layer- trees 15-70% and second layer mixed of shrubs and grassland, almost all broad leaf trees remain green all year. Canopy is never without green foliage
124	Open forest, deciduous broad leaf	Top layer- trees 15-70% and second layer mixed of shrubs and grassland, consists of seasonal broad leaf tree communities with an annual cycle of leaf-on and leaf-off
125	Open forest, mixed	Open forest, mix of types
126	Open forest, unknown	Open forest, not matching any of the other definitions
20	Shrubs	Woody perennial plants with persistent and woody stems and without a main stem being less than 5m. The shrub foliage can be either evergreen or deciduous.
30	Herbaceous	Plants without persistent stems or shoots above ground and lacking firm structure. Tree and shrub cover is less than 10%
90	Herbaceous Wetland	Lands with a permanent mixture of water and herbaceous or woody vegetation. The vegetation can be present in salt, brackish, or fresh water.
100	Moss and lichen	Moss and lichen
60	Bare/sparse vegetation	Lands with exposed soil, sand, or rocks and never has more than 10% vegetation cover during any time of the year
40	Cultivated and managed vegetation/agriculture	Lands covered with temporary crops followed by harvest and a bare soil period.
50	Urban/built up	Land covered by buildings or other man-made structures
70	Snow and ice	Land under snow or ice throughout the year
80	Permanent water bodies	Lakes, reservoirs, and rivers. Can be either fresh or salt-water bodies

200	Open sea	Oceans, seas. Can be either fresh or salt-water bodies.
-----	----------	---

1090

1091

1092

1093       **2.4.17 Segment\_Woody Vegetation Fractional Cover**

1094       (parameter = segment\_cover). Woody vegetation fractional cover derived  
1095 from the 2019 Copernicus 100 m shrub and forest fractional cover data products. The  
1096 woody cover fractional cover is the simple addition of the forest fractional cover with  
1097 the shrub fractional cover. The ATL08 woody vegetation fractional cover value shall  
1098 be the pixel value at the segment latitude/longitude. The Copernicus data products  
1099 can be found at <https://lcviewer.vito.be/download>

1100       **2.4.18 Segment\_watermask**

1101       (parameter = segment\_watermask). Water mask (i.e., flag) indicating inland  
1102 water as referenced from the Global Raster Water Mask at 250 m spatial resolution  
1103 (Carroll et al, 2009; available online at <http://glcf.umd.edu/data/watermask/>). 0 =  
1104 no water; 1 = water.

1105       **2.4.19 Segment\_snowcover**

1106       (parameter = segment\_snowcover). Daily snowcover mask (i.e., flag)  
1107 indicating a likely presence of snow or ice within each segment produced from best  
1108 available source used for reference. The snow mask will be the same snow mask as  
1109 used for ATL09 Atmospheric Products: NOAA snow-ice flag. 0=ice free water;  
1110 1=snow free land; 2=snow; 3=ice.

1111       **2.4.20 Urban\_flag**

1112       **2.4.21 (parameter = urban\_flag). Segment estimated urban cover flag as**  
1113       **derived from the Global Urban Footprint (GUF) data product. GUF**  
1114       **is a global mapping of urban areas derived from the TerraSAR-X**

1115                   **and TanDEM-X satellites. The GUF maps at a resolution of ~12 m**  
1116                   **(0.4 arcseconds). Due to differences in resolution, the ATL08 GUF**  
1117                   **value is set based upon a 4x4 block of pixels about the 100 m**  
1118                   **segment latitude/longitude . If ANY of the pixels the GUF pixels are**  
1119                   **labeled as urban, the ATL08 GUF value is set to urban. The GUF**  
1120                   **urban flag is set as -1 = undetermined, 0 = not urban, 1 = urban.**  
1121                   **The GUF data are available from DLR**  
1122                   **[https://www.dlr.de/eoc/en/desktopdefault.aspx/tabid-](https://www.dlr.de/eoc/en/desktopdefault.aspx/tabid-9628/16557_read-40454/)**  
1123                   **[9628/16557\\_read-40454/](https://www.dlr.de/eoc/en/desktopdefault.aspx/tabid-9628/16557_read-40454/)Surface Type**

1124                   (parameter = surf\_type). The surface type for a given segment is determined at  
1125 the major frame rate (every 200 shots, or ~140 meters along-track) and is a two-  
1126 dimensional array surf\_type(n, nsurf), where n is the major frame number, and nsurf  
1127 is the number of possible surface types such that surf\_type(n,isurf) is set to 0 or 1  
1128 indicating if surface type isurf is present (1) or not (0), where isurf = 1 to 5 (land,  
1129 ocean, sea ice, land ice, and inland water) respectively.

#### 1130                   **2.4.22 ATL08\_region**

1131                   (parameter = atl08\_region). The ATL08 regions that encompass the ATL03  
1132 granule being processed through the ATL08 algorithm. The ATL08 regions are shown  
1133 by Figure 2.3.

#### 1134                   **2.4.23 Last\_segment\_extend**

1135                   (parameter = last\_seg\_extend). The distance (km) that the last ATL08 10 km  
1136 processing segment is either extended beyond 10 km or uses data from the previous  
1137 10 km processing segment to allow for enough data for processing the ATL03 photons  
1138 through the ATL08 algorithm. If the last portion of an ATL03 granule being processed  
1139 would result in a segment with less than 3.4 km (170 geosegments) worth of data,  
1140 that last portion is added to the previous 10 km processing window to be processed  
1141 together as one extended ATL08 processing segment. The resulting last\_seg\_extend  
1142 value would be a positive value of distance beyond 10 km that the ATL08 processing  
1143 segment was extended by. If the last ATL08 processing segment would be less than

1144 10 km but greater than 3.4 km, a portion extending from the start of current ATL08  
 1145 processing segment backwards into the previous ATL08 processing segment would  
 1146 be added to the current ATL08 processing segment to make it 10 km in length. The  
 1147 distance of this backward data gathering would be reported in last\_seg\_extend as a  
 1148 negative distance value. Only new 100 m ATL08 segment products generated from  
 1149 this backward extension would be reported. All other segments that are not extended  
 1150 will report a last\_seg\_extend value of 0.

1151 **2.4.24 Brightness\_flag**

1152 (parameter = brightness\_flag). Based upon the classification of the photons  
 1153 within each 100 m, this parameter flags ATL08 segments where the mean number of  
 1154 ground photons per shot exceed a value of 3. This calculation can be made as the total  
 1155 number of ground photons divided by the number of ATLAS shots within the 100 m  
 1156 segment. A value of 0 = indicates non-bright surface, value of 1 indicates bright  
 1157 surface, and a value of 2 indicates “undetermined” due to clouds or other factors. The  
 1158 brightness is computed initially on the 10 km processing segment. If the ground  
 1159 surface is determined to be bright for the entire 10 km segment, the brightness is then  
 1160 calculated at the 100 m segment size.

1161

1162 **2.5 Subgroup: Beam data**

1163 The subgroup for beam data contains basic information on the geometry and  
 1164 pointing accuracy for each beam.

1165 Table 2.5. Summary table for beam parameters for the ATL08 product.

Group	Data Type	Units	Description	Source
segment_id_beg	Integer		First along-track segment_id number in 100-m segment	ATL03
segment_id_end	Integer		Last along-track segment_id number in 100-m segment	ATL03

---

<b>ref_elev</b>	Float	Elevation of the unit pointing vector for the reference photon in the local ENU frame in radians. The angle is measured from East-North plane and positive towards up	ATL03
<b>ref_azimuth</b>	Float	Azimuth of the unit pointing vector for the reference photon in the ENU frame in radians. The angle is measured from North and positive toward East.	ATL03
<b>atlas_pa</b>	Float	Off nadir pointing angle of the spacecraft	ATL03
<b>rgt</b>	Integer	The reference ground track (RGT) is the track on the earth at which the vector bisecting laser beams 3 and 4 is pointed during repeat operations	ATL03
<b>sigma_h</b>	Float	Total vertical uncertainty due to PPD and POD	ATL03
<b>sigma_along</b>	Float	Total along-track uncertainty due to PPD and POD knowledge	ATL03
<b>sigma_across</b>	Float	Total cross-track uncertainty due to PPD and POD knowledge	ATL03
<b>sigma_topo</b>	Float	Uncertainty of the geolocation knowledge due to local topography (Equation 1.3)	computed
<b>sigma_atlas_land</b>	Float	Total uncertainty that includes sigma_h plus the geolocation uncertainty due to local slope Equation 1.2	computed
<b>psf_flag</b>	integer	Flag indicating sigma_atlas_land (aka PSF) as computed in Equation 1.2 exceeds a value of 1m.	computed

---

---

<b>layer_flag</b>	Integer	Cloud flag indicating presence of clouds or blowing snow	ATL09
<b>cloud_flag_atm</b>	Integer	Cloud confidence flag from ATL09 indicating clear skies	ATL09
<b>msw_flag</b>	Integer	Multiple scattering warning product produced on ATL09	ATL09
<b>cloud_fold_flag</b>	integer	Cloud flag to indicate potential of high clouds that have “folded” into the lower range bins	ATL09
<b>asr</b>	Float	Apparent surface reflectance	ATL09
<b>snr</b>	Float	Background signal to noise level	Computed
<b>solar_azimuth</b>	Float	The azimuth (in degrees) of the sun position vector from the reference photon bounce point position in the local ENU frame. The angle is measured from North and is positive towards East.	ATL03g
<b>solar_elevation</b>	Float	The elevation of the sun position vector from the reference photon bounce point position in the local ENU frame. The angle is measured from the East-North plane and is positive Up.	ATL03g
<b>n_seg_ph</b>	Integer	Number of photons within each land segment	computed
<b>ph_ndx_beg</b>	Integer	Photon index begin	computed
<b>sat_flag</b>	Integer	Flag derived from full_sat_fract and near_sat_fract on the ATL03 data product	computed

---



1167           **2.5.1** Georeferenced\_segment\_number\_beg

1168           (parameter = segment\_id\_beg). The first along-track segment\_id in each 100-m  
1169 segment. Each 100-m segment consists of five sequential 20-m segments provided  
1170 from the ATL03 product, which are labeled as segment\_id. The segment\_id is a seven  
1171 digit number that uniquely identifies each along track segment, and is written at the  
1172 along-track geolocation segment rate (i.e. ~20m along track). The four digit RGT  
1173 number can be combined with the seven digit segment\_id number to uniquely define  
1174 any along-track segment number. Values are sequential, with 0000001 referring to  
1175 the first segment after the equatorial crossing of the ascending node.

1176           **2.5.2** Georeferenced\_segment\_number\_end

1177           (parameter = segment\_id\_end). The last along-track segment\_id in each 100-m  
1178 segment. Each 100-m segment consists of five sequential 20-m segments provided  
1179 from the ATL03 product, which are labeled as segment\_id. The segment\_id is a seven  
1180 digit number that uniquely identifies each along track segment, and is written at the  
1181 along-track geolocation segment rate (i.e. ~20m along track). The four digit RGT  
1182 number can be combined with the seven digit segment\_id number to uniquely define  
1183 any along-track segment number. Values are sequential, with 0000001 referring to  
1184 the first segment after the equatorial crossing of the ascending node.

1185           **2.5.3** Beam\_coelevation

1186           (parameter = ref\_elev). Elevation of the unit pointing vector for the reference  
1187 photon in the local ENU frame in radians. The angle is measured from East-North  
1188 plane and positive towards up.

1189           **2.5.4** Beam\_azimuth

1190           (parameter = ref\_azimuth). Azimuth of the unit pointing vector for the  
1191 reference photon in the ENU frame in radians. The angle is measured from North and  
1192 positive toward East.

1193           **2.5.5** ATLAS\_Pointing\_Angle

1194           (parameter = atlas\_pa). Off nadir pointing angle (in radians) of the satellite to  
1195 increase spatial sampling in the non-polar regions.

1196           **2.5.6** Reference\_ground\_track

1197           (parameter = rgt). The reference ground track (RGT) is the track on the earth  
1198 at which the vector bisecting laser beams 3 and 4 (or GT2L and GT2R) is pointed  
1199 during repeat operations. Each RGT spans the part of an orbit between two ascending  
1200 equator crossings and are numbered sequentially. The ICESat-2 mission has 1387  
1201 RGTs, numbered from 0001xx to 1387xx. The last two digits refer to the cycle number.

1202           **2.5.7** Sigma\_h

1203           (parameter = sigma\_h). Total vertical uncertainty due to PPD (Precise Pointing  
1204 Determination), POD (Precise Orbit Determination), and geolocation errors.  
1205 Specifically, this parameter includes radial orbit error,  $\sigma_{orbit}$ , tropospheric errors,  
1206  $\sigma_{Trop}$ , forward scattering errors,  $\sigma_{forwardscattering}$ , instrument timing errors,  $\sigma_{timing}$ ,  
1207 and off-nadir pointing geolocation errors. The component parameters are pulled  
1208 from ATL03 and ATL09. Sigma\_h is the root sum of squares of these terms as detailed  
1209 in Equation 1.1. The sigma\_h reported here is the mean of the sigma\_h values reported  
1210 within the five ATL03 geosegments that are used to create the 100 m ATL08 segment.

1211           **2.5.8** Sigma\_along

1212           (parameter = sigma\_along). Total along-track uncertainty due to PPD and POD  
1213 knowledge. This parameter is pulled from ATL03.

1214           **2.5.9** Sigma\_across

1215           (parameter = sigma\_across). Total cross-track uncertainty due to PPD and  
1216 POD knowledge. This parameter is pulled from ATL03.

1217           **2.5.10** Sigma\_topo

1218           (parameter = sigma\_topo). Uncertainty in the geolocation due to local surface  
1219 slope as described in Equation 1.3. The local slope is multiplied by the 6.5 m  
1220 geolocation uncertainty factor that will be used to determine the geolocation  
1221 uncertainty. The geolocation error will be computed from a 100 m sample due to the  
1222 local slope calculation at that scale.

1223           **2.5.11** Sigma\_ATLAS\_LAND

1224           (parameter = sigma\_atlas\_land). Total vertical geolocation error due to  
1225 ranging, and local surface slope. The parameter is computed for ATL08 as described  
1226 in Equation 1.2. The geolocation error will be computed from a 100 m sample due to  
1227 the local slope calculation at that scale.

1228           **2.5.12** PSF\_flag

1229           (parameter = psf\_flag). Flag indicating that the point spread function  
1230 (computed as sigma\_atlas\_land) has exceeded 1m.

1231           **2.5.13** Layer\_flag

1232           (parameter = layer\_flag). Flag is a combination of multiple ATL09 flags and  
1233 takes daytime/nighttime into consideration. A value of 1 means clouds or blowing  
1234 snow is likely present. A value of 0 indicates the likely absence of clouds or blowing  
1235 snow. If no ATL09 product is available for an ATL08 segment, an invalid value will be  
1236 reported. Since the cloud flags from the ATL09 product are reported at an along-track  
1237 distance of 250 m, we will report the highest value of the ATL09 flags at the ATL08  
1238 resolution (100 m). Thus, if a 100 m ATL08 segment straddles two values from  
1239 ATL09, the highest cloud flag value will be reported on ATL08. This reporting strategy  
1240 holds for all the cloud flags reported on ATL08.

1241           **2.5.14** Cloud\_flag\_atm

1242           (parameter = cloud\_flag\_atm). Cloud confidence flag from ATL09 that indicates  
1243 the number of cloud or aerosol layers identified in each 25Hz atmospheric profile. If  
1244 the flag is greater than 0, aerosols or clouds could be present.

1245           **2.5.15** MSW

1246           (parameter = msw\_flag). Multiple scattering warning flag with values from -1 to  
1247 5 as computed in the ATL09 atmospheric processing and delivered on the ATL09 data  
1248 product. If no ATL09 product is available for an ATL08 segment, an invalid value will  
1249 be reported. MSW flags:

1250                               -1 = signal to noise ratio too low to determine presence of  
1251                               cloud or blowing snow  
1252                               0 = no\_scattering  
1253                               1 = clouds at > 3 km  
1254                               2 = clouds at 1-3 km  
1255                               3 = clouds at < 1 km  
1256                               4 = blowing snow at < 0.5 optical depth  
1257                               5 = blowing snow at >= 0.5 optical depth

1258           **2.5.16** Cloud Fold Flag

1259           (parameter = cloud\_fold\_flag). Clouds occurring higher than 14 to 15 km in the  
1260 atmosphere will be folded down into the lower portion of the atmospheric profile.

1261           **2.5.17** Computed\_Apparent\_Surface\_Reflectance

1262           (parameter = asr). Apparent surface reflectance computed in the ATL09  
1263 atmospheric processing and delivered on the ATL09 data product. If no ATL09  
1264 product is available for an ATL08 segment, an invalid value will be reported.

1265           **2.5.18 Signal\_to\_Noise\_Ratio**

1266           (parameter = snr). The Signal to Noise Ratio of geolocated photons as  
1267 determined by the ratio of the superset of ATL03 signal and DRAGANN found signal  
1268 photons used for processing the ATL08 segments to the background photons (i.e.,  
1269 noise) within the same ATL08 segments.

1270           **2.5.19 Solar\_Azimuth**

1271           (parameter = solar\_azimuth). The azimuth (in degrees) of the sun position  
1272 vector from the reference photon bounce point position in the local ENU frame. The  
1273 angle is measured from North and is positive towards East.

1274           **2.5.20 Solar\_Elevation**

1275           (parameter = solar\_elevation). The elevation of the sun position vector from  
1276 the reference photon bounce point position in the local ENU frame. The angle is  
1277 measured from the East-North plane and is positive up.

1278           **2.5.21 Number\_of\_segment\_photons**

1279           (parameter = n\_seg\_ph). Number of photons in each land segment.

1280           **2.5.22 Photon\_Index\_Begin**

1281           (parameter = ph\_ndx\_beg). Index (1-based) within the photon-rate data of  
1282 the first photon within this each land segment.

1283           **2.5.23 Saturation Flag**

1284           (parameter = sat\_flag) Saturation flag derived from the ATL03 saturation  
1285 flags full\_sat\_frac. The saturation flags on the ATL03 data product (full\_sat\_frac)  
1286 are the percentage of photons determined to be saturated within each geosegment.  
1287 For the ATL08 saturation flag, a value of 0 will indicate no saturation. A value of 1  
1288 will indicate the average of all 5 geosegment full\_sat\_frac values was over 0.2. This  
1289 value of 1 is an indication of standing water or saturated soils. If an ATL08 segment  
1290 is not fully populated with 5 values for full\_sat\_frac, a value of -1 will be set.

1291        sat\_flag:     -1 indicates not enough valid data to make determination  
1292                    0 indicates no saturation in ATL08 segment  
1293                    1 indicates saturation in ATL08 segment  
1294  
1295  
1296  
1297

## 1298 **3 ALGORITHM METHODOLOGY**

1299 For the ecosystem community, identification of the ground and canopy surface  
1300 is by far the most critical task, as meeting the science objective of determining global  
1301 canopy heights hinges upon the ability to detect both the canopy surface and the  
1302 underlying topography. Since a space-based photon counting laser mapping system  
1303 is a relatively new instrument technology for mapping the Earth's surface, the  
1304 software to accurately identify and extract both the canopy surface and ground  
1305 surface is described here. The methodology adopted for ATL08 establishes a  
1306 framework to potentially accept multiple approaches for capturing both the upper  
1307 and lower surface of signal photons. One method used is an iterative filtering of  
1308 photons in the along-track direction. This method has been found to preserve the  
1309 topography and capture canopy photons, while rejecting noise photons. An advantage  
1310 of this methodology is that it is self-parameterizing, robust, and works in all  
1311 ecosystems if sufficient photons from both the canopy and ground are available. For  
1312 processing purposes, along-track data signal photons are parsed into  $L$ -km segment  
1313 of the orbit which is recommended to be 10 km in length.

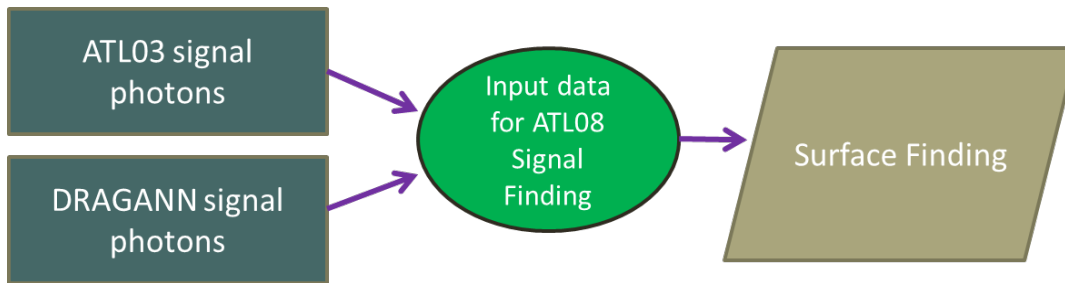
1314

### 1315 **3.1 Noise Filtering**

1316 Solar background noise is a significant challenge in the analysis of photon  
1317 counting laser data. Range measurement data created from photon counting lidar  
1318 detectors typically contain far higher noise levels than the more common photon  
1319 integrating detectors available commercially in the presence of passive, solar  
1320 background photons. Given the higher detection sensitivity for photon counting  
1321 devices, a background photon has a greater probability of triggering a detection event  
1322 over traditional integral measurements and may sometimes dominate the dataset.  
1323 Solar background noise is a function of the surface reflectance, topography, solar  
1324 elevation, and atmospheric conditions. Prior to running the surface finding  
1325 algorithms used for ATL08 data products, the superset of output from the GSFC  
1326 medium-high confidence classed photons (ATL03 signal\_conf\_ph: flags 3-4) and the

1327 output from DRAGANN will be considered as the input data set. ATL03 input data  
1328 requirements include the latitude, longitude, height, segment delta time, segment ID,  
1329 and a preliminary signal classification for each photon. The motivation behind  
1330 combining the results from two different noise filtering methods is to ensure that all  
1331 of the potential signal photons for land surfaces will be provided as input to the  
1332 surface finding software. The description of the methodology for the ATL03  
1333 classification is described separately in the ATL03 ATBD. The methodology behind  
1334 DRAGANN is described in the following section.

1335



1336

1337 Figure 3.1. Combination of noise filtering algorithms to create a superset of input data for  
1338 surface finding algorithms.

1339

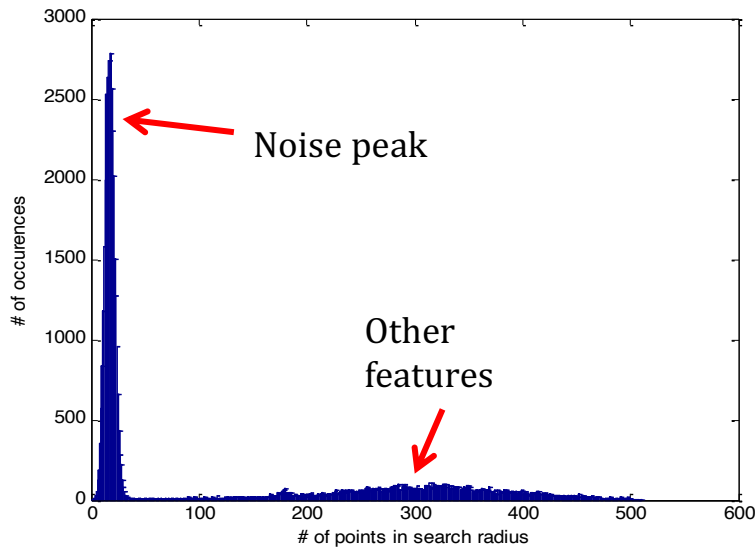
### 1340 3.1.1 DRAGANN

1341 The Differential, Regressive, and Gaussian Adaptive Nearest Neighbor  
1342 (DRAGANN) filtering technique was developed to identify and remove noise photons  
1343 from the photon counting data point cloud. DRAGANN utilizes the basic premise that  
1344 signal photons will be closer in space than random noise photons. The first step of the  
1345 filtering is to implement an adaptive nearest neighbor search. By using an adaptive  
1346 method, different thresholds can be applied to account for variable amounts of  
1347 background noise and changing surface reflectance along the data profile. This search  
1348 finds an effective radius by computing the probability of finding P number of points  
1349 within a search area. For MABEL and mATLAS, P=20 points within the search area





1379



1380

1381 Figure 3.2. Histogram of the number of photons within a search radius. This histogram is  
1382 used to determine the threshold for the DRAGANN approach.

1383

1384 Once the radius has been computed, DRAGANN counts the number of points  
1385 within the radius for each point and histograms that set of values. The distribution of  
1386 the number of points, Figure 3.2, reveals two distinct peaks; a noise peak and a signal  
1387 peak. The motivation of DRAGANN is to isolate the signal photons by determining a  
1388 threshold based on the number of photons within the search radius. The noise peak  
1389 is characterized as having a large number of occurrences of photons with just a few  
1390 neighboring photons within the search radius. The signal photons comprise the broad  
1391 second peak. The first step in determining the threshold between the noise and signal  
1392 is to implement Gaussian fitting to the number of photons distribution (i.e., the  
1393 distribution shown in Figure 3.2). The Gaussian function has the form

1394

1395

$$g(x) = ae^{-\frac{(x-b)^2}{2c^2}} \quad \text{Eqn. 3.3}$$

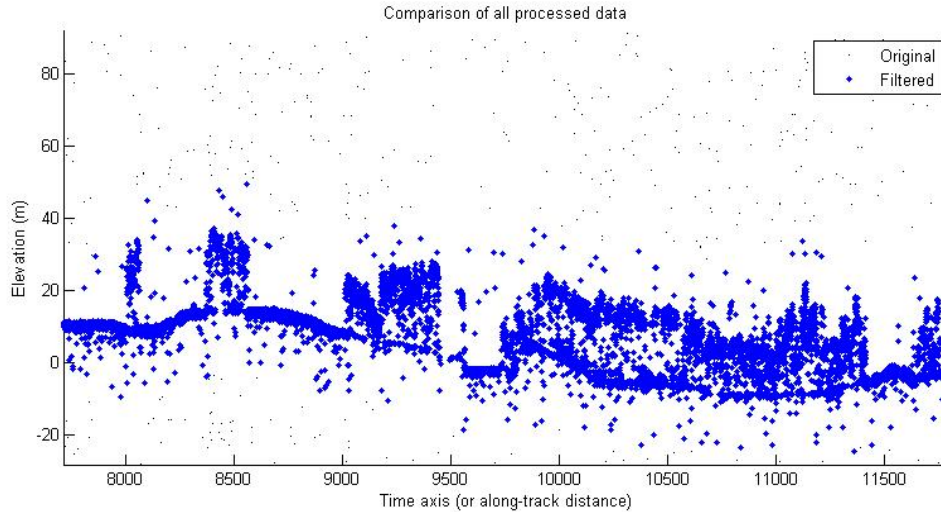
1396

1397 where  $a$  is the amplitude of the peak,  $b$  is the center of the peak, and  $c$  is the standard  
1398 deviation of the curve. A first derivative sign crossing method is one option to identify  
1399 peaks within the distribution.

1400 To determine the noise and signal Gaussians, up to ten Gaussian curves are fit  
1401 to the histogram using an iterative process of fitting and subtracting the max-  
1402 amplitude peak component from the histogram until all peaks have been extracted.  
1403 Then, the potential Gaussians pass through a rejection process to eliminate those with  
1404 poor statistical fits or other apparent errors (Goshtasby and O'Neill, 1994; Chauve et  
1405 al. 2008). A Gaussian with an amplitude less than  $1/5$  of the previous Gaussian and  
1406 within two standard deviations of the previous Gaussian should be rejected. Once the  
1407 errant Gaussians are rejected, the final two remaining are assumed to represent the  
1408 noise and signal. These are separated based on the remaining two Gaussian  
1409 components within the histogram using the logic that the leftmost Gaussian is noise  
1410 (low neighbor counts) and the other is signal (high neighbor counts).

1411 The intersection of these two Gaussians (noise and signal) determines a data  
1412 threshold value. The threshold value is the parameter used to distinguish between  
1413 noise points and signal points when the point cloud is re-evaluated for surface finding.  
1414 In the event that only one curve passes the rejection process, the threshold is set at  
1415  $1 \sigma$  above the center of the noise peak.

1416 An example of the noise filtered product from DRAGANN is shown in Figure  
1417 3.3. The signal photons identified in this process will be combined with the coarse  
1418 signal finding output available on the ATL03 data product.



1419

1420 Figure 3.3. Output from DRAGANN filtering. Signal photons are shown as blue.

1421 Figure 3.3 provides an example of along-track (profiling) height data collected  
 1422 in September 2012 from the MABEL (ICESat-2 simulator) over vegetation in North  
 1423 Carolina. The photons have been filtered such that the signal photons returned from  
 1424 vegetation and the ground surface are remaining. Noise photons that are adjacent to  
 1425 the signal photons are also retained in the input dataset; however, these should be  
 1426 classified as noise photons during the surface finding process. It is possible that some  
 1427 additional outlying noise may be retained during the DRAGANN process when noise  
 1428 photons are densely grouped, and these photons should be filtered out before the  
 1429 surface finding process. Estimates of the ground surface and canopy height can then  
 1430 be derived from the signal photons.

1431

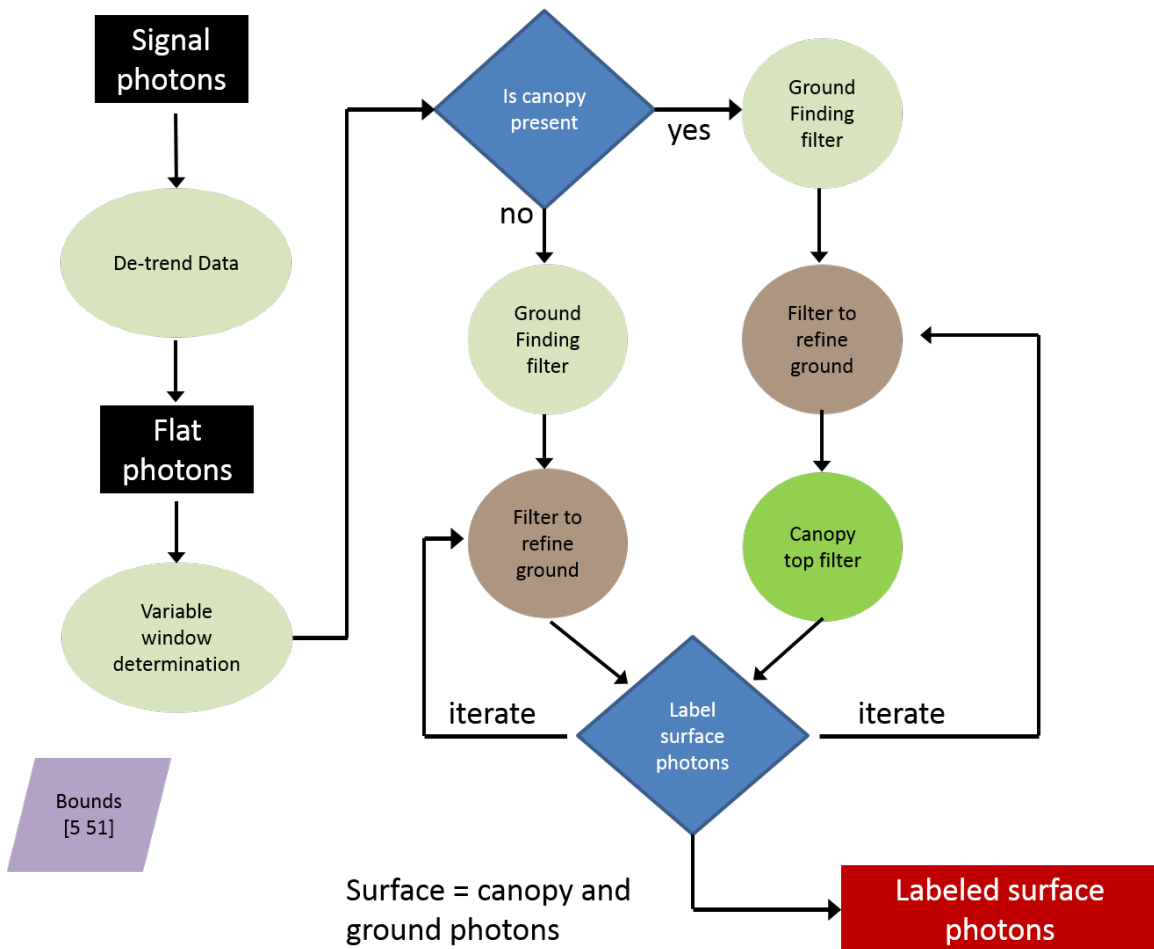
### 1432 **3.2 Surface Finding**

1433 Once the signal photons have been determined, the objective is to find the  
 1434 ground and canopy photons from within the point cloud. With the expectation that  
 1435 one algorithm may not work everywhere for all biomes, we are employing a  
 1436 framework that will allow us to combine the solutions of multiple algorithms into one  
 1437 final composite solution for the ground surface. The composite ground surface  
 1438 solution will then be utilized to classify the individual photons as ground, canopy, top

1439 of canopy, or noise. Currently, the framework described here utilizes one algorithm  
1440 for finding the ground surface and canopy surface. Additional methods, however,  
1441 could be integrated into the framework at a later time. Figure 3.4 below describes the  
1442 framework.

1443

1444



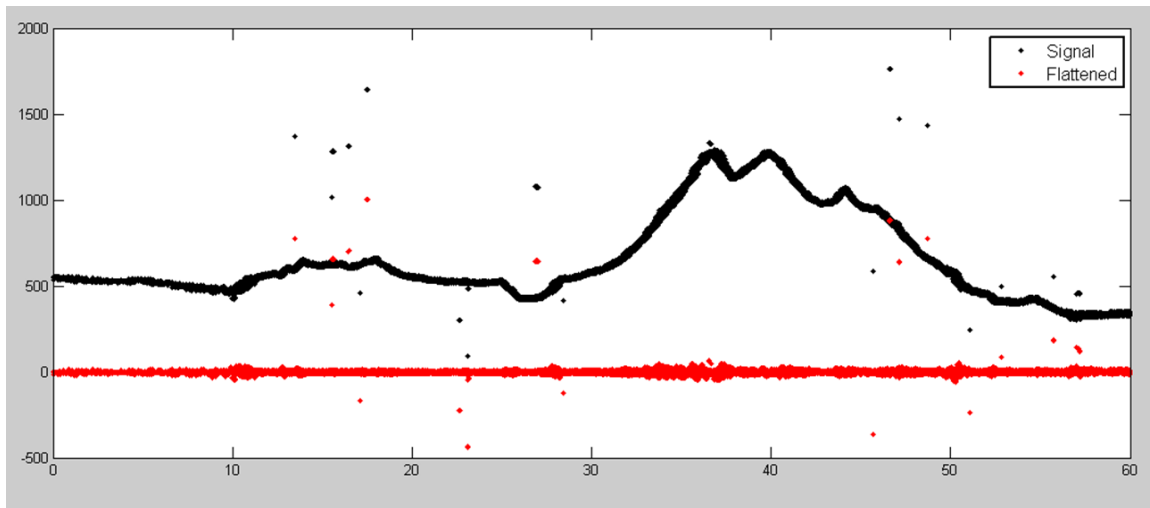
1445

1446 Figure 3.4. Flowchart of overall surface finding method.

1447

1448 **3.2.1 De-trending the Signal Photons**

1449 An important step in the success of the surface finding algorithm is to remove  
1450 the effect of topography on the input data, thus improving the performance of the  
1451 algorithm. This is done by de-trending the input signal photons by subtracting a  
1452 heavily smoothed “surface” that is derived from the input data. Essentially, this is a  
1453 low pass filter of the original data and most of the analysis to detect the canopy and  
1454 ground will subsequently be implemented on the high pass data. The amount of  
1455 smoothing that is implemented in order to derive this first surface is dependent upon  
1456 the relief. For segments where the relief is high, the smoothing window size is  
1457 decreased so topography isn’t over-filtered.



1458  
1459 Figure 3.5. Plot of Signal Photons (black) from 2014 MABEL flight over Alaska and de-  
1460 trended photons (red).

1461

1462 **3.2.2 Canopy Determination**

1463 A key factor in the success of the surface finding algorithm is for the software  
1464 to automatically **account for the presence of canopy** along a given  $L$ -km segment.  
1465 Due to the large volume of data, this process has to occur in an automated fashion,  
1466 allowing the correct methodology for extracting the surface to be applied to the data.  
1467 In the absence of canopy, the iterative filtering approach to finding ground works

1468 extremely well, but if canopy does exist, we need to accommodate for that fact when  
1469 we are trying to recover the ground surface.

1470 For ATL08 product regions over Antarctica (regions 7, 8, 9, 10) and Greenland  
1471 (region 11), the algorithm will assume only ground photons (canopy flag = 0) (see  
1472 Figure 2.2).

1473

### 1474 3.2.3 Variable Window Determination

1475 The method for generating a best estimated terrain surface will vary depending  
1476 upon whether canopy is present. *L-km segments* without canopy are much easier to  
1477 analyze because the ground photons are usually continuous. *L-km segments* with  
1478 canopy, however, require more scrutiny as the number of signal photons from ground  
1479 are fewer due to occlusion by the vegetation.

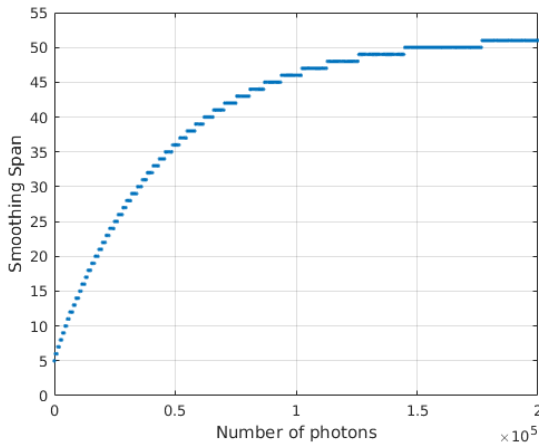
1480 There are some common elements for finding the terrain surface for both cases  
1481 (canopy/no canopy) and with both methods. In both cases, we will use a variable  
1482 windowing span to compute statistics as well as filter and smooth the data. For  
1483 clarification, the window size is variable for each *L-km segment*, but it is constant  
1484 within the *L-km segment*. For the surface finding algorithm, we will employ a  
1485 Savitzky-Golay smoothing/median filtering method. Using this filter, we compute a  
1486 variable smoothing parameter (or window size). It is important to bound the filter  
1487 appropriately as the output from the median filter can lose fidelity if the scan is over-  
1488 filtered.

1489 We have developed an empirically-determined shape function, bound between  
1490 [5 51], that sets the window size (*Sspan*) based on the number of photons within each  
1491 *L-km segment*.

$$1492 \quad Sspan = \text{ceil}[5 + 46 * (1 - e^{-a*length})] \quad \text{Eqn. 3.4}$$

$$1493 \quad a = \frac{\log\left(1 - \frac{21}{51-5}\right)}{-28114} \approx 21 \times 10^{-6} \quad \text{Eqn. 3.5}$$

1494 where  $a$  is the shape parameter and length is the total number of photons in the  $L$ -km  
1495 segment. The shape parameter,  $a$ , was determined using data collected by MABEL and  
1496 is shown in Figure 3.6. It is possible that the model of the shape function, or the  
1497 filtering bounds, will need to be adjusted once ICESat-2/ATLAS is on orbit and  
1498 collecting data.



1499

1500 Figure 3.6. Shape Parameter for variable window size.

1501

### 1502 3.2.4 Compute descriptive statistics

1503 To help characterize the input data and initialize some of the parameters used  
1504 in the algorithm, we employ a moving window to compute descriptive statistics on  
1505 the de-trended data. The moving window's width is the smoothing span function  
1506 computed in Equation 5 and the window slides  $\frac{1}{4}$  of its size to allow of overlap  
1507 between windows. By moving the window with a large overlap helps to ensure that  
1508 the approximate ground location is returned. The statistics computed for each  
1509 window step include:

- 1510 • Mean height
- 1511 • Min height
- 1512 • Max height
- 1513 • Standard deviation of heights



1514

1515           Dependent upon the amount of vegetation within each window, the estimated  
1516 ground height is estimated using different statistics. A standard deviation of the  
1517 photon elevations computed within each moving window are used to classify the  
1518 vertical spread of photons as belonging to one of four classes with increasing amounts  
1519 of variation: open, canopy level 1, canopy level 2, canopy level 3. The canopy indices  
1520 are defined in Table 3.1.

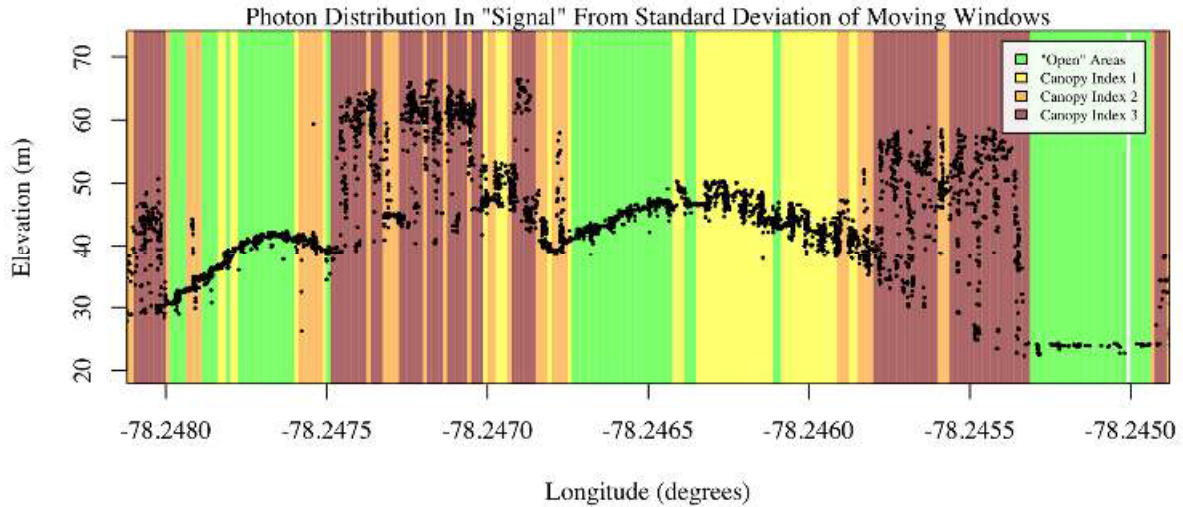
1521

1522 Table 3.1. Standard deviation ranges utilized to qualify the spread of photons within  
1523 moving window.

Name	Definition	Lower Limit	Upper Limit
Open	Areas with little or no spread in signal photons determined due to low standard deviation	N/A	Photons falling within 1 <sup>st</sup> quartile of Standard deviation
Canopy Level 1	Areas with small spread in signal photons	1 <sup>st</sup> quartile	Median
Canopy Level 2	Areas with a medium amount of spread	Median	3 <sup>rd</sup> quartile
Canopy Level 3	Areas with high amount of spread in signal photons	3 <sup>rd</sup> quartile	N/A

1524

1525



1526

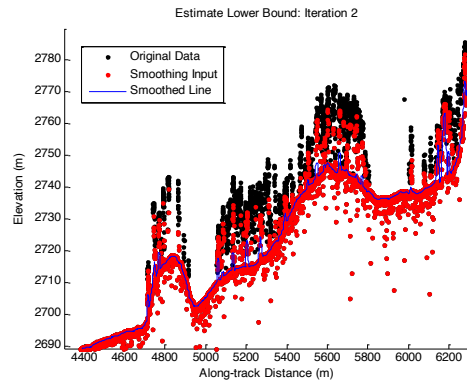
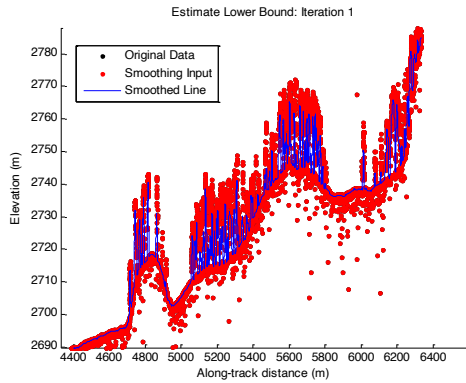
1527 Figure 3.7. Illustration of the standard deviations calculated for each moving window to  
 1528 identify the amount of spread of signal photons within a given window.

1529

### 1530 **3.2.5 Ground Finding Filter (Iterative median filtering)**

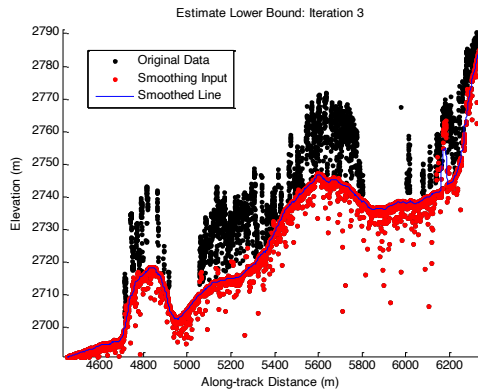
1531 A combination of an iterative median filtering and smoothing filter approach  
 1532 will be employed to derive the output solution of both the ground and canopy  
 1533 surfaces. The input to this process is the set of de-trended photons. Finding the  
 1534 ground in the presence of canopy often poses a challenge because often there are  
 1535 fewer ground photons underneath the canopy. The algorithm adopted here uses an  
 1536 iterative median filtering approach to retain/eliminate photons for ground finding in  
 1537 the presence of canopy. When canopy exists, a smoothed line will lay somewhere  
 1538 between the canopy top and the ground. This fact is used to iteratively label points  
 1539 above the smoothed line as canopy. The process is repeated five times to eliminate  
 1540 canopy points that fall above the estimated surface as well as noise points that fall  
 1541 below the ground surface. An example of iterative median filtering is shown in Figure  
 1542 3.8. The final median filtered line is the preliminary surface estimate. A limitation of  
 1543 this approach, however, is in cases of dense vegetation and few photons reaching the  
 1544 ground surface. In these instances, the output of the median filter may lie within the  
 1545 canopy.

1546



1547

1548



1549

1550 Figure 3.8. Three iterations of the ground finding concept for  $L$ -km segments with canopy.

1551

### 1552 3.3 Top of Canopy Finding Filter

1553 Finding the top of the canopy surface uses the same methodology as finding  
1554 the ground surface, except now the de-trended data are “flipped” over. The “flip”  
1555 occurs by multiplying the photons heights by -1 and adding the mean of all the heights  
1556 back to the data. The same procedure used to find the ground surface can be used to  
1557 find the indices of the top of canopy points.

1558

1559 **3.4 Classifying the Photons**

1560           Once a composite ground surface is determined, photons falling within the  
1561 point spread function of the surface are labeled as ground photons. Based on the  
1562 expected performance of ATLAS, the point spread function should be approximately  
1563 35 cm rms. Signal photons that are not labeled as ground and are below the ground  
1564 surface (buffered with the point spread function) are considered noise, but keep the  
1565 signal label.

1566           The top of canopy photons that are identified can be used to generate an upper  
1567 canopy surface through a shape-preserving surface fitting method. All signal photons  
1568 that are not labeled ground and lie above the ground surface (buffered with the point  
1569 spread function) and below the upper canopy surface are considered to be canopy  
1570 photons (and thus labeled accordingly). Signal photons that lie above the top of  
1571 canopy surface are considered noise, but keep the signal label.

1572

1573	FLAGS,	0 = noise
1574		1 = ground
1575		2 = canopy
1576		3 = TOC (top of canopy)

1577

1578           The final ground and canopy classifications are flags 1 – 3. The full canopy is  
1579 the combination of flags 2 and 3.

1580

1581 **3.5 Refining the Photon Labels**

1582           During the first iteration of the algorithm, it is possible that some photons are  
1583 mislabeled; most likely this would be noise photons mislabeled as canopy. To reject  
1584 these mislabeled photons, we apply three criteria:

- 1585           a) If top of canopy photons are 2 standard deviations above a  
1586           smoothed median top of canopy surface
- 1587           b) If there are less than 3 canopy indices within a 15m radius

1588 c) If, for 500 signal photon segments, the number of canopy photons  
1589 is < 5% of the total (when SNR > 1), or < 10% of the total (when SNR  
1590 <= 1). This minimum number of canopy indices criterion implies a  
1591 minimum amount of canopy cover within a region.

1592 There are also instances where the ground points will be redefined. This  
1593 reassigning of ground points is based on how the final ground surface is determined.  
1594 Following the “iterate” steps in the flowchart shown in Figure 3.4, if there are no  
1595 canopy indices identified for the *L-km* segment, the final ground surface is  
1596 interpolated from the identified ground photons and then will undergo a final round  
1597 of median filtering and smoothing.

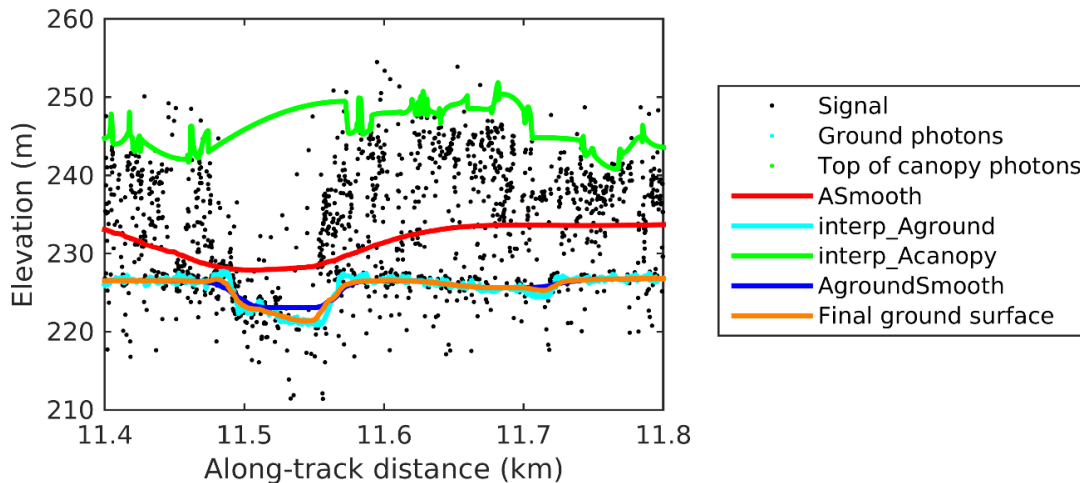
1598 If canopy photons are identified, the final ground surface is interpolated based  
1599 upon the level/amount of canopy at that location along the segment. The final ground  
1600 surface is a composite of various intermediate ground surfaces, defined thusly:

**ASmooth** heavily smoothed surface used to de-trend the signal data

**Interp\_Aground** interpolated ground surface based upon the identified ground  
photons

**AgroundSmooth** median filtered and smoothed version of Interp\_Aground

1601



1602

1603 Figure 3.9. Example of the intermediate ground and top of canopy surfaces calculated from  
 1604 MABEL flight data over Alaska during July 2014.

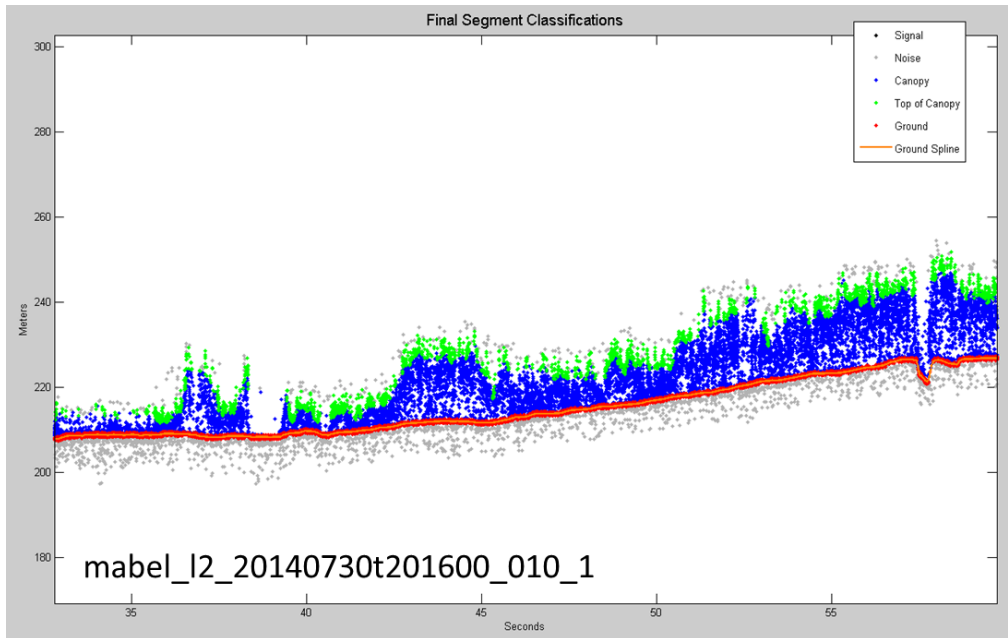
1605

1606 During the first round of ground surface refinement, where there are canopy  
 1607 photons identified in the segment, the ground surface at that location is defined by  
 1608 the smoothed ground surface (AgroundSmooth) value. Else, if there is a location  
 1609 along-track where the standard deviation of the ground-only photons is greater than  
 1610 the 75% quartile for all signal photon standard deviations (i.e., canopy level 3), then  
 1611 the ground surface at that location is a weighted average between the interpolated  
 1612 ground surface (Interp\_Aground\*1/3) and the smoothed interpolated ground surface  
 1613 (AgroundSmooth\*2/3). For all remaining locations long the segment, the ground  
 1614 surface is the average of the interpolated ground surface (Interp\_Aground) and the  
 1615 heavily smoothed surface (ASmooth).

1616 The second round of ground surface refinement is simpler than the first.  
 1617 Where there are canopy photons identified in the segment, the ground surface at that  
 1618 location is defined by the smoothed ground surface (AgroundSmooth) value again.  
 1619 For all other locations, the ground surface is defined by the interpolated ground  
 1620 surface (Interp\_Aground). This composite ground surface is run through the median  
 1621 and smoothing filters again.

1622 The pseudocode for this surface refining process can be found in section 4.10.

1623 Examples of the ground and canopy photons for several MABEL lines are  
1624 shown in Figures 3.10 – 3.12.



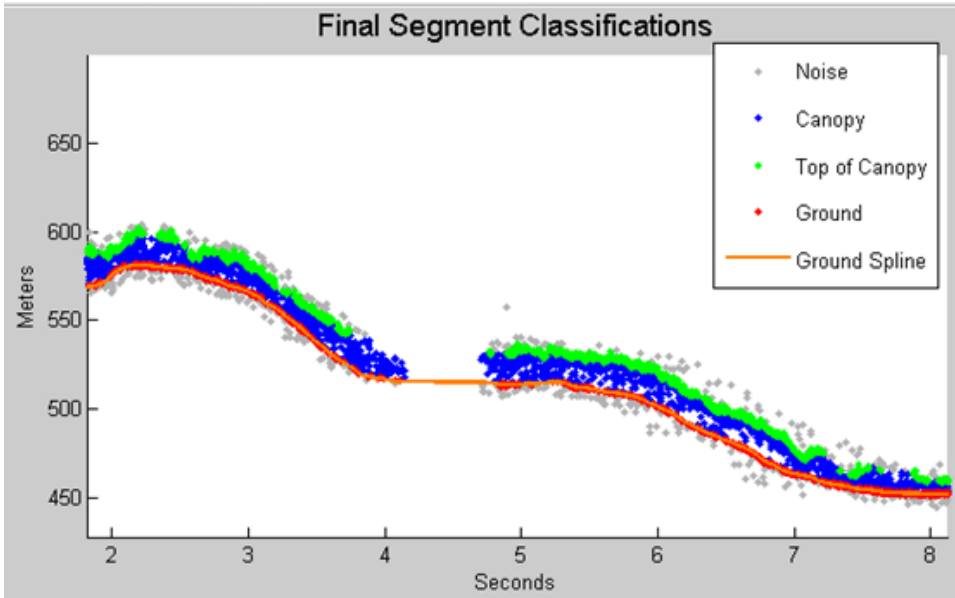
1625

1626 Figure 3.10. Example of classified photons from MABEL data collected in Alaska 2014.

1627 Red photons are photons classified as terrain. Green photons are classified as top of canopy.

1628 Canopy photons (shown as blue) are considered as photons lying between the terrain

1629 surface and top of canopy.



1630

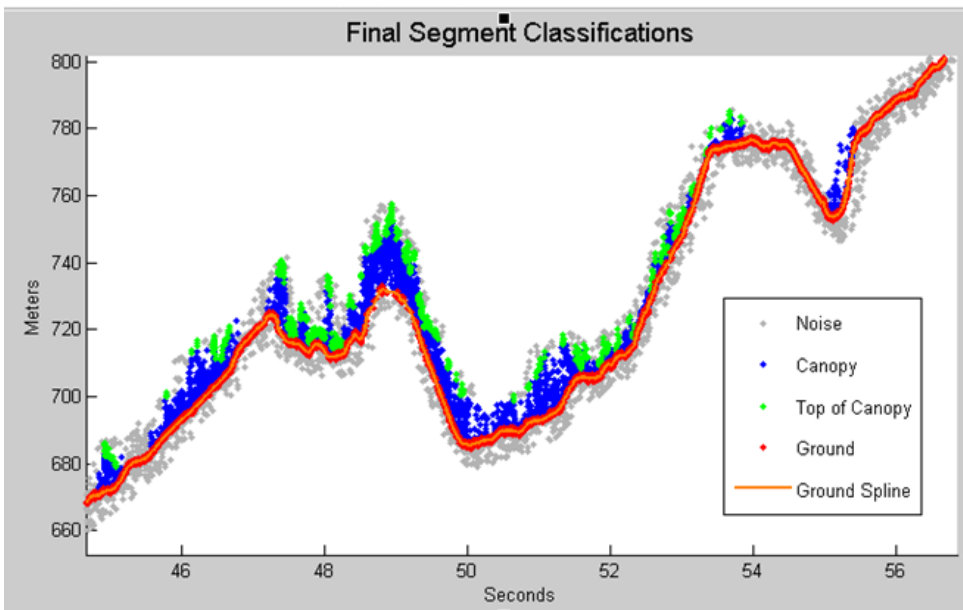
1631 Figure 3.11. Example of classified photons from MABEL data collected in Alaska 2014.

1632 Red photons are photons classified as terrain. Green photons are classified as top of canopy.

1633 Canopy photons (shown as blue) are considered as photons lying between the terrain

1634 surface and top of canopy.

1635



1636

1637 Figure 3.12. Example of classified photons from MABEL data collected in Alaska 2014.

1638 Red photons are photons classified as terrain. Green photons are classified as top of canopy.



1639 Canopy photons (shown as blue) are considered as photons lying between the terrain  
1640 surface and top of canopy.

1641

### 1642 **3.6 Canopy Height Determination**

1643 Once a final ground surface is determined, canopy heights for individual  
1644 photons are computed by removing the ground surface height for that photon's  
1645 latitude/longitude. These relative canopy height values will be used to compute the  
1646 canopy statistics on the ATL08 data product.

1647

### 1648 **3.7 Link Scale for Data products**

1649 The link scale for each segment within which values for vegetation parameters  
1650 will be derived will be defined over a fixed distance of 100 m. A fixed segment length  
1651 ensures that canopy and terrain metrics are consistent between segments, in addition  
1652 to increased ease of use of the final products. A size of 100 m was selected as it should  
1653 provide approximately 140 photons (a statistically sufficient number) from which to  
1654 make the calculations for terrain and canopy height.

1655

1656 **4. ALGORITHM IMPLEMENTATION**

1657 Prior to running the surface finding algorithms used for ATL08 data products, the  
1658 superset of output from the GSFC medium-high confidence classed photons (ATL03  
1659 signal\_conf\_ph: flags 3-4) and the output from DRAGANN will be considered as the input  
1660 data set. ATL03 input data requirements include the along-track time, latitude, longitude,  
1661 height, and classification for each photon. The motivation behind combining the results  
1662 from two different noise filtering methods is to ensure that all of the potential signal  
1663 photons for land surfaces will be provided as input to the surface finding software.

1664 Some additional quality checks are also described here prior to implementing the  
1665 ATL08 software. The first check utilizes the POD\_PPD flag on ATL03. In instances where  
1666 the satellite is maneuvering or the pointing/ranging solutions are suspect, ATL08 will not  
1667 use those data. Thus, data will only flow to the ATL08 algorithm when the POD\_PPD flag  
1668 is set to 0 which indicates ‘nominal’ conditions.

1669 A second quality check pertains to the flags set on the ATL03 photon quality flag  
1670 (quality\_ph). Currently, ATL03 quality\_ph flags are described as:

1671 0 = nominal conditions

1672 1 = possible after-pulse (this identifies the after pulses that occur between 2.3 and  
1673 5 m below the surface)

1674 2 = possible late impulse response effect (this flag identifies additional detector  
1675 effects 5 – 50 m below the surface).

1676 3 = possible TEP crossing.

1677 For this release of the software, we want to mention that there are cases of after-pulsing  
1678 that occur 0.5 – 2.3 m below the surface that are considered nominal with the quality\_ph  
1679 flag. The output from the DRAGANN algorithm (i.e. the DRAGANN flag) will be set to a  
1680 value of 0 when ATL03 quality\_ph flags are greater than 0 such that they are ignored in  
1681 the ATL08 algorithm.

1682

1683 A third quality check pertains to the signal photons (DRAGANN + ATL03 signal  
 1684 confidence photons) and whether those heights are near the surface heights. To pass this  
 1685 check, signal photons that lie 120 m above the reference DEM will be disregarded. Signal  
 1686 photons lying below the reference DEM will be allowed to continue for additional ATL08  
 1687 processing. The motivation for this quality check is to eliminate ICESat-2 photons that are  
 1688 reflecting from clouds rather than the true surface.

1689 Table 4.1. Input parameters to ATL08 classification algorithm.

Name	Data Type	Long Name	Units	Description	Source
<b>delta_time</b>	DOUBLE	GPS elapsed time	seconds	Elapsed GPS seconds since start of the granule for a given photon. Use the metadata attribute granule_start_seconds to compute full gps time.	ATL03
<b>lat_ph</b>	FLOAT	latitude of photon	degrees	Latitude of each received photon. Computed from the ECEF Cartesian coordinates of the bounce point.	ATL03
<b>lon_ph</b>	FLOAT	longitude of photon	degrees	Longitude of each received photon. Computed from the ECEF Cartesian coordinates of the bounce point.	ATL03
<b>h_ph</b>	FLOAT	height of photon	meters	Height of each received photon, relative to the WGS-84 ellipsoid.	ATL03
<b>sigma_h</b>	FLOAT	height uncertainty	m	Estimated height uncertainty (1-sigma) for the reference photon.	ATL03
<b>signal_conf_ph</b>	UINT_1_LE	photon signal confidence	counts	Confidence level associated with each photon event selected as signal (0-noise, 1- added to allow for buffer but algorithm classifies as background, 2-low, 3-med, 4-high).	ATL03
<b>segment_id</b>	UNIT_32	along-track segment ID number	unitless	A seven-digit number uniquely identifying each along-track segment. These are sequential, starting with one for the first segment after an ascending equatorial crossing node.	ATL03

<b>cab_prof</b>	FLOAT	Calibrated Attenuated Backscatter	unitless	Calibrated Attenuated Backscatter from 20 to -1 km with vertical resolution of 30m	ATL09
<b>dem_h</b>	FLOAT	DEM Height	meters	Best available DEM (in priority of GIMP/ANTARCTIC/GMTED/MSS) value at the geolocation point. Height is in meters above the WGS84 Ellipsoid.	ATL09

1690

1691 Table 4.2. Additional external parameters referenced in ATL08 product.

Name	Data Type	Long Name	Units	Description	Source
<b>atlas_pa</b>				Off nadir pointing angle of the spacecraft	
<b>ground_track</b>				Ground track, as numbered from left to right: 1 = 1L, 2 = 1R, 3 = 2L, 4 = 2R, 5 = 3L, 6 = 3R	
<b>dem_h</b>				Reference DEM height	ANC06
<b>ref_azimuth</b>	FLOAT	azimuth	radians	Azimuth of the unit pointing vector for the reference photon in the local ENU frame in radians. The angle is measured from north and positive towards east.	ATL03
<b>ref_elev</b>	FLOAT	elevation	radians	Elevation of the unit pointing vector for the reference photon in the local ENU frame in radians. The angle is measured from east-north plane and positive towards up.	ATL03
<b>rgt</b>	INTEGER_2	reference ground track	unitless	The reference ground track (RGT) is the track on the Earth at which a specified unit vector within the observatory is pointed. Under nominal operating conditions, there will be no data collected along the RGT, as the RGT is spanned by GT2L and GT2R. During slews or off-pointing, it is possible that ground tracks	ATL03

				may intersect the RGT. The ICESat-2 mission has 1,387 RGTs.	
<b>sigma_along</b>	DOUBLE	along-track geolocation uncertainty	meters	Estimated Cartesian along-track uncertainty (1-sigma) for the reference photon.	ATL03
<b>sigma_across</b>	DOUBLE	across-track geolocation uncertainty	meters	Estimated Cartesian across-track uncertainty (1-sigma) for the reference photon.	ATL03
<b>surf_type</b>	INTEGER_1	surface type	unitless	Flags describing which surface types this interval is associated with. 0=not type, 1=is type. Order of array is land, ocean, sea ice, land ice, inland water.	ATL03 , Section 4
<b>layer_flag</b>	Integer	Consolidated cloud flag	unitless	Flag indicating the presence of clouds or blowing snow with good confidence	ATL09
<b>cloud_flag_asr</b>	Integer(3)	Cloud probability from ASR	unitless	Cloud confidence flag, from 0 to 5, indicating low, med, or high confidence of clear or cloudy sky	ATL09
<b>msw_flag</b>	Byte(3)	Multiple scattering warning flag	unitless	Flag with values from 0 to 5 indicating presence of multiple scattering, which may be due to blowing snow or cloud/aerosol layers.	ATL09
<b>asr</b>	Float(3)	Apparent surface reflectance	unitless	Surface reflectance as modified by atmospheric transmission	ATL09
<b>snow_ice</b>	INTEGER_1	Snow Ice Flag	unitless	NOAA snow-ice flag. 0=ice free water; 1=snow free land; 2=snow; 3=ice	ATL09

1692

#### 1693 **4.1 Cloud based filtering**

1694 It is possible for the presence of clouds to affect the number of surface photon  
1695 returns through signal attenuation, or to cause false positive classifications of  
1696 ground or canopy photons on low cloud returns. Either of these cases would reduce  
1697 the accuracy of the ATL08 product. To improve the performance of the ATL08  
1698 algorithm, ideally all clouds would be identified prior to processing through the  
1699 ATL08 algorithm. There will be instances, however, where low lying clouds (e.g.

1700 <800 m above the ground surface) may be difficult to identify. Currently, ATL08  
1701 provides an ATL09 derived cloud flag (layer\_flag) on its 100 m product and  
1702 encourages the user to make note of the presence of clouds when using ATL08  
1703 output. Unfortunately at present, a review of on-orbit data from ATL03 and ATL09  
1704 indicate that the cloud layer flag is not being set correctly in the ATL09 algorithm.  
1705 Ultimately, the final cloud based filtering process used in the ATL08 algorithm will  
1706 most likely be derived from parameters/flag on the ATL09 data product. Until the  
1707 ATL09 cloud flags are proven reliable, however, a preliminary cloud screening  
1708 method is presented below. This methodology utilizes the calibrated attenuated  
1709 backscatter on the ATL09 data product to identify (and subsequently remove for  
1710 processing) clouds or other problematic issues (i.e. incorrectly telemetered  
1711 windows). Using this new method, telemetered windows identified as having either  
1712 low or no surface signal due to the presence of clouds (likely above the telemetered  
1713 band), as well as photon returns suspected to be clouds instead of surface returns,  
1714 will be omitted from the ATL08 processing. This process, however, will not identify  
1715 the extremely low clouds (i.e. <800 m). The steps are as follows:

- 1716 1. Match up the ATL09 calibrated attenuated backscatter (cab\_prof) columns to  
1717 the ATL03 granule being processed using segment ID.
- 1718 2. Flip the matching cab\_prof vertical columns so that the elevation bins go  
1719 from low to high.
- 1720 3. For each of the matching ATL09 cab\_prof vertical columns, perform a cubic  
1721 Savitsky-Golay smoothing filter with a span size of 15 vertical bins. Call this  
1722 cab\_smooth.
- 1723 4. Perform the same smoothing filter on each horizontal row of the cab\_smooth  
1724 output, this time using a span size of 7 horizontal bins. Call this  
1725 cab\_smoother.
- 1726 5. Create a low\_signal logical array the length of the number of matching ATL09  
1727 columns and set to false.
- 1728 6. For each column of cab\_smoother:  
1729 a. Set any values below 0 to 0.

- 1730           b. Set a logical array of cab\_smoother bins that are below 15 km in  
1731           elevation to true. Call this cab15.
- 1732           c. Using the ATL09 dem\_h value for that column, find the ATL09  
1733           cab\_smoother bins that are 240 m above and 240 m below (~8 ATL09  
1734           vertical bins each direction) the dem\_h value. The bins found here that  
1735           are also within cab15 are designated as sfc\_bins.
- 1736           d. Find the maximum peak value of cab\_smoother within the sfc\_bins, if  
1737           any. This will represent the surface peak.
- 1738           e. Find the maximum value of cab\_smoother that is higher in elevation  
1739           than the sfc\_bins and within cab15, if any. This will represent the  
1740           cloud peak.
- 1741           f. If there is no surface peak, set the low\_signal flag to true.
- 1742           g. If there are both surface and cloud peak values returned, determine a  
1743           surface peak / cloud peak ratio. If that ratio is less than or equal to 0.4,  
1744           set low\_signal flag for that column to true.
- 1745        7. After each matching ATL09 column of cab\_smoother has been analyzed for  
1746        low signal, assign the low\_signal flag to an ATL03 photon resolution logical  
1747        array by matching up the ATL03 photon segment\_id values to the ATL09  
1748        range of segment IDs for each ATL09 cab\_prof column.
- 1749        8. For each ATL09 cab\_prof column where the low\_signal flag was not set, check  
1750        for any ATL03 photons greater than 800 meters (TBD) in elevation away  
1751        (higher or lower) from the ATL09 dem\_h value. Assign an ATL03 photon  
1752        resolution too\_far\_signal flag to true when this conditional is met.
- 1753        9. A logical array mask is created for any ATL03 photons that have either the  
1754        low\_signal flag or the too\_far\_signal flag set to true such that those photons  
1755        will not be further processed by the ATL08 function.

1756

#### 1757 **4.2 Preparing ATL03 data for input to ATL08 algorithm**

- 1758        1. At times, cloud attenuation will lead to a reduced L-km with a length that is  
1759        not a multiple of 100 meters. If the last 100m land segment of the L-km

1760 segment contains fewer than 5 ATL03 20m geosegments and the current L-  
1761 km segment is not the last one of the granule, do not report output for this  
1762 last 100m land segment. Retain the starting geosegment of this land segment  
1763 and begin the next L-km segment here.

1764 2. Break up data into *L-km* segments. Segments equivalent of 10 km in along-  
1765 track distance of an orbit would be appropriate.

1766 a. If the last portion of an ATL03 granule being processed would result  
1767 in an *L-km* segment with less than 3.4 km (170 geosegments) worth of  
1768 data, that last portion is added to the previous *L-km* processing  
1769 window to be processed together as one extended *L-km* processing  
1770 segment.

1771 i. The resulting **last\_seg\_extend** value would be reported as a  
1772 positive value of distance beyond 10 km that the ATL08  
1773 processing segment was extended by.

1774 b. If the last *L-km* segment would be less than 10 km but greater than 3.4  
1775 km, a portion extending from the start of current *L-km* processing  
1776 segment backwards into the previous *L-km* processing segment would  
1777 be added to the current ATL08 processing segment to make it 10 km  
1778 in length. Only new 100 m ATL08 segment products generated from  
1779 this backward extension would be reported.

1780 i. The distance of this backward data gathering would be  
1781 reported in **last\_seg\_extend** as a negative distance value.

1782 c. All other segments that are not extended will report a last\_seg\_extend  
1783 value of 0.

1784 3. Add a buffer of 200 m (or 10 segment\_id's) to both ends of each *L-km*  
1785 segment. The total processing segment length is ( $L\text{-km} + 2*\text{buffer}$ ), but will  
1786 be referred to as *L-km* segments for simplicity.

1787 a. The first *L-km* segment from an ATL03 granule would only have a  
1788 buffer at the end, and the last *L-km* segment from an ATL03 granule  
1789 would only have a buffer at the beginning.

1790 4. The input data for ATL08 algorithm is X, Y, Z, T (where T is time).



1791

### 1792 **4.3 Noise filtering via DRAGANN**

1793 DRAGANN will use ATL03 photons with all signal classification flags (0-4). These  
1794 will include both signal and noise photons. This section give a broad overview of the  
1795 DRAGANN function. See Appendix A for more details.

- 1796 1. Determine the relative along-track time, ATT, of each geolocated photon  
1797 from the beginning of each *L-km* segment.
- 1798 2. Rescale the ATT with equal-time spacing between each data photon, keeping  
1799 the relative beginning and end time values the same.
- 1800 3. Normalize the height and rescaled ATT data from 0 – 1 for each *L-km*  
1801 segment based on the min/max of each field. So,  $\text{normtime} = (\text{time} -$   
1802  $\text{mintime})/(\text{maxtime} - \text{mintime})$ .
- 1803 4. Build a kd-tree based on normalized Z and normalized and rescaled ATT.
- 1804 5. Determine the search radius starting with Equation 3.1.  $P$ =[determined by  
1805 preprocessor; see Sec 4.3.1], and  $V_{\text{total}} = 1$ .  $N_{\text{total}}$  is the number of photons  
1806 within the data *L-km* segment. Solve for  $V$ .
- 1807 6. Now that you know  $V$ , determine the radius using Equation 3.2.
- 1808 7. Compute the number of neighbors for each photon using this search radius.
- 1809 8. Generate a histogram of the neighbor count distribution. As illustrated in  
1810 Figure 3.2, the noise peak is the first peak (usually with the highest  
1811 amplitude).
- 1812 9. Determine the 10 highest peaks of the histogram.
- 1813 10. Fit Gaussians to the 10 highest peaks. For each peak,
  - 1814 a. Compute the amplitude,  $a$ , which is located at peak position  $b$ .
  - 1815 b. Determine the width,  $c$ , by stepping one bin at a time away from  $b$  and  
1816 finding the last histogram value that is  $> \frac{1}{2}$  the amplitude,  $a$ .
  - 1817 c. Use the amplitude and width to fit a Gaussian to the peak of the  
1818 histogram, as described in Equation 3.3.
  - 1819 d. Subtract the Gaussian from the histogram, and move on to calculate  
1820 the next highest peak's Gaussian.

1821 e. Reject Gaussians that are too near ( $< 2$  standard deviations) and  
1822 amplitude too low ( $< 1/5$  previous amplitude) from the previous  
1823 signal Gaussian.

1824 11. Reject any of the returned Gaussians with imaginary components.

1825 12. Determine if there is a narrow noise Gaussian at the beginning of the  
1826 histogram. These typically occur when there is little noise, such as during  
1827 nighttime passes.

1828 a. Search for the Gaussian with the highest amplitude,  $a$ , in the first 5%  
1829 of the histogram

1830 b. Check if the highest amplitude is  $\geq 1/10$  of the maximum of all  
1831 Gaussian amplitudes

1832 c. Check if the width,  $c$ , of the Gaussian with the highest amplitude is  $\leq$   
1833 4 bins

1834 d. If these three conditions are met, save the  $[a,b,c]$  values as  $[a_0,b_0,c_0]$ .  
1835 e. If the three conditions are not met, search again within the first 10%.  
1836 Repeat the process, incrementing the percentage of histogram  
1837 searched by 5% up to 30%. As soon as the conditions are met, save  
1838 the  $[a_0,b_0,c_0]$  values and break out of the percentage histogram search  
1839 loop.

1840 13. If a narrow noise peak was found, sort the remaining Gaussians from largest  
1841 to smallest area, estimated by  $a*c$ , then append  $[a_0,b_0,c_0]$  to the beginning of  
1842 the sorted  $[a,b,c]$  arrays. If a narrow noise peak was not found, sort all  
1843 Gaussians by largest to smallest area.

1844 a. If a narrow noise peak was not found, check in sorted order if one of  
1845 the Gaussians are in the first 10% of the histogram. If so, it becomes  
1846 the first Gaussian.

1847 b. Reject any Gaussians that are fully contained within another.

1848 c. Reject Gaussians whose centers are within 3 standard deviations of  
1849 another, unless only two Gaussians remain

1850 14. If there are two or more Gaussians remaining, they are referred to as  
1851 Gaussian 1 and Gaussian 2, assumed to be the noise and signal Gaussians.

- 1852 15. Determine the threshold value that will define the cutoff between noise and  
1853 signal.
- 1854 a. If the absolute difference of the two Gaussians becomes near zero,  
1855 defined as  $< 1e-8$ , set the first bin index where that occurs, past the  
1856 first Gaussian peak location, as the threshold. This would typically be  
1857 set if the two Gaussians are far away from each other.
- 1858 b. Else, the threshold value is the intersection of the two Gaussians,  
1859 which can be estimated as the first bin index past the first Gaussian  
1860 peak location and before the second Gaussian where there is a  
1861 minimum absolute difference between the two Gaussians.
- 1862 c. If there is only one Gaussian, it is assumed to be the noise Gaussian,  
1863 and the threshold is set to  $b + c$ .
- 1864 16. Label all photons having a neighbor count above the threshold as signal.
- 1865 17. Label all photons having a neighbor count below the threshold as noise.
- 1866 18. Reject noise photons.
- 1867 19. Retain signal photons for feeding into next step of processing.
- 1868 20. Use Logical OR to combine DRAGANN signal photons with ATL03 medium-  
1869 high confidence signal photons (flags 3-4) as ATL08 signal photons.
- 1870 21. Calculate a signal to noise ratio (SNR) for the  $L$ - $km$  segment by dividing the  
1871 number of ATL08 signal photons by the number of noise (i.e., all – signal)  
1872 photons.

#### 1873 4.3.1 DRAGANN Quality Assurance

1874 Based upon on-orbit data, there are instances where only noise photons are selected  
1875 as signal photons following running through DRAGANN. These instances usually  
1876 occur to telemetered windows with low signal, signal attenuation near the surface  
1877 due to fog, haze (or other atmospheric properties). If any  $d\_flag$  results in the 10 km  
1878 = 1

- 1879 1. For each 20 m  $segment\_id$  that has a  $d\_flag = 1$ , build a histogram of 5 m  
1880 height bins using the height of only the DRAGANN-flagged photons  
1881 ( $d\_flag=1$ )

1882           2. If the number of bins indicates that all d\_flag photons fall within the same  
1883           vertical 60 m, do nothing and move to the next geosegment.  
1884           3. If the d\_flag photons fall outside of 60 m, calculate the median and  
1885           standard deviation of the histogram counts.  
1886           4. If the maximum value of the histogram counts is greater than the median  
1887           + 3\*standard deviation, a surface peak has been detected based on the  
1888           relative photon density within the 5 meter steps. Else, set all d\_flag = 0  
1889           for this geosegment.  
1890           5. Set all d\_flag = 0 from 3 height bins below the detected peak to the bottom  
1891           of the telemetry window.  
1892           6. Starting with the peak count bin (surface), step upwards bin by bin and  
1893           check if 12 bin counts (60 meters of height bins) above surface are less  
1894           than 0.5 \* histogram median. If so, for all photons above current height in  
1895           loop + 60 meters, set all d\_flag = 0 and exit bin-by-bin loop.  
1896           7. Starting with one bin above the peak count bin (surface), again step  
1897           upwards bin by bin. For each iteration, calculate the standard deviation of  
1898           the bin counts including only the current bin to the highest height bin and  
1899           call this noise standard deviation. If all remaining vertical height bins  
1900           from current bin to highest height bin are less than 2\* histogram  
1901           standard deviation, or if the noise standard deviation is less than 1.0, or if  
1902           this bin and the next 2 higher bins each have counts less than the peak bin  
1903           count (entire histogram) - 3\*histogram standard deviation, then set all  
1904           d\_flag = 0 for all heights above this level and exit bin-by-bin loop  
1905           8. For a final check, construct a new histogram, with median and standard  
1906           deviation, using the corrected d\_flag results and only where d\_flag = 1. If  
1907           the histogram median is greater than 0.0 and the standard deviation is  
1908           greater than 0.75\*median, set all d\_flag in this geosegment = 0. This  
1909           indicates results not well constrained about a detectible surface.  
1910

#### 1911 4.3.2 Preprocessing to dynamically determine a DRAGANN parameter

1912 While a default value of  $P=20$  was found to work well when testing with MABEL  
1913 flight data, further testing with simulated data showed that  $P=20$  is not sufficient in  
1914 cases of very low or very high noise. Additional testing with real ATL03 data have  
1915 shown the ground signal to be much stronger, and the canopy signal to be much  
1916 weaker, than originally anticipated. Therefore, a preprocessing step for dynamically  
1917 calculating  $P$  and running the core DRAGANN function is described in this  
1918 subsection. This assumes  $L$ -km to be 10 km (with additional  $L$ -km buffering).

- 1919 1. Define a DRAGANN processing window of 170 segments ( $\sim 3.4$  km),  
1920 and a buffer of 10 segments ( $\sim 200$  m).
- 1921 2. The buffer is applied to both sides of each DRAGANN processing  
1922 window to create buffered DRAGANN processing windows  
1923 (referenced as “buffered window” for the rest of this section) that will  
1924 overlap the DRAGANN processing windows next to them.
- 1925 3. For each buffered window within the  $L$ -km segment, calculate a  
1926 histogram of points with 1 m elevation bins.
- 1927 4. For each buffered window histogram, calculate the median counts.
- 1928 5. Bins with counts below the buffered window median count value are  
1929 estimated to be noise. Calculate the mean count of noise bins.
- 1930 6. Bins with counts above the buffered window median count value are  
1931 estimated to be signal. Calculate the mean count of signal bins.
- 1932 7. Determine the time elapsed over the buffered window.
- 1933 8. Calculate estimated noise and signal rates for each buffered window  
1934 by multiplying each window’s mean counts of noise bins and signal  
1935 bins, determined from steps 5 and 6 above, by  $1/(\text{elapsed time})$  to  
1936 return the rates in terms of points/meter[elevation]/second[across].
- 1937 9. Calculate a noise ratio for each window by dividing the noise rate by  
1938 the signal rate.
- 1939 10. If, for all the buffered windows in the  $L$ -km segment, the noise rate is  
1940 less than 20 and the noise ratio is less than 0.15; OR any noise rate is

1941 0; OR any signal rate is greater than 1000: re-calculate steps 3-9  
1942 using the entire *L-km* segment. Continue with the following steps  
1943 using results from the one *L-km* window (instead of multiple buffered  
1944 windows).

1945 11. Now, determine the DRAGANN parameter, *P*, for each buffered  
1946 window based on the following conditionals:

1947 a. If the signal rate is NaN (i.e., an invalid value), set the signal  
1948 index array to empty and move on to the next buffered  
1949 window.

1950 b. If noise rate < 20 || noise ratio < 0.15:  
1951  $P = \text{signal rate}$   
1952 If signal rate is < 5,  $P = 5$ ; if signal rate > 20,  $P = 20$

1953 c. Else  $P = 20$ .

1954 12. Run DRAGANN on the buffered window points using the calculated *P*.

1955 13. If DRAGANN fails to find a signal (i.e., only one Gaussian found), run  
1956 DRAGANN again with  $P = 10$ .

1957 14. If DRAGANN still fails to find a signal, try to determine *P* a second time  
1958 using the following conditionals:

1959 a. If (noise rate >= 20) ...  
1960 && (signal rate > 100) ...  
1961 && (signal rate < 250),  
1962  $P = (\text{signal rate})/2$

1963 b. Else if signal rate >= 250,  
1964 if noise rate >= 250,  
1965  $P = (\text{noise rate}) * 1.1$   
1966 else,  
1967  $P = 250$

1968 c. Else,  $P = \text{mean}(\text{noise rate}, \text{signal rate})$

1969 15. Run DRAGANN on the buffered window points using the newly  
1970 calculated *P*.

1971 a. If still no signal points are found, set a dragannError flag.

1972 16. If signal points were found by DRAGANN, for each buffered window  
1973 calculate a signal check by dividing the number of signal points found  
1974 via DRAGANN by the number of total points in the buffered window.

1975 17. If dragannError has been set, or there are suspect signal statistics, the  
1976 following snippet of pseudocode will check those conditionals and try  
1977 to iteratively find a better P value to run DRAGANN with:  
1978  
1979 try\_count = 0  
1980  
1981 While dragannError ...  
1982 || ( (noise rate >= 30) ...  
1983 && (signal check > noise ratio) ...  
1984 && (noise ratio >= 0.15) ) ...  
1985 || (signal check < 0.001):  
1986  
1987 if P < 3,  
1988 break  
1989 else,  
1990 P = P\*0.75  
1991 end  
1992  
1993 if try\_count < 2  
1994 Clear out signal index results from previous DRAGANN run  
1995 Re-run DRAGANN with new P value  
1996 Recalculate the signal check  
1997 end  
1998  
1999 if no signal index results are returned  
2000 P = P\*0.75  
2001 end  
2002  
2003 try\_count = try\_count + 1  
2004  
2005 end

2006  
2007 18. If no signal photons are found by DRAGANN because only one  
2008 Gaussian was found, set the threshold as b+c (i.e., one standard  
2009 deviation away from the Gaussian peak location) for a final DRAGANN  
2010 run. Otherwise, set the signal index array to empty and move on to the  
2011 next buffered window.

- 2012 19. Assign the signal values found from DRAGANN for each buffered  
 2013 window to the original DRAGANN processing window range of points.  
 2014 20. Combine signal points from each DRAGANN processing window back  
 2015 into one  $L$ - $km$  array of signal points for further processing.

2016

### 2017 4.3.3 Iterative DRAGANN processing

2018 It is possible in processing segments with high noise rates that DRAGANN will  
 2019 incorrectly identify clusters of noise as signal. One way to reduce these false positive  
 2020 noise clusters is to run the alternative DRAGANN process (Sec 4.3.1) again with the  
 2021 input being the signal output photons from the first run through alternative  
 2022 DRAGANN. Note that this methodology is still being tested, so by default this option  
 2023 should not be set.

- 2024 1. If  $SNR < 1$  (TBD) from alternative DRAGANN run, run alternative DRAGANN  
 2025 process again using the output signal photons from first DRAGANN run as the  
 2026 input to the second DRAGANN run.  
 2027 2. Recalculate SNR based on output of second DRAGANN run.

2028

2029

### 2030 4.4 Compute Filtering Window

- 2031 1. Next step is to run a surface filter with a variable window size (variable in  
 2032 that it will change from  $L$ - $km$  segment to  $L$ - $km$  segment). The window-size is  
 2033 denoted as Window.  
 2034 2.  $Sspan = ceil[5 + 46 * (1 - e^{-a*length})]$ , where  $length$  is the number of  
 2035 photons in the segment.  
 2036 3.  $a = \frac{\log\left(1 - \frac{21}{51-5}\right)}{-28114} \approx 21 \times 10^{-6}$ , where  $a$  is the shape parameter for the window  
 2037 span.  
 2038



2039 **4.5 De-trend Data**

- 2040 1. The input data are the signal photons identified by DRAGANN and the ATL03  
2041 classification (signal\_conf\_ph) values of 3-4.
- 2042 2. Generate a rough surface by connecting all unique (time) photons to each  
2043 other. Let's call this surface interp\_A.
- 2044 3. Run a median filter through interp\_A using the window size set by the  
2045 software. Output = Asmooth.
- 2046 4. Define a reference DEM limit (ref\_dem\_limit) as 120 m (TBD).
- 2047 5. Remove any Asmooth values further than the ref\_dem\_limit threshold from  
2048 the reference DEM, and interpolate the Asmooth surface based on the  
2049 remaining Asmooth values. The interpolation method to use is the shape  
2050 preserving piecewise cubic Hermite interpolating polynomial – hereafter  
2051 labeled as “pchip” (Fritsch & Carlson, 1980).
- 2052 6. Compute the approximate relief of the *L-km* segment using the 95<sup>th</sup> - 5<sup>th</sup>  
2053 percentile heights of the signal photons. We are going to filter Asmooth again  
2054 and the smoothing is a function of the relief.
- 2055 7. Define the SmoothSize using the conditional statements below. The  
2056 SmoothSize will be used to detrend the data as well as to create an  
2057 interpolated ground surface later.
- 2058 SmoothSize = 2 \* Window
- 2059 • If relief >= 900, SmoothSize = round(SmoothSize/4)
  - 2060 • If relief >= 400 && <= 900, SmoothSize = round(SmoothSize/3)
  - 2061 • If relief >= 200 && <= 400, SmoothSize = round(SmoothSize/2)
- 2062 8. Greatly smooth Asmooth by first running Asmooth 10 times through a  
2063 median filter then a smoothing filter with a moving average method on the  
2064 result. Both the median filter and the smoothing filter use a window size of  
2065 SmoothSize.
- 2066 9. Create a second smooth line (Asmooth2) that roughly follows the ground and  
2067 Asmooth2 will be used only for detrending data during initial ground

2068 estimation. Asmooth2 is created by running five iterations of a median filter  
2069 and smoothing using SmoothSize defined in 4.6.7. The threshold for removing  
2070 photons is 1 m above each iteration.

2071

#### 2072 **4.6 Filter outlier noise from signal**

- 2073 1. If there are any signal data that are 150 meters above Asmooth, remove them  
2074 from the signal data set.
- 2075 2. If the standard deviation of the detrended signal is greater than 10 meters,  
2076 remove any signal value from the signal data set that is 2 times the standard  
2077 deviation of the detrended signal below Asmooth or Asmooth2.
- 2078 3. Calculate a new Asmooth surface by interpolating (pchip method) a surface  
2079 from the remaining signal photons and median filtering using the Window  
2080 size, then median filter and smooth (moving average method) 10 times again  
2081 using the SmoothSize.
- 2082 4. Calculate a new Asmooth2 surface by interpolating a surface from remaining  
2083 signal photons and repeat **step 4.6.9**.
- 2084 5. Detrend the signal photons by subtracting the signal height values from the  
2085 Asmooth2 surface height values. Use the Asmooth2 detrended heights for the  
2086 initial ground estimate surface finding.
- 2087 6. Other calculations for canopy and ground finding will utilize detrended from  
2088 the original Asmooth.

2089

#### 2090 **4.7 Finding the initial ground estimate**

- 2091 1. At this point, the initial signal photons have been noise filtered and de-  
2092 trended and should have the following format: X, Y, detrended Z, T (T=time).  
2093 From this, the input data into the ground finding will be the ATD (along track  
2094 distance) metric (such as time) and the detrended Z height values.
- 2095 2. Define a medianSpan as  $\text{round}(\text{Window} * 2/3)$ .

- 2096 3. Calculate the background neighbor density of the subsurface photons using  
 2097 ALL available photons (the non-detrended data). This step is run on all  
 2098 photons including noise photons. Histogram the photons in 0.5 m vertical  
 2099 bins and a 60 m horizontal bin.
- 2100 4. To avoid including zero population bins in the histogram signal tracking  
 2101 process, identify the bin with the maximum bin count among bins 3 – 7  
 2102 (starting at the lowest height) across each 60 m within the 10-km processing  
 2103 window.
- 2104 5. Calculate the mean of those maximum bin values to represent the noise count  
 2105 for the 10-km window.
- 2106 6. The following steps are run on the detrended signal photons.
- 2107 7. Calculate the brightness of the surface for each 60 m to be histogrammed via  
 2108 the calculation in Section 2.4.21. If a bright surface is detected, skip steps 8  
 2109 and 9
- 2110 8. Determine the lowest 0.5 m histogram height bin for each 60 m along track,  
 2111 in the detrended heights where:
- 2112 a. The neighbor density is 10 x greater than the background density and  
 2113 b. The neighbor density is greater than the histogram population median  
 2114 plus 1/3 of the population standard deviation.
- 2115 9. The photons with detrended heights above this bin are masked from  
 2116 consideration in the initial ground height estimate. Detrended signal photons  
 2117 implies that the d\_flag photons.
- 2118 10. Identifying the ground surface is an iterative process. Start by assuming that  
 2119 all the input signal height photons are the ground. The first goal is the cut  
 2120 out the lower height excess photons in order to find a lower bound for  
 2121 potential ground photons. This process is done 5 times and an offset of 4  
 2122 meters is subtracted from the resulting lower bound. The smoothing filter  
 2123 uses a moving average again:
- 2124 for j=1:5  
 2125 cutOff = median filter (ground, medianSpan)

```

2126         cutOff = smooth filter (cutOff, Window)
2127         ground = ground( (cutOff - ground) > -1 )
2128     end
2129     lowerbound = median filter (ground, medianSpan*3)
2130     middlebound = smooth filter (lowerbound, Window)
2131     lowerbound = smooth filter (lowerbound, Window) - 4
2132 end;
2133 11. Create a linearly interpolated surface along the lower bound points and only
2134     keep input photons above that line as potential ground points:
2135
2136         top = input( input > interp(lowerbound) )
2137
2138 12. The next goal is to cut out excess higher elevation photons in order to find an
2139     upper bound to the ground photons. This process is done 3 times and an
2140     offset of 1 meter is added to the resulting upper bound. The smoothing filter
2141     uses a moving average:
2142
2143     for j = 1:3
2144         cutOff = median filter (top, medianSpan)
2145         cutOff = smooth filter (cutOff, Window)
2146         top = top( (cutOff - top) > -1 )
2147     end
2148     upperbound = median filter (top, medianSpan)
2149     upperbound = smooth filter (upperbound, Window) + 1
2150
2151 13. Create a linearly interpolated surface along the upper bound points and
2152     extract the points between the upper and lower bounds as potential ground
2153     points:
2154
2155         ground = input( ( input > interp(lowerbound) ) & ...
2156             ( input < interp(upperbound) ) )
2157
2158 14. Refine the extracted ground points to cut out more canopy, again using the
2159     moving average smoothing:

```

```

2154         For j = 1:2
2155             cutOff = median filter (ground, medianSpan)
2156             cutOff = smooth filter (cutOff, Window)
2157             ground = ground( (cutOff - ground) > -1 )
2158         end

2159     15. Run the ground output once more through a median filter using window side
2160         medianSpan and a smoothing filter using window size Window, but this time
2161         with the Savitzky-Golay method.
2162     16. Finally, linearly interpolate a surface from the ground points.
2163     17. The first estimate of canopy points are those indices of points that are
2164         between 2 and 150 meters above the estimated ground surface. Save these
2165         indices for the next section on finding the top of canopy.
2166     18. The output from the final iteration of ground points is temp_interpA – an
2167         interpolated ground estimate.
2168     19. Find ground indices that lie within 10 m below and 0.5 m above of
2169         temp_interpA .
2170     20. Apply the ground indices to the original heights (i.e., not the de-trended data)
2171         to label ground photons.
2172     21. Interpolate a ground surface using the pchip method based on the ground
2173         photons. Output is interp_Aground.

```

2174

#### 2175 **4.8 Find the top of the canopy**

```

2176     1. The input are the ATD metric (i.e., time), and the de-trended Z values indexed
2177         by the canopy indices extracted from step 4.7(17).
2178     2. Flip this data over so that we can find a canopy “surface” by multiplying the
2179         de-trended canopy heights by -1.0 and adding the mean(heights).
2180     3. Finding the top of canopy is also an iterative process. Follow the same steps
2181         described in 4.7(2) – 4.7(16), but use the canopy indexed and flipped Z
2182         values in place of the ground input.

```

- 2183 4. Final retained photons are considered top of canopy photons. Use the indices  
2184 of these photons to define top of canopy photons in the original (not de-  
2185 trended) Z values.
- 2186 5. Build a kd-tree on canopy indices using elevation data detrended with  
2187 Asmooth.
- 2188 6. If there are less than three canopy indices within a 100m radius, reassign  
2189 these photons to noise photons. Initially, a value of 15 m was used for the  
2190 search radius. In Release 004 of the algorithm, this value was increased to  
2191 100 m to include more top of canopy photons that were not captured in the  
2192 initial canopy spline estimate.

2193

#### 2194 **4.9 Compute statistics on de-trended (Asmooth) data**

- 2195 1. The input data have been noise filtered and de-trended (Asmooth) and  
2196 should have the following input format: X, Y, detrended Z, T.
- 2197 2. The input data will contain signal photons as well as a few noise photons  
2198 near the surface.
- 2199 3. Compute statistics of heights in the along-track direction using a sliding  
2200 window. Using the window size (window), compute height statistics for all  
2201 photons that fall within each window. These include max height, median  
2202 height, mean height, min height, and standard deviation of all photon heights.  
2203 Additionally, in each window compute the median height and standard  
2204 deviation of just the initially classified top of canopy photons, and the  
2205 standard deviation of just the initially classified ground photon heights.  
2206 Currently only the median top of canopy, and all STD variables are being  
2207 utilized, but it's possible that other statistics may be incorporated as  
2208 changes/improvements are made to the code.
- 2209 4. Slide the window  $\frac{1}{4}$  of the window span and recompute statistics along the  
2210 entire *L-km* segment. This results in one value for each statistic for each  
2211 window.

- 2212 5. Determine canopy index categories for each window based upon the total  
 2213 distribution of STD values for all signal photons along the *L-km* segment  
 2214 based on STD quartiles.
- 2215 6. Open canopy have STD values falling within the 1<sup>st</sup> quartile.
- 2216 7. Canopy Level 1 has STD values falling from 1<sup>st</sup> quartile to median STD value.
- 2217 8. Canopy Level 2 has STD values falling from median STD value to 3<sup>rd</sup> quartile.
- 2218 9. Canopy Level 3 has STD values falling from 3<sup>rd</sup> quartile to max STD.
- 2219 10. Linearly interpolate the window STD values (both for all photons and  
 2220 ground-only photons) back to the native along-track resolution and calculate  
 2221 the interpolated all-photon STD quartiles to create an interpolated canopy  
 2222 level index. This will be used later for interpolating a ground surface.  
 2223

2224 **4.10 Refine Ground Estimates**

- 2225 1. Detrend the interpolated ground surface using Asmooth. Smooth the  
 2226 detrended interpolated ground surface 10 times. All further ground surface  
 2227 smoothing use the moving average method:

2228 For j= 1:10

2229           AgroundSmooth = median filter (interp\_Aground, SmoothSize\*3)

2230           AgroundSmooth = smooth filter (AgroundSmooth, SmoothSize)

2231 End

2232

- 2233 2. This output (AgroundSmooth) from the filtering/smoothing function is an  
 2234 intermediate ground solution and it will be used to estimate the final  
 2235 solution.

- 2236 3. If there are **no canopy indices** identified along the entire segment AND relief  
 2237 >400 m

2238           FINALGROUND = median filter (Asmooth, SmoothSize)

2239           FINALGROUND = smooth filter (FINALGROUND, SmoothSize)

```

2240         Else
2241             FINALGROUND = AgroundSmooth
2242         end
2243     4. If there are canopy indices identified along the segment:
2244         If there is a canopy photon identified at a location along-track above the
2245         ground surface, then at that location along-track
2246             FINALGROUND = AgroundSmooth
2247         else if there is a location along-track where the interpolated ground STD has
2248         an interpolated canopy level >= 3
2249             FINALGROUND = Interp_Aground*1/3 + AgroundSmooth*2/3
2250         else
2251             FINALGROUND = Interp_Aground*1/2 + Asmooth*1/2
2252         end
2253     5. Smooth the resulting interpolated ground surface (FINALGROUND) once
2254         using a median filter with window size of 9 then a smoothing filter twice with
2255         window size of 9. Select ground photons that lie within the point spread
2256         function (PSF) of FINALGROUND.
2257     6. PSF is determined by sigma_atlas_land (Eq. 1.2) calculated at the photon
2258         resolution and thresholded between 0.5 to 1 m.
2259         a. Estimate the terrain slope by taking the gradient of FINALGROUND.
2260             Gradient is reported at the center of ((finalground(n+1)-
2261             finalground(n-1))/(dist_x(n+1)-dist_x(n-1))/2
2262         b. Linearly interpolate the sigma_h values to the photon resolution.
2263         c. Calculate sigma_topo (Eq. 1.3) at the photon resolution.
2264         d. Calculate sigma_atlas_land at the photon resolution using the sigma_h
2265             and sigma_topo values at the photon resolution.
2266         e. Set PSF equal to sigma_atlas_land.
2267             i. Any PSF < 0.5 m is set to 0.5 m as the minimum PSF.

```



2268                   ii. Any PSF > 1 m is set to 1 m as the maximum PSF. Set psf\_flag to  
2269                   true.

2270

#### 2271 **4.11 Canopy Photon Filtering**

2272       1. The first canopy filter will remove photons classified as top of canopy that  
2273       are significantly above a smoothed median top of canopy surface. To  
2274       calculate the smoothed median top of canopy surface:

2275           a. Linearly interpolate the median and standard deviation canopy  
2276           window statistics, calculated from 4.9 (3), to the top of canopy photon  
2277           resolution. Output variables: interpMedianC, interpStdC.

2278           b. Calculate a canopy window size using Eq. 3.4, where *length* = number  
2279           of top of canopy photons. Output variable: winC.

2280           c. Create the median filtered and smoothed top of canopy surface,  
2281           smoothedC, using a locally weighted linear regression smoothing  
2282           method, “lowess” (Cleveland, 1979):

2283                   smoothedC = median filter ( interpMedianC, winC )

2284

2285                   if SNR > 1, canopySmoothSpan = winC\*2;

2286                   else, canopySmoothSpan = smoothSpan;

2287

2288                   smoothedC = smooth filter ( smoothedC, canopySmoothSpan )

2289           d. Add the detrended heights back into the smoothedC surface:

2290                   smoothedC = smoothedC + Asmooth

2291       2. Set canopy height thresholds based on the interpolated top of canopy STD:

2292           If SNR > 1, canopySTDthresh = 3; else, canopySTDthresh = 2;

2293           canopy\_height\_thresh = canopySTDthresh\*interpStdC

2294           high\_cStd = canopy\_height\_thresh > 10

2295                    low\_cStd = canopy\_height\_thresh < 3

2296                    canopy\_height\_thresh(high\_cStd) =

2297                    canopy\_height\_thresh(high\_cStd)/2

2298                    canopy\_height\_thresh(low\_cStd) = 3

2299                    3. Relabel as noise any top of canopy photons that are higher than smoothedC +

2300                    canopy\_height\_thresh.

2301                    4. Next, interpolate a top of canopy surface using the remaining top of canopy

2302                    photons (here we are trying to create an upper bound on canopy points). The

2303                    interpolation method used is pchip. This output is named interp\_Acanopy.

2304                    5. Photons falling below interp\_Acanopy and above FINALGROUND+PSF are

2305                    labeled as canopy points.

2306                    6. For 500 signal photon segments, if number of all canopy photons (i.e., canopy

2307                    and top of canopy) is:

2308                                       < 5% of the total (when SNR > 1), OR

2309                                       < 10% of the total (when SNR <= 1),

2310                    relabel the canopy photons as noise.

2311                    7. Interpolate, using the pchip method, a new top of canopy surface from the

2312                    filtered top of canopy photons. This output is again named interp\_Acanopy.

2313                    8. Again, label photons that lie between interp\_Acanopy and

2314                    FINALGROUND+PSF as canopy photons.

2315                    9. Since the canopy points have been relabeled, we need to do a final

2316                    refinement of the ground surface:

2317                    If canopy is present at any location along-track

2318                                       FINALGROUND = AgroundSmooth (at that location)

2319                    Else if canopy is not present at a location along-track

2320                                       FINALGROUND = interp\_Aground

2321 Smooth the resulting interpolated ground surface (FINALGROUND) once  
2322 using a median filter with window size of SmoothSize (SmoothSize = 9), then  
2323 a moving average smoothing filter twice with window size of SmoothSize  
2324 (SmoothSize = 9)

2325 10. Relabel ground photons based on this new (and last) FINALGROUND solution  
2326 +/- a recalculated PSF (via steps in 4.10 (6)). Points falling below the buffer  
2327 are labeled as noise.

2328 11. Using Interp\_Acanopy and this last FINALGROUND solution + PSF buffer,  
2329 label all photons that lie between the two as canopy photons.

2330 12. Repeat the canopy cover filtering: For 500 signal photon segments, if  
2331 number of all canopy photons (i.e., canopy and top of canopy) is:  
2332 < 5% of the total (when SNR > 1), OR  
2333 < 10% of the total (when SNR <= 1),  
2334 relabel the canopy photons as noise. This is the last canopy labeling step.

2335

#### 2336 **4.12 Compute individual Canopy Heights**

- 2337 1. At this point, each photon will have its final label assigned in  
2338 **classed\_pc\_flag**: 0 = noise, 1 = ground, 2 = canopy, 3 = top of canopy.
- 2339 2. For each individual photon labeled as canopy or top of canopy, subtract the Z  
2340 height value from the interpolated terrain surface, FINALGROUND, at that  
2341 particular position in the along-track direction.
- 2342 3. The relative height for each individual canopy or top of canopy photon will  
2343 be used to calculate canopy products described in Section 4.15. Additional  
2344 canopy products will be calculated using the absolute heights, as described in  
2345 Section 4.15.1.

2346

2347 **4.13 Final photon classification QA check**

- 2348 1. Find any ground, canopy, or top of canopy photons that have elevations  
2349 further than the `ref_dem_limit` from the reference DEM elevation value.  
2350 Convert these to the noise classification.
- 2351 2. Find any relative heights of canopy or top of canopy photons that are greater  
2352 than 150 m above the interpolated ground surface, `FINALGROUND`. Convert  
2353 these to the noise classification.
- 2354 3. Find any `FINALGROUND` elevations that are further than the `ref_dem_limit`  
2355 from the reference DEM elevation value. Convert those `FINALGROUND`  
2356 elevations to an invalid value, and convert any classified photons at the same  
2357 indices to noise.
- 2358 4. If more than 50% of photons are removed in a segment, set `ph_removal_flag`  
2359 to true.

2360

2361 **4.14 Compute segment parameters for the Land Products**

- 2362 1. For each 100 m segment, determine the classed photons (photons classified  
2363 as ground, canopy, or top of canopy).
- 2364 a. If there are fewer than 50 classed photons in a 100 m segment, do not  
2365 calculate land or canopy products.
- 2366 b. If there are 50 or more classed photons in a 100 m segment, extract  
2367 the ground photons to create the land products.
- 2368 2. If the number of ground photons > 5% of the total number of classed photons  
2369 within the segment (this control value of 5% can be modified once on orbit):
- 2370 a. Compute statistics on the ground photons: mean, median, min, max,  
2371 standard deviation, mode, and skew. These heights will be reported  
2372 on the product as **`h_te_mean`**, **`h_te_median`**, **`h_te_min`**, **`h_te_max`**,  
2373 **`h_te_mode`**, and **`h_te_skew`** respectively described in Table 2.1.
- 2374 b. Compute the standard deviation of the ground photons about the  
2375 interpolated terrain surface, `FINALGROUND`. This value is reported as  
2376 **`h_te_std`** in Table 2.1.

- 2377 c. Compute the residuals of the ground photon Z heights about the  
 2378 interpolated terrain surface, FINALGROUND. The product is the root  
 2379 sum of squares of the ground photon residuals combined with the  
 2380 **sigma\_atlas\_land** term in Table 2.5 as described in Equation 1.4. This  
 2381 parameter reported as **h\_te\_uncertainty** in Table 2.1.
- 2382 d. Compute a linear fit on the ground photons and report the slope. This  
 2383 parameter is **terrain\_slope** in Table 2.1.
- 2384 e. Calculate a best fit terrain elevation at the mid-point location of the  
 2385 100 m segment:
- 2386 i. Calculate each terrain photon's distance along-track into the  
 2387 100 m segment using the corresponding ATL03 20 m products  
 2388 segment\_length and dist\_ph\_along, and determine the mid-  
 2389 segment distance (expected to be 50 m ± 0.5 m).
- 2390 1. Use the mid-segment distance to linearly interpolate a  
 2391 mid-segment time (**delta\_time** in Table 2.4). Use the  
 2392 mid-segment time to linearly interpolate other mid-  
 2393 segment parameters: interpolated terrain surface,  
 2394 FINALGROUND, as **h\_te\_interp** (Table 2.1); **latitude**  
 2395 and **longitude** (Table 2.4).
- 2396 ii. Calculate a linear fit, as well as 3<sup>rd</sup> and 4<sup>th</sup> order polynomial fits  
 2397 to the terrain photons in the segment.
- 2398 iii. Create a slope-adjusted and weighted mid-segment variable,  
 2399 weightedZ, from the linear fit: Use terrain\_slope to apply a  
 2400 slope correction to each terrain photon by subtracting the  
 2401 terrain photon heights from the linear fit. Determine the mid-  
 2402 segment location of the linear fit, and add that height to the  
 2403 slope corrected terrain photons. Apply a linear weighting to  
 2404 each photon based on its distance to the mid-segment location:  
 2405  $1 / \sqrt{(\text{photon distance along} - \text{mid-segment distance})^2}$  ).  
 2406 Calculate the weighted mid-segment terrain height, weightedZ:

2407                   sum( each adjusted terrain height \* its weight ) / sum(all  
2408                   weights).

2409                   iv. Determine which of the three fits is best by calculating the  
2410                   mean and standard deviation of the fit errors. If one of the fits  
2411                   has both the smallest mean and standard deviations, use that  
2412                   fit. Else, use the fit with the smallest standard deviation. If  
2413                   more than one fit has the same smallest mean and/or standard  
2414                   deviation, use the fit with the higher polynomial.

2415                   v. Use the best fit to define the mid-segment elevation. This  
2416                   parameter is **h\_te\_best\_fit** in Table 2.1.

2417                               1. If h\_te\_best\_fit is farther than 3 m from h\_te\_interp (best  
2418                               fit diff threshold), check if: there are terrain photons on  
2419                               both sides of the mid-segment location; or the elevation  
2420                               difference between weightedZ and h\_te\_interp is  
2421                               greater than the best fit diff threshold; or the number of  
2422                               ground photons in the segment is <= 5% of total  
2423                               number of classified photons per segment. If any of  
2424                               those cases are present, use h\_te\_interp as the corrected  
2425                               h\_te\_best\_fit. Otherwise use weightedZ as the corrected  
2426                               h\_te\_best\_fit.

2427                   f. Compute the difference of the median ground height from the  
2428                   reference DTM height. This parameter is **h\_dif\_ref** in Table 2.4.  
2429

2430                   3. If the number of ground photons in the segment <= 5% of total number of  
2431                   classified photons per segment,

2432                               a. Report an invalid value for terrain products: **h\_te\_mean,**  
2433                               **h\_te\_median, h\_te\_min, h\_te\_max, h\_te\_mode, h\_te\_skew, h\_te\_std,**  
2434                               **and h\_te\_uncertainty** respectively as described in Table 2.1.

2435                               b. If the number of ground photons in the segment is <= 5% of total  
2436                               number of classified photons in the segment, compute **terrain\_slope**

2437 via a linear fit of the interpolated ground surface, FINALGROUND,  
2438 instead of the ground photons.  
2439 c. Report the mid-segment interpolated terrain surface, FinalGround, as  
2440 **h\_te\_interp** as described in Table 2.1, and report **h\_te\_best\_fit** as the  
2441 h\_te\_interp value.  
2442

#### 2443 **4.15 Compute segment parameters for the Canopy Products**

- 2444 1. For each 100 m segment, determine the classed photons (photons classified as  
2445 ground, canopy, or top of canopy).
  - 2446 a) If there are fewer than 50 classed photons in a 100 m segment, do not  
2447 calculate land or canopy products.
  - 2448 b) If there are 50 or more classed photons in a 100 m segment, extract all  
2449 canopy photons (i.e., canopy and top of canopy; henceforth referred to  
2450 as “canopy” unless otherwise noted) to create the canopy products.
- 2451 2. Only compute canopy height products if the number of canopy photons is >  
2452 5% of the total number of classed photons within the segment (this control  
2453 value of 5% can be modified once on orbit).
  - 2454 a) If the number of ground photons is also > 5% of the total number of  
2455 classed photons within the segment, set **canopy\_rh\_conf** to 2.
  - 2456 b) If the number of ground photons is < 5% of the total number of classed  
2457 photons within the segment, continue with the relative canopy height  
2458 calculations, but set canopy\_rh\_conf to 1.
  - 2459 c) If the number of canopy photons is < 5% of the total number of classed  
2460 photons within the segment, regardless of ground percentage, set  
2461 canopy\_rh\_conf to 0 and report an invalid value for each canopy height  
2462 variable.
- 2463 3. Again, the relative heights (height above the interpolated ground surface,  
2464 FINALGROUND) have been computed already. All parameters derived in the  
2465 section are based on relative heights.

- 2466 4. Sort the heights and compute a cumulative distribution of the heights. Select  
 2467 the height associated with the 98% maximum height. This value is **h\_canopy**  
 2468 listed in Table 2.2.
- 2469 5. Compute statistics on the relative canopy heights. Min, Mean, Median, Max and  
 2470 standard deviation. These values are reported on the product as  
 2471 **h\_min\_canopy**, **h\_mean\_canopy**, **h\_max\_canopy**, and **canopy\_openness**  
 2472 respectively in Table 2.2.
- 2473 6. Using the cumulative distribution of relative canopy heights, select the heights  
 2474 associated with the **canopy\_h\_metrics** percentile distributions (10, 15, 20, 25,  
 2475 30, 35, 40, 45, 50, 55, 60, 65, 70, 75, 80, 85, 90, 95), and report as listed in Table  
 2476 2.2.
- 2477 7. Compute the difference between h\_canopy and canopy\_h\_metrics(50). This  
 2478 parameter is **h\_dif\_canopy** reported in Table 2.2 and represents an amount of  
 2479 canopy depth.
- 2480 8. Compute the standard deviation of all photons that were labeled as Top of  
 2481 Canopy (flag 3) in the photon labeling portion. This value is reported on the  
 2482 data product as **toc\_roughness** listed in Table 2.2.
- 2483 9. The quadratic mean height, **h\_canopy\_quad** is computed by

2484 
$$qmh = \sqrt{\frac{\sum_{i=1}^{N_{ca}} h_i^2}{N_{ca}}}$$

2485 where  $N_{ca}$  is the number of canopy photons in the segment and  $h_i$  are the  
 2486 individual canopy heights.

2487

#### 2488 **4.15.1 Canopy Products calculated with absolute heights**

- 2489 1. The absolute canopy height products are calculated if the number of canopy  
 2490 photons is > 5% of the total number of classed photons within the segment.  
 2491 No number of ground photons threshold is applied for these. Absolute  
 2492 canopy heights are first determined as the relative heights of individual  
 2493 photons above the estimated terrain surface. Once those cumulative



2494 distribution is made, the absolute heights are the relative heights plus the  
2495 best fit terrain height ( $h_{te\_bestfit}$ ).

2496 2. The **centroid\_height** parameter in Table 2.2 is represented by all the classed  
2497 photons for the segment (canopy & ground). To determine the centroid  
2498 height, compute a cumulative distribution of all absolute classified heights  
2499 and select the median height.

2500 3. Calculate **h\_canopy\_abs**, the 98<sup>th</sup> percentile of the absolute canopy heights.

2501 4. Compute statistics on the absolute canopy heights: Min, Mean, Median, and  
2502 Max. These values are reported on the product as **h\_min\_canopy\_abs**,  
2503 **h\_mean\_canopy\_abs**, and **h\_max\_canopy\_abs**, respectively, as described in  
2504 Table 2.2.

2505 5. Again, using the cumulative distribution of relative canopy heights, select the  
2506 heights associated with the **canopy\_h\_metrics\_abs** percentile distributions  
2507 (10, 15, 20, 25, 30, 35, 40, 45, 50, 55, 60, 65, 70, 75, 80, 85, 90, 95) and then  
2508 added to the  $h_{te\_bestfit}$ , and report as listed in Table 2.2.

#### 2509 **4.16 Record final product without buffer**

2510 1. Now that all products have be determined via processing of the *L-km*  
2511 segment with the buffer included, remove the products that lie within the  
2512 buffer zone on each end of the *L-km* segment.

2513 2. Record the final *L-km* products and move on to process the next *L-km*  
2514 segment.

2515

2516

2517 **5 DATA PRODUCT VALIDATION STRATEGY**

2518 Although there are no Level-1 requirements related to the accuracy and precision  
2519 of the ATL08 data products, we are presenting a methodology for validating terrain  
2520 height, canopy height, and canopy cover once ATL08 data products are created.  
2521 Parameters for the terrain and canopy will be provided at a fixed size of 100 m along  
2522 the ground track referred to as a segment. Validation of the data parameters should  
2523 occur at the 100 m segment scale and residuals of uncertainties are quantified (i.e.  
2524 averaged) at the 5-km scale. This 5-km length scale will allow for quantification of  
2525 errors and uncertainties at a local scale which should reflect uncertainties as a  
2526 function of surface type and topography.

2527

2528 **5.1 Validation Data**

2529 Swath mapping airborne lidar is the preferred source of validation data for the  
2530 ICESat-2 mission due to the fact that it is widely available and the errors associated  
2531 with most small-footprint, discrete return data sets are well understood and  
2532 quantified. Profiling airborne lidar systems (such as MABEL) are more challenging to  
2533 use for validation due to the low probability of exact overlap of flightlines between  
2534 two profiling systems (e.g. ICESat-2 and MABEL). In order for the ICESat-2 validation  
2535 exercise to be statistically relevant, the airborne data should meet the requirements  
2536 listed in Table 5.1. Validation data sets should preferably have a minimum average  
2537 point density of 5 pts/m<sup>2</sup>. In some instances, however, validation data sets with a  
2538 lower point density that still meet the requirements in Table 5.1 may be utilized for  
2539 validation to provide sufficient spatial coverage.

2540 Table 5.1. Airborne lidar data vertical height (*Z* accuracy) requirements for validation data.

ICESat-2 ATL08 Parameter	Airborne lidar (rms)
Terrain height	<0.3 m over open ground (vertical) <0.5 m (horizontal)

---

Canopy height	<2 m temperate forest, < 3 m tropical forest
Canopy cover	n/a

---

2541

2542 Terrain and canopy heights will be validated by computing the residuals between the  
2543 ATL08 terrain and canopy height value, respectively, for a given 100 m segment and  
2544 the terrain height (or canopy height) of the validation data for that same  
2545 representative distance. Canopy cover on the ATL08 data product shall be validated  
2546 by computing the relative canopy cover ( $cc = \text{canopy returns}/\text{total returns}$ ) for the  
2547 same representative distance in the airborne lidar data.

2548 It is recommended that the validation process include the use of ancillary data sets  
2549 (i.e. Landsat-derived annual forest change maps) to ensure that the validation results  
2550 are not errantly biased due to non-equivalent content between the data sets.

2551 Using a synergistic approach, we present two options for acquiring the required  
2552 validation airborne lidar data sets.

2553

2554 **Option 1:**

2555 We will identify and utilize freely available, open source airborne lidar data as the  
2556 validation data. Potential repositories of this data include OpenTopo (a NSF  
2557 repository or airborne lidar data), NEON (a NSF repository of ecological monitoring  
2558 in the United States), and NASA GSFC (repository of G-LiHT data). In addition to  
2559 small-footprint lidar data sets, NASA Mission data (i.e. ICESat and GEDI) can also be  
2560 used in a validation effort for large scale calculations.

2561

2562 **Option 2:**

2563 Option 2 will include Option 1 as well as the acquisition of additional airborne lidar  
2564 data that will benefit multiple NASA efforts.

2565 GEDI: With the launch of the Global Ecosystems Dynamic Investigation  
2566 (GEDI) mission in 2018, there are tremendous synergistic activities for  
2567 data validation between both the ICESat-2 and GEDI missions. Since the  
2568 GEDI mission, housed on the International Space Station, has a  
2569 maximum latitude of 51.6 degrees, much of the Boreal zone will not be  
2570 mapped by GEDI. The density of GEDI data will increase as latitude  
2571 increases north to 51.6 degrees. Since the data density for GEDI would  
2572 be at its highest near 51.6 degrees, we would propose to acquire  
2573 airborne lidar data in a “GEDI overlap zone” that would ample  
2574 opportunity to have sufficient coverage of benefit to both ICESat-2 and  
2575 GEDI for calibration and validation.

2576 We recommend the acquisition of new airborne lidar collections that will meet our  
2577 requirements to best validate ICESat-2 as well as be beneficial for the GEDI mission.  
2578 In particular, we would like to obtain data over the following two areas:

- 2579 1) Boreal forest (as this forest type will NOT be mapped with GEDI)
- 2580 2) GEDI high density zone (between 50 to 51.6 degrees N). Airborne lidar data  
2581 in the GEDI/ICESat-2 overlap zone will ensure cross-calibration between  
2582 these two critical datasets which will allow for the creation of a global,  
2583 seamless terrain, canopy height, and canopy cover product for the  
2584 ecosystem community.

2585 In both cases, we would fly data with the following scenario:

2586 Small-footprint, full-waveform, dual wavelength (green and NIR), high point density  
2587 (>20 pts/m<sup>2</sup>) and, over low and high relief locations. In addition, the newly acquired  
2588 lidar data must meet the error accuracies listed in Table 5.1.

2589 Potential candidate acquisition areas include: Southern Canadian Rocky Mountains  
2590 (near Banff), Pacific Northwest mountains (Olympic National Park, Mt. Baker-  
2591 Snoqualmie National Forest), and Sweden/Norway. It is recommended that the

2592 airborne lidar acquisitions occur during the summer months to avoid snow cover in  
 2593 either 2016 or 2017 prior to launch of ICESat-2.

2594

2595 **5.2 Internal QC Monitoring**

2596 In addition to the data product validation, internal monitoring of data  
 2597 parameters and variables is required to ensure that the final ATL08 data quality  
 2598 output is trustworthy. Table 5.2 lists a few of the computed parameters that should  
 2599 provide insight into the performance of the surface finding algorithm within the  
 2600 ATL08 processing chain.

2601 Table 5.2. ATL08 parameter monitoring.

Group	Description	Source	Monitor	Validate in Field
<b>h_te_median</b>	Median terrain height for segment	computed		Yes against airborne lidar data. The airborne lidar data should have an absolute accuracy of <30 cm rms.
<b>n_te_photons</b> <b>n_ca_photons</b> <b>n_toc_photons</b>	Number of classed (sum of terrain, canopy, and top of canopy) photons in a 100 m segment	computed	Yes. Build an internal counter for the number of segments in a row where there aren't enough photons (currently a minimum of 50 photons)	

---

<b>h_te_interp</b>	Interpolated terrain surface height, FINALGROUND	computed	per 100 m segment is used) Difference h_te_interp and h_te_median and determine if the value is > a specified threshold. 2 m is suggested as the threshold value. This is an internal check to evaluate whether the median elevation for a segment is roughly the same as the interpolated surface height.	
<b>h_dif_ref</b>	Difference between h_te_median and ref_dem	computed	This value will be computed and flagged if the difference is > 25 m. The reference DEM is the onboard DEM.	
<b>h_canopy</b>	95% height of individual canopy heights for segment	computed	Yes, > a specified threshold (e.g. 60 m)	Yes against airborne lidar data. The

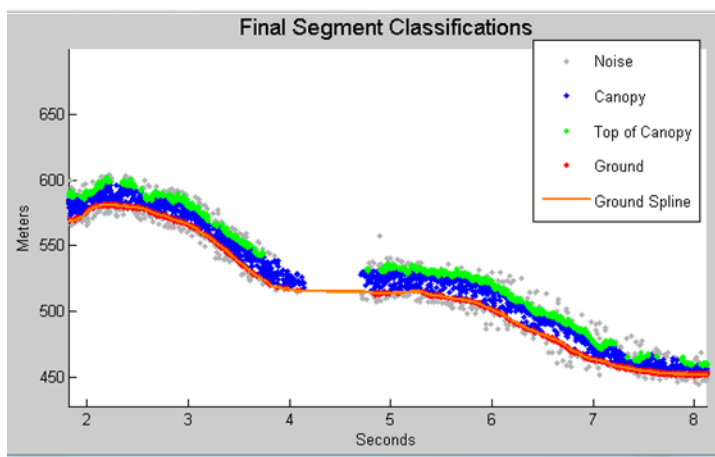
---

---

				canopy heights derived from airborne lidar data should have a relative accuracy <2 m in temperate forest, <3 m in tropical forest
<b>h_dif_canopy</b>	Difference between h_canopy and canopy_h_metrics(50)	computed	Yes, this is an internal check to make sure the calculations on canopy height are not suspect	
<b>psf_flag</b>	Flag is set if computed PSF exceeds 1m	computed	Yes, this is an internal check to make sure the calculations are not suspect	
<b>ph_removal_flag</b>	Flag is set if more than 50% of classified photons in a segment is removed during final QA check	computed		
<b>dem_removal_flag</b>	Flag is set if more than 20% of classified photons in a segment is removed due to a large distance from the reference DEM	computed	Yes, this will check if bad results are due to bad DEM values or because too much noise was labeled as signal	

---

2603 In addition to the monitoring parameters listed in Table 5.2, a plot such as what is  
2604 shown in Figure 5.1 would be helpful for internal monitoring and quality  
2605 assessment of the ATL08 data product. Figure 5.1 illustrates in graphical form what  
2606 the input point cloud look like in the along-track direction, the classifications of each  
2607 photon, and the estimated ground surface (FINALGROUND).



2608

2609 Figure 5.1. Example of *L-km* segment classifications and interpolated ground surface.

2610



2611 The following parameters are to be calculated and placed in the QA/QC group on the  
 2612 HDF5 data file, based on Table 5.2 of the ATL08 ATBD. Statistics shall be computed  
 2613 on a per-granule basis and reported on the data product. If any parameter meets the  
 2614 QA trigger conditional, an alert will be sent to the ATL08 ATBD team for product  
 2615 review.

2616 Table 5.3. QA/QC trending and triggers.

QA/QC trending description	QA trigger conditional
Percentage of segments with > 50 classed photons	None
Max, median, and mean of the number of contiguous segments with < 50 classed photons	None
Number and percentage of segments with difference in $h_{te\_interp} - h_{te\_median}$ is greater than a specified threshold (2 m TBD)	> 50 segments in a row
Max, median, and mean of $h_{diff\_ref}$ over all segments	None
Percentage of segments where $h_{diff\_ref} > 25$ m	Percentage > 75%
Percentage of segments where the $h_{canopy}$ is > 60m	None
Max, median, and mean of $h_{diff}$	None
Percentage of segments where $psf\_flag$ is set	Percentage > 75%
Percentage of classified photons removed in a segment during final photon QA check	Percentage > 50% (i.e., $ph\_removal\_flag$ is set to true)
Percentage of classified photons removed in a segment during the reference DEM threshold removal process	Percentage > 20% (i.e., $dem\_removal\_flag$ is set to true)

2617

2618

2619 **6 REFERENCES**

2620

2621 Carroll, M. L., Townshend, J. R., DiMiceli, C. M., Noojipady, P., & Sohlberg, R. A.  
2622 (2009). A new global raster water mask at 250 m resolution. *International Journal of*  
2623 *Digital Earth*, 2(4), 291–308. <http://doi.org/10.1080/17538940902951401>

2624 Channan, S., K. Collins, and W. R. Emanuel (2014). Global mosaics of the standard  
2625 MODIS land cover type data. University of Maryland and the Pacific Northwest  
2626 National Laboratory, College Park, Maryland, USA.

2627 Chauve, Adrien, et al. (2008). Processing full-waveform lidar data: modelling raw  
2628 signals. *International archives of photogrammetry, remote sensing and spatial*  
2629 *information sciences 2007*, 102-107.

2630 Cleveland, W. S. (1979). Robust Locally Weighted Regression and Smoothing  
2631 Scatterplots. *Journal of the American Statistical Association*, 74(368), 829–836.  
2632 <http://doi.org/10.2307/2286407>

2633 Friedl, M.A., D. Sulla-Menashe, B. Tan, A. Schneider, N. Ramankutty, A. Sibley and X.  
2634 Huang (2010). MODIS Collection 5 global land cover: Algorithm refinements and  
2635 characterization of new datasets, 2001-2012, Collection 5.1 IGBP Land Cover,  
2636 Boston University, Boston, MA, USA.

2637 Fritsch, F.N., and Carlson, R.E. (1980). Monotone Piecewise Cubic Interpolation.  
2638 *SIAM Journal on Numerical Analysis*, 17(2), 238–246.  
2639 <http://doi.org/10.1137/0717021>

2640 Goshtasby, A., and O'Neill, W.D. (1994). Curve fitting by a Sum of Gaussians.  
2641 *Graphical Models and Image Processing*, 56(4), 281-288.

2642 Goetz and Dubayah (2011). Advances in remote sensing technology and  
2643 implications for measuring and monitoring forest carbon stocks and change. *Carbon*  
2644 *Management*, 2(3), 231-244. doi:10.4155/cmt.11.18

2645 Hall, F.G., Bergen, K., Blair, J.B., Dubayah, R., Houghton, R., Hurtt, G., Kellndorfer, J.,  
2646 Lefsky, M., Ranson, J., Saatchi, S., Shugart, H., Wickland, D. (2011). Characterizing 3D  
2647 vegetation structure from space: Mission requirements. *Remote sensing of*  
2648 *environment*, 115(11), 2753-2775

2649 Harding, D.J., (2009). Pulsed laser altimeter ranging techniques and implications for  
2650 terrain mapping, in *Topographic Laser Ranging and Scanning: Principles and*  
2651 *Processing*, Jie Shan and Charles Toth, eds., CRC Press, Taylor & Francis Group, 173-  
2652 194.

2653 Neuenschwander, A.L. and Magruder, L.A. (2016). The potential impact of vertical  
2654 sampling uncertainty on ICESat-2/ATLAS terrain and canopy height retrievals for  
2655 multiple ecosystems. *Remote Sensing*, 8, 1039; doi:10.3390/rs8121039

2656 Neuenschwander, A.L. and Pitts, K. (2019). The ATL08 Land and Vegetation Product  
2657 for the ICESat-2 Mission. *Remote Sensing of Environment*, 221, 247-259.  
2658 <https://doi.org/10.1016/j.rse.2018.11.005>

2659 Neumann, T., Brenner, A., Hancock, D., Robbins, J., Saba, J., Harbeck, K. (2018). ICE,  
2660 CLOUD, and Land Elevation Satellite – 2 (ICESat-2) Project Algorithm Theoretical  
2661 Basis Document (ATBD) for Global Geolocated Photons (ATL03).

2662 Olson, D. M., Dinerstein, E., Wikramanayake, E. D., Burgess, N. D., Powell, G. V. N.,  
2663 Underwood, E. C., D'Amico, J. A., Itoua, I., Strand, H. E., Morrison, J. C., Loucks, C. J.,  
2664 Allnutt, T. F., Ricketts, T. H., Kura, Y., Lamoreux, J. F., Wettengel, W. W., Hedao, P.,  
2665 Kassem, K. R. (2001). Terrestrial ecoregions of the world: a new map of life on Earth.  
2666 *Bioscience*, 51(11), 933-938.

2667

2668 **Appendix A**

2669 **DRAGANN Gaussian Deconstruction**

2670 John Robbins

2671 20151021

2672

2673 Updates made by Katherine Pitts:

2674 20170808

2675 20181218

2676

2677 **Introduction**

2678 This document provides a verbal description of how the DRAGANN (Differential,  
2679 Regressive, and Gaussian Adaptive Nearest Neighbor) filtering system deconstructs  
2680 a histogram into Gaussian components, which can also be called *iteratively fitting a*  
2681 *sum of Gaussian Curves*. The purpose is to provide enough detail for ASAS to create  
2682 operational ICESat-2 code required for the production of the ATL08, Land and  
2683 Vegetation product. This document covers the following Matlab functions within  
2684 DRAGANN:

- 2685 • mainGaussian\_dragann
  - 2686 • findpeaks\_dragann
  - 2687 • peakWidth\_dragann
  - 2688 • checkFit\_dragann
- 2689

2690 Components of the k-d tree nearest-neighbor search processing and histogram  
2691 creation were covered in the document, *DRAGANN k-d Tree Investigations*, and have  
2692 been determined to function consistently with UTexas DRAGANN Matlab software.

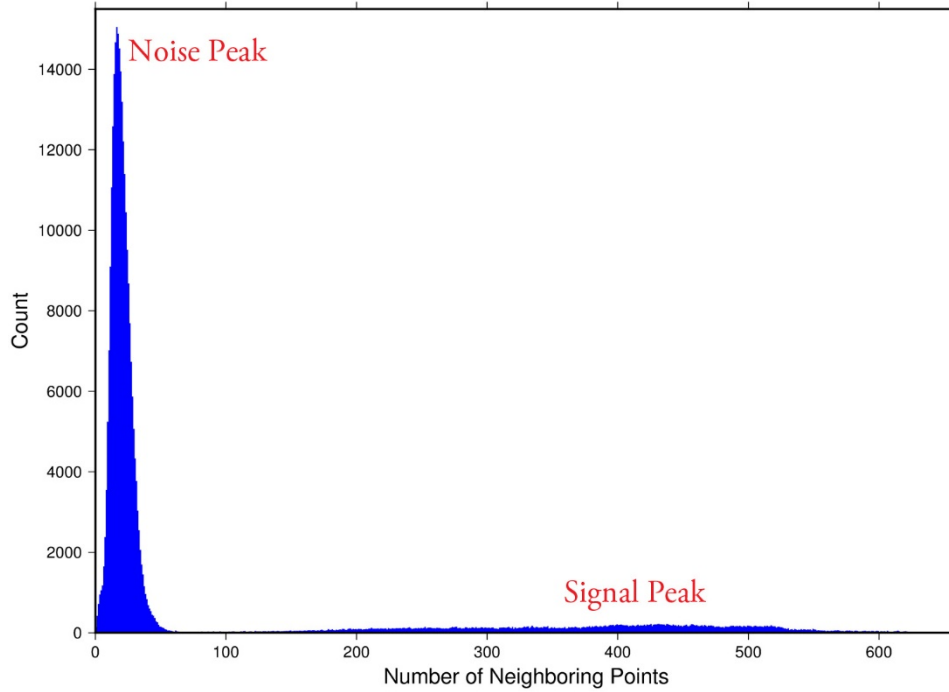
2693

2694 **Histogram Creation**

2695 Steps to produce a histogram of nearest-neighbor counts from a normalized photon  
2696 cloud segment have been completed and confirmed. Figure A.1 provides an example  
2697 of such a histogram. The development, below, is specific to the two-dimensional  
2698 case and is provided as a review.

2699 The histogram represents the frequency (count) of the number of nearby photons  
2700 within a specified radius, as ascertained for each point within the photon cloud. The  
2701 radius,  $R$ , is established by first normalizing the photon cloud in time (x-axis) and in  
2702 height (y-axis), i.e., both sets of coordinates (time & height) run from 0 to 1; then an  
2703 average radius for finding 20 points is determined based on forming the ratio of 20  
2704 to the total number of the photons in the cloud ( $N_{total}$ ):  $20/N_{total}$ .

2705



2706

2707 **Figure A.1.** Histogram for Mabel data, channel 43 from SE-AK flight on July 30, 2014  
 2708 at 20:16.

2709 Given that the total area of the normalized photon cloud is, by definition, 1, then this  
 2710 ratio gives the average area,  $A$ , in which to find 20 points. A corresponding radius is  
 2711 found by the square root of  $A/\pi$ . A single equation describing the radius, as a  
 2712 function of the total number of photons in the cloud (remembering that this is done  
 2713 in the cloud normalized, two-dimensional space), is given by

2714 
$$R = \sqrt{\frac{20/N_{total}}{\pi}} \quad (\text{A.1})$$

2715 For the example in Figure A.1,  $R$  was found to be 0.00447122. The number of  
 2716 photons falling into this radius, at each point in the photon cloud, is given along the  
 2717 x-axis; a count of their number (or frequency) is given along the y-axis.

2718

2719 **Gaussian Peak Removal**

2720

2721 At this point, the function, `mainGaussian_dragann`, is called, which passes the  
 2722 histogram and the number of peaks to detect (typically set to 10).

2723 This function essentially estimates (i.e., fits) a sequence of Gaussian curves, from  
 2724 larger to smaller. It determines a Gaussian fit for the highest histogram peak, then  
 2725 removes it before determining the fit for the next highest peak, etc. In concept, the  
 2726 process is an iterative sequential-removal of the ten largest Gaussian components  
 2727 within the histogram.

2728 In the process of *sequential least-squares*, parameters are re-estimated when input  
2729 data is incrementally increased and/or improved. The present problem operates in  
2730 a slightly reverse way: the data set is fixed (i.e., the histogram), but components  
2731 within the histogram (independent Gaussian curve fits) are removed sequentially  
2732 from the histogram. The paper by *Goshtasby & O'Neill* (1994) outlines the concepts.

2733 Recall that a Gaussian curve is typically written as

$$2734 \quad y = a \cdot \exp(-(x - b)^2 / 2c^2) \quad (\text{A.2})$$

2735 where  $a$  = the height of the peak;  $b$  = position of the peak; and  $c$  = width of the bell  
2736 curve.

2737 The function, `mainGaussian_dragann`, computes the  $[a, b, c]$  values for the ten  
2738 highest peaks found in the histogram. At initialization, these  $[a, b, c]$  values are set to  
2739 zero. The process begins by locating histogram peaks via the function,  
2740 `findpeaks_dragann`.

2741

## 2742 **Peak Finding**

2743 As input arguments, the `findpeaks_dragann` function receives the histogram and a  
2744 minimum peak size for consideration (typically set to zero, which means all peaks  
2745 will be found). An array of index numbers (i.e., the “number of neighboring points”,  
2746 values along x-axis of Figure A.1) for all peaks is returned and placed into the  
2747 variable `peaks`.

2748 The methodology for locating each peak goes like this: The function first computes  
2749 the derivatives of the histogram. In Matlab there is an intrinsic function, called `diff`,  
2750 which creates an array of the derivatives. `Diff` essentially computes the differences  
2751 along sequential, neighboring values. “ $Y = \text{diff}(X)$  calculates differences between  
2752 adjacent elements of  $X$ .” [from Matlab Reference Guide] Once the derivatives are  
2753 computed, then `findpeaks_dragann` enters a loop that looks for changes in the sign  
2754 of the derivative (positive to negative). It skips any derivatives that equal zero.

2755 For the  $k$ th derivative, the “*next*” derivative is set to  $k+1$ . A test is made whereby if  
2756 the  $k+1$  derivative equals zero and  $k+1$  is less than the total number of histogram  
2757 values, then increment “*next*” to  $k+2$  (i.e., find the next negative derivative). The test  
2758 is iterated until the start of the “down side” of the peak is found (i.e., these iterations  
2759 handle cases when the peak has a flat top to it).

2760 When a sign change (positive to negative) is found, the function then computes an  
2761 approximate index location (variable *maximum*) of the peak via

$$2762 \quad \text{maximum} = \text{round} \left( \frac{\text{next} - k}{2} \right) + k \quad (\text{A.3})$$

2763 These values of *maximum* are retained in the peaks array (which can be *grown* in  
2764 Matlab) and returned to the function mainGaussian\_dragann.

2765 Next, back within mainGaussian\_dragann, there are two tests to determine whether  
2766 the first or last elements of the histogram are peaks. This is done since the  
2767 findpeaks\_dragann function will not detect peaks at the first or last elements, based  
2768 solely on derivatives. The tests are:

2769 If ( histogram(1) > histogram(2) && max(histogram)/histogram(1) < 20 ) then  
2770 insert a value of 1 to the very first element of the peaks array (again, Matlab can  
2771 easily “grow” arrays). Here, max(histogram) is the highest peak value across the  
2772 whole histogram.

2773 For the case of the last histogram value (say there are N-bins), we have

2774 If ( histogram(N) > histogram(N-1) && max(histogram)/histogram(N) < 4 ) then  
2775 insert a value of N to the very last element of the peaks array.

2776 One more test is made to determine whether there any peaks were actually found  
2777 for the whole histogram. If none were found, then the function,  
2778 mainGaussian\_dragann, merely exits.

2779

## 2780 **Identifying and Processing upon the Ten Highest Peaks**

2781 The function, mainGaussian\_dragann, now begins a loop to analyze the ten highest  
2782 peaks. It begins the  $n^{\text{th}}$  loop (where  $n$  goes from 1 to 10) by searching for the largest  
2783 peak among all remaining peaks. The index number, as well as the magnitude of the  
2784 peak, are retained in a variable, called maximum, with dimension 2.

2785 In each pass in the loop, the  $[a,b,c]$  values (see eq. 2) are retained as output of the  
2786 function. The values of  $a$  and  $b$  are set equal to the index number and peak  
2787 magnitude saved in maximum(1) and maximum(2), respectively. The  $c$ -value is  
2788 determined by calling the function, peakWidth\_dragann.

### 2789 *Determination of Gaussian Curve Width*

2790 The function, peakWidth\_dragann, receives the whole histogram and the index  
2791 number (maximum(1)) of the peak for which the value  $c$  is needed, as arguments.  
2792 For a specific peak, the function essentially searches for the point on the histogram  
2793 that is about  $\frac{1}{2}$  the size of the peak and that is furthest away from the peak being  
2794 investigated (left and right of the peak). If the two sides (left and right) are  
2795 equidistant from the peak, then the side with the smallest value is chosen ( $> \frac{1}{2}$   
2796 peak).

2797 Upon entry, it first initializes  $c$  to zero. Then it initializes the index values left, xL and  
2798 right, xR as index-1 and index+1, respectively (these will be used in a loop,



2799 described below). It next checks whether the  $n^{\text{th}}$  peak is the first or last value in the  
2800 histogram and treats it as a special case.

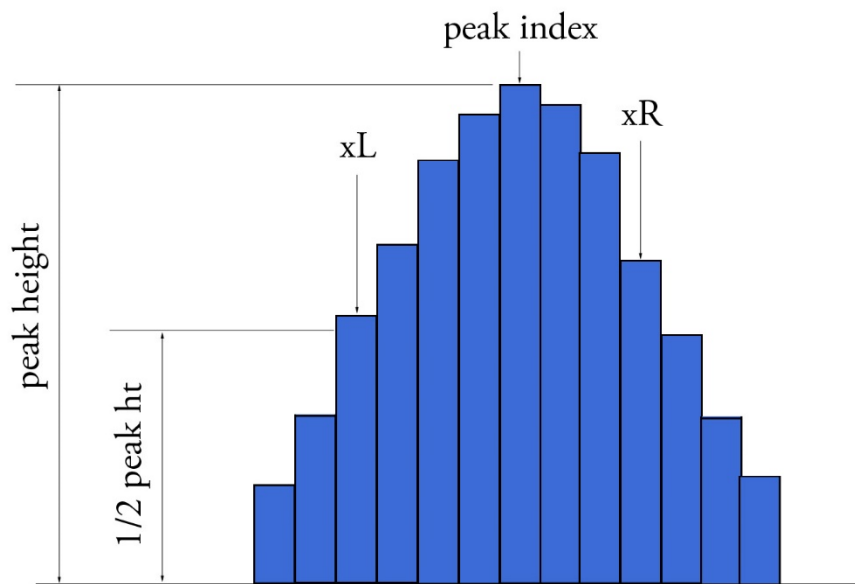
2801 At initialization, first and last histogram values are treated as follows:

2802 If first bin of histogram (peak = 1), set left = 1 and  $xL = 1$ .

2803 If last bin of histogram, set right =  $m$  and  $xR = m$ , where  $m$  is the final index of the  
2804 histogram.

2805 Next, a search is made to the left of the peak for a nearby value that is smaller than  
2806 the peak value, but larger than half of the peak value. A while-loop does this, with  
2807 the following conditions: (a) left > 0, (b) histogram value at left is  $\geq$  half of histo  
2808 value at peak and (c) histo value at left is  $\leq$  histo value at peak. When these  
2809 conditions are all true, then  $xL$  is set to left and left is decremented by 1, so that the  
2810 test can be made again. When the conditions are no longer met (i.e., we've moved to  
2811 a bin in the histogram where the value drops below half of the peak value), then the  
2812 program breaks out of the while loop.

2813 This is followed by a similar search made upon values to the right of the peak. When  
2814 these two while-loops are complete, we then have the index numbers from the  
2815 histogram representing bins that are above half the peak value. This is shown in  
2816 Figure A.2.



2817

2818 **Figure A.2.** Schematic representation of a histogram showing  $xL$  and  $xR$  parameters  
2819 determined by the function `peakWidth_dragann`.

2820 A test is made to determine which of these is furthest from the middle of the peak. In  
2821 Figure A.2,  $xL$  is furthest away and the variable  $x$  is set to equal  $xL$ . The histogram

2822 “height” at  $x$ , which we call  $V_x$ , is used (as well as  $x$ ) in an inversion of Equation A.2  
2823 to solve for  $c$ :

$$2824 \quad c = \sqrt{\frac{-(x-b)^2}{2\ln\left(\frac{V_x}{a}\right)}} \quad (\text{A.4})$$

2825 The function, `peakWidth_dragann`, now returns the value of  $c$  and control returns to  
2826 the function, `mainGaussian_dragann`.

2827 The `mainGaussian_dragann` function then picks-up with a test on whether the  
2828 returned value of  $c$  is zero. If so, then use a value of 4, which is based on an *a priori*  
2829 understanding that  $c$  usually falls between 4 and 6. If the value of  $c$  is not zero, then  
2830 add 0.5 to  $c$ .

2831 At this point, we have the  $[a,b,c]$  values of the Gaussian for the  $n^{\text{th}}$  peak. Based on  
2832 these values, the Gaussian curve is computed (via Equation A.2) and it is removed  
2833 (subtracted) from the current histogram (and put into a new variable called  
2834 `newWave`).

2835 After a Gaussian curve is removed from the current histogram, the following peak  
2836 width calculations could potentially have a  $V_x$  value less than 1 from  $a$ . This would  
2837 cause the width,  $c$ , to be calculated as unrealistically large. Therefore, a check is put  
2838 in place to determine if  $a - V_x < 1$ . If so,  $V_x$  is set to a value of  $a - 1$ .

### 2839 *Numeric Optimization Steps*

2840 The first of the optimization steps utilizes a Full Width Half Max (*FWHM*) approach,  
2841 computed via

$$2842 \quad FWHM = 2c\sqrt{2\ln 2} \quad (\text{A.5})$$

2843 A left range,  $L_r$ , is computed by  $L_r = \text{round}(b - FWHM/2)$ . This tested to make sure it  
2844 doesn't go off the left edge of the histogram. If so, then it is set to 1.

2845 Similarly, a right range,  $R_r$ , is computed by  $R_r = \text{round}(b + FWHM/2)$ . This is also tested  
2846 to be sure that it doesn't go off the right edge of the histogram. If so, then it is set to  
2847 the index value for the right-most edge of the histogram.

2848 Using these new range values, create a temporary segment (between  $L_r$  and  $R_r$ ) of  
2849 the `newWave` histogram, this is called `errorWave`. Also, set three delta parameters  
2850 for further optimization:

2851  $\Delta C = 0.05;$        $\Delta B = 0.02;$        $\Delta A = 1$

2852 The temporary segment, `errorWave` is passed to the function `checkFit_dragann`,  
2853 along with a set of zero values having the same number of elements as `errorWave`,  
2854 the result, at this point, is saved into a variable called `oldError`. The function,  
2855 `checkFit_dragann`, computes the sum of the squares of the difference between two

2856 histogram segments (in this case, errorWave and zeros with the same number of  
2857 elements as errorWave). Hence, the result, oldError, is the sum of the squares of the  
2858 values of errorWave. This function is applied in optimization loops, to refine the  
2859 values of  $b$  and  $c$ , described below.

2860 *Optimization of the  $b$ -parameter.* The do-loop operates at a maximum of 1000 times.  
2861 It's purpose is to refine the value of  $b$ , in 0.02 increments. It increments the value of  
2862  $b$  by DeltaB, to the right, and computes a new Gaussian curve based on  $b+\Delta b$ , which  
2863 is then removed from the histogram with the result going into the variable  
2864 newWave. As before, checkFit\_dragann is called by passing the range-limited part of  
2865 newWave (errorWave) and returning a new estimate of the error (newError) which  
2866 is then checked against oldError to determine which is smaller. If newError is  $\geq$   
2867 oldError, then the value of  $b$  that produced oldError is retained, and the testing loop  
2868 is exited.

2869 *Optimization of the  $c$ -parameter.* Now the value of  $c$  is optimized, first to the left,  
2870 then to the right. It is performed independently of, but similarly, to the  $b$ -parameter,  
2871 using do-loops with a maximum of 1000 passes. These loops increment (to right) or  
2872 decrement (to left) by a value of 0.05 (DeltaC) and use checkFit\_dragann to, again,  
2873 check the quality of the fit. The loops (right and left) kick-out when the fit is found to  
2874 be smallest.

2875 The final, optimized Gaussian curve is now removed (subtracted) from the  
2876 histogram. After removal, a statement "corrects" any histogram values that may  
2877 drop below zero, by setting them to zero. This could happen due to any mis-fit of the  
2878 Gaussian.

2879 The  $n^{\text{th}}$  loop is concluded by examining the peaks remaining in the histogram  
2880 without the peak just processed by sending the  $n^{\text{th}}$ -residual histogram back into the  
2881 function findpeaks\_dragann. If the return of peak index numbers from  
2882 findpeaks\_dragann reveals more than 1 peak remaining, then the index numbers for  
2883 peaks that meet these three criteria are retained in an array variable called these:

- 2884 1. The peak must be located above  $b(n)-2*c(n)$ , and
  - 2885 2. The peak must be located below  $b(n)+2*c(n)$ , and
  - 2886 3. The height of the peak must be  $< a(n)/5$ .
- 2887

2888 The peaks meeting all three of these criteria are to be eliminated from further  
2889 consideration. What this accomplishes is eliminate the nearby peaks that have a size  
2890 lower than the peak just previously analyzed; thus, after their elimination, only  
2891 leaving peaks that are further away from the peak just processed and are  
2892 presumably "real" peaks. The  $n^{\text{th}}$  iteration ends here, and processing begins with the  
2893 revised histogram (after having removed the peak just analyzed).

2894

## 2895 **Gaussian Rejection**

2896 The function mainGaussian\_dragann returns the  $[a,b,c]$  parameters for the ten  
2897 highest peaks from the original histogram. The remaining code in dragann examines  
2898 each of the ten Gaussian peaks and eliminates the ones that fail to meet a variety of  
2899 conditions. This section details how this is accomplished.

2900 First, an approximate area,  $area1=a*c$ , is computed for each found peak and  $b$ , for all  
2901 ten peaks, being the index of the peaks, are converted to an actual value via  
2902  $b+\min(\text{numptsinrad})-1$  (call this  $allb$ ).

2903 Next, a rejection is made for all peaks that have any component of  $[a,b,c]$  that are  
2904 imaginary (Matlab isreal function is used to confirm that all three components are  
2905 real, in which case it passes).

2906 To check for a narrow noise peak at the beginning of the histogram in cases of low  
2907 noise rates, such as during nighttime passes, a check is made to first determine if the  
2908 highest Gaussian amplitude,  $a$ , within the first 5% of the histogram is  $\geq 1/10$  \* the  
2909 maximum amplitude of all Gaussians. If so, that peak's Gaussian width,  $c$ , is checked  
2910 to determine if it is  $\leq 4$  bins. If neither of those conditions are met in the first 5%,  
2911 the conditions are rechecked for the first 10% of the histogram. This process is  
2912 repeated up to 30% of the histogram, in 5% intervals. Once a narrow noise peak is  
2913 found, the process breaks out of the incremental 5% histogram checks, and the  
2914 noise peak values are returned as  $[a0, b0, c0]$ .

2915 If a narrow noise peak was found, the remaining peak area values,  $area1 (a*c)$ , then  
2916 pass through a descending sort; if no narrow noise peak was found, all peak areas go  
2917 through the descending sort. So now, the  $[a,allb,c]$ -values are sorted from largest  
2918 "area" to smallest, these are placed in arrays  $[a1, b1, c1]$ . If a narrow noise peak was  
2919 found, it is then appended to the beginning of the  $[a1, b1, c1]$  arrays, such that  $a1 =$   
2920  $[a0 a1]$ ,  $b1 = [b0 b1]$ ,  $c1 = [c0 c1]$ .

2921 In the case that a narrow noise peak was not found, a test is made to check that at  
2922 least one of the peaks is within the first 10% of the whole histogram. It is done  
2923 inside a loop that works from peak 1 to the number of peaks left at this point. This  
2924 loop first tests whether the first (sorted) peak is within the first 10% of the  
2925 histogram; if so, then it simply kicks out of the loop. If not, then it places the loop's  
2926 current peak into a holder ( $ihold$ ) variable, increments the loop to the next peak and  
2927 runs the same test on the second peak, etc. Here's a Matlab code snippet:

```
2928 inds = 1:length(a1);  
2929 for i = 1:length(b1)  
2930     if b1(i) <= min(numptsinrad) + 1/10*max(numptsinrad)  
2931         if i==1  
2932             break;  
2933         end  
2934         ihold = inds(i);  
2935         for j = i:-1:2  
2936             inds(j) = inds(j-1);  
2937         end  
2938         inds(1) = ihold;
```

```

2939         break
2940     end
2941 end
2942

```

2943 The j-loop expression gives the `init_val:step_val:final_val`. The semi-colon at the end  
 2944 of statements causes Matlab to execute the expression without printout to the user's  
 2945 screen. When this loop is complete, then the indexes (`inds`) are re-ordered and  
 2946 placed back into the `[a1,b1,c1]` and `area1` arrays.

2947 Next, are tests to reject any Gaussian peak that is entirely encompassed by another  
 2948 peak. A Matlab code snippet helps to describe the processing.

```

2949 % reject any gaussian if it is fully contained within another
2950 isR = true(1,length(a1));
2951 for i = 1:length(a1)
2952     ai = a1(i);
2953     bi = b1(i);
2954     ci = c1(i);
2955     aset = (1-(c1/ci).^2);
2956     bset = ((c1/ci).^2*2*bi - 2*b1);
2957     cset = -(2*c1.^2.*log(a1/ai)-b1.^2+(c1/ci).^2*bi^2);
2958     realset = (bset.^2 - 4*aset.*cset >= 0) | (a1 > ai);
2959     isR = isR & realset;
2960 end
2961 a2 = a1(isR);
2962 b2 = b1(isR);
2963 c2 = c1(isR);
2964

```

2965 The logical array `isR` is initialized to all be true. The i-do-loop will run through all  
 2966 peaks. The computations are done in array form with the variables `aset,bset,cset` all  
 2967 being arrays of `length(a1)`. At the bottom of the loop, `isR` remains "true" when  
 2968 either of the conditions in the expression for `realset` is met (the single "|" is a logical  
 2969 "or"). Also, the nomenclature, "." and ".", denote element-by-element array  
 2970 operations (not matrix operations). Upon exiting the i-loop, the array variables  
 2971 `[a2,b2,c2]` are set to the `[a1,b1,c1]` that remain as "true." [At this point, in our test  
 2972 case from channel 43 of East-AK Mable flight on 20140730 @ 20:16, six peaks are  
 2973 still retained: 18, 433, 252, 33, 44.4 and 54.]

2974 Next, reject Gaussian peaks whose centers lay within  $3\sigma$  of another peak, unless only  
 2975 two peaks remain. The code snippet looks like this:

```

2976 isR = true(1, length(a2));
2977 for i = 1:length(a2)
2978     ai = a2(i);
2979     bi = b2(i);
2980     ci = c2(i);
2981     realset = (b2 > bi+3*ci | b2 < bi-3*ci | b2 == bi);
2982     realset = realset | a2 > ai;
2983     isR = isR & realset;
2984 end
2985 if length(a2) == 2
2986     isR = true(1, 2);
2987 end
2988 a3 = a2(isR);

```

```
2989     b3 = b2(isR);
2990     c3 = c2(isR);
2991
```

2992 Once again, the isR array is initially set to “true.” Now, the array, realset, is tested  
2993 twice. In the first line, one of three conditions must be true. In the second line, if  
2994 realset is true or  $a2 > ai$ , then it remains true. At this point, we’ve pared down, from  
2995 ten Gaussian peaks, to two Gaussian peaks; one represents the noise part of the  
2996 histogram; the other represents the signal part.

2997 If there are less than two peaks left, a thresholding/histogram error message is  
2998 printed out. If the lastTryFlag is not set, DRAGANN ends its processing and an empty  
2999 IDX value is returned. The lastTryFlag is set in the preprocessing function which  
3000 calls DRAGANN, as multiple DRAGANN runs may be tried until sufficient signal is  
3001 found.

3002 If there are two peaks left, then set the array [a,b,c] to those two peaks. [At this  
3003 point, in our test case from channel 43 of East-AK Mable flight on 20140730 @  
3004 20:16, the two peaks are: 18 and 433.]

3005

### 3006 **Gaussian Thresholding**

3007 With the two Gaussian peaks identified as noise and signal, all that is left is to  
3008 compute the threshold value between the Gaussians.

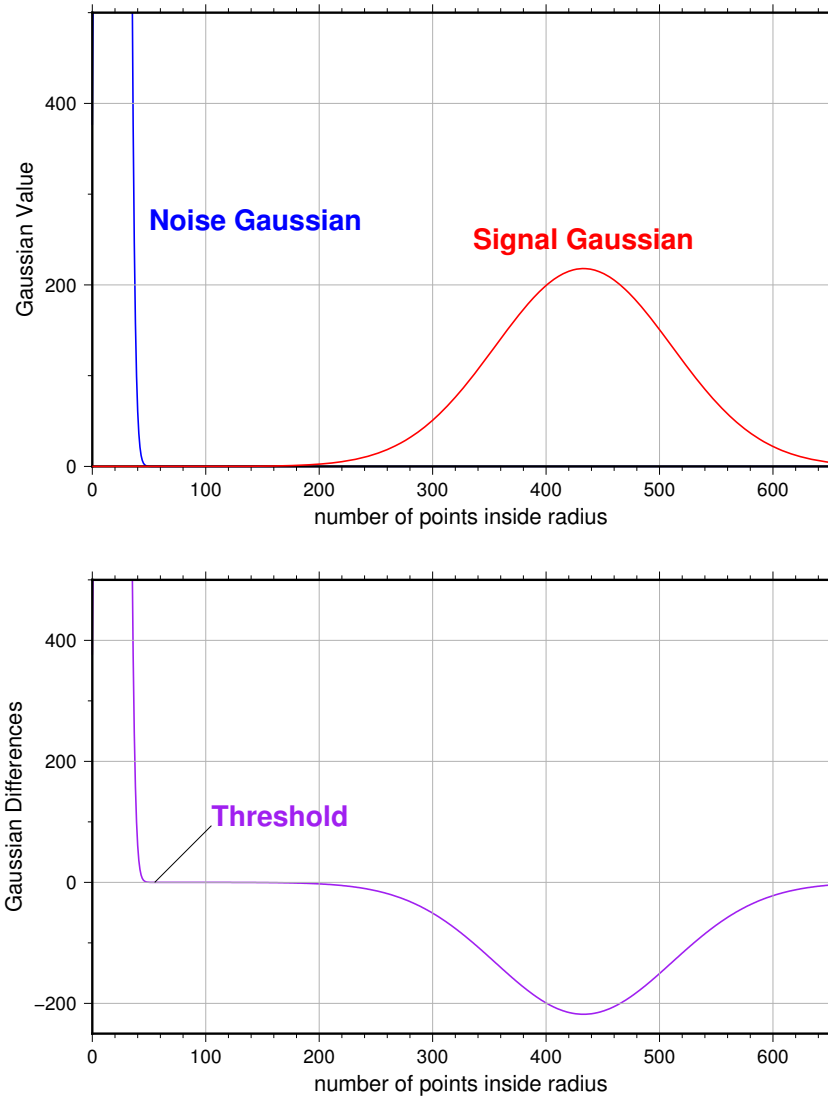
3009 An array of xvals is established running from  $\min(\text{numptsinrad})$  to  
3010  $\max(\text{numptsinrad})$ . In our example, xvals has indices between 0 and 653. For each  
3011 of these xvals, Gaussian curves (allGauss) are computed for the two Gaussian peaks  
3012 [a,b,c] determined at the end of the previous section. This computation is performed  
3013 via a function called gaussmaker which receives, as input, the xvals array and the  
3014 [a,b,c] parameters for the two Gaussian curves. An array of heights of the Gaussian  
3015 curves is returned by the function, computed with Equation A.2. In Matlab, the  
3016 allGauss array has dimension  $2 \times 654$ . An array, noiseGauss is set to be equal to the  
3017 1<sup>st</sup> column of allGauss.

3018 An if-statement checks whether the b array has more than 1 element (i.e., consisting  
3019 of two peaks), if so, then nextGauss is set to the 2<sup>nd</sup> column of allGauss, and a  
3020 difference, noiseGauss-nextGauss, is computed.

3021 The following steps are restricted to be between the two main peaks. First, the first  
3022 index of the absolute value of the difference that is near-zero (defined as  $1e-8$ ) is  
3023 found, if it exists, and put into the variable diffNearZero. This is expected to be found  
3024 if the two Gaussians are far away from each other in the histogram.

3025 Second, the point (i.e., index) is found of the minimum of the absolute value of the  
3026 difference; this index is put into variable, signchanges. This point is where the sign  
3027 changes from positive to negative as one moves left-to-right, up the Gaussian curve

3028 differences (noise minus next will be positive under the peak of the noise curve, and  
3029 negative under the next (signal) curve). Figure A.3 (top) shows the two Gaussian  
3030 curves. The bottom plot shows their differences.



3031

3032 **Figure A.3.** Top: two remaining Gaussian curves representing the noise (blue) and  
3033 signal (red) portions of the histogram in Figure A.1. Bottom: difference noise –  
3034 signal of the two Gaussian curves. The threshold is defined as the point where the  
3035 sign of the differences change.

3036 If there is any value stored in `diffNearZero`, that value is now saved into the variable  
3037 `threshNN`. Else, the value of the threshold in `signchanges` is saved into `threshNN`,  
3038 concluding the if-statement for `b` having more than 1 element.

3039 An else clause ( $b \neq 1$ ), merely sets threshNN to  $b+c$ , i.e., 1-standard deviation away  
3040 from mean of the (presumably) noise peak.

3041 The final step is mask the signal part of the histogram where all indices above the  
3042 threshNN index are set to logical 1 (true). This is applied to the numptsinrad array,  
3043 which represents the photon cloud. After application, dragann returns the cloud  
3044 with points in the cloud identified as “signal” points.

3045 The Matlab code has a few debug statements that follow, along with about 40 lines  
3046 for plotting.

3047

### 3048 **References**

3049 Goshtasby, A & W. D. O’Neill, Curve Fitting by a Sum of Gaussians, *CVGIP: Graphical*  
3050 *Models and Image Processing*, V. 56, No. 4, 281-288, 1994.